Quadram Institute, Analytical Sciences Unit

USING INFRARED SPECTROSCOPY TO EVALUATE PHYSIOLOGICAL AGEING IN STORED POTATOES (*SOLANUM TUBEROSUM*)

Jessica M. R. Garnett, *MChem*

September 2018

A thesis submitted to the University of East Anglia for the degree of Doctor of Philosophy

ABSTRACT

The potato tuber is one of world's largest food crops and in most growing regions is only harvested once a year. A proportion of tubers must therefore be stored efficiently to ensure there are enough provisions to last until the next harvest. Dormancy break during storage causes reduced tuber quality and potentially considerable losses.

The aim of this work has been to determine whether Vis/NIR Spectroscopy can be used to monitor tuber dormancy, and further, to predict the onset of sprouting within a potato tuber.

Small changes in Chlorophyll (Chl) production can be tracked in the tissue under the surface skin of a potato tuber, using a Vis/NIR spectrometer equipped with a fibre-optic probe. A static experimental setup yielded precise measurements of these subtle changes when the tuber was stimulated with light, long before visible greening occurred. It was found that there is a greater capacity for Chl production around the apical buds or "eyes" of a tuber compared with the surrounding tissue.

These results held true for several cultivars from multiple harvests over the four years of the project. The technique however is very sensitive to the exact positioning of the tuber-probe alignment, due to the highly localised area of increased activity in the Chl production under an eye and the shape of the tuber itself.

Although Chl is not produced in tubers whilst kept in cold dark storage, a tuber's capacity to produce Chl once removed was found to change over the course of long-term storage. This behaviour was well fitted by a generalised logistic function. Prediction of the onset of dormancy break could be made from the shape of the curve from individual tuber batches. A proviso throughout is that sufficient tubers need to be analysed to obtain a meaningful batch average. The large tuber-to-tuber variance in behaviour remains the greatest challenge to translating this work into real world settings.

CONTENTS

LIST OF FIGURES

LIST OF TABLES

ACKNOWLEDGEMENTS

INTRODUCTION

1.1 THE POTATO CROP

1.1.1 Origin, Production and Consumption

The social significance of the potato (*Solanum tuberosum*) is found foremost in the Peruvian archaeological record. Ceramic pottery resembling potatoes has been dated back to 400 A.D. (Harris, 1992). These artefacts are known to belong to the Mochica, Chimu and Ina cultures. Not only have the vessels represented the vegetable itself, but also as embodying a life form (Kidder, 1967). An example of this can be seen by the *Potato-Mother* shown in FIGURE 1:1. Graves and Cabieses (2001) suggested that the Andean people saw a link between the potato and the supernatural world, implied by designs in which human figures and animals appear to sprout from the potato's eyes. Whatever the reason, it certainly shows the importance of the potato for the Andean people during this time.

Figure 1:1 The Potato-Mother, located at the Penn Museum, Philadelphia, USA. Donated by Mrs. George W. Childs Drexel (1939). Brick red and creamy white, height; 7 ¾ inches. Object No. 39-20-32.

It is known therefore that the potato is of ancient origin. Further archaeological and genetic evidence indicated that wild species first occurred in the Andes of modern-day Peru and Bolivia and were domesticated in South America over 8000 years ago (Bradshaw and Ramsay, 2009, Brush et al., 1981). The potato is a tuberous crop from the perennial nightshade plant *Solanum tuberosum;* the edible tuber is a starch food group (Hoover, 2001). The modern cultivated potato was first recorded in the Canary Islands during the 16th century (Hawkes and Francisco-Ortega, 1993). However, the origin of the European potato has long been in dispute; DNA analysis has shown a wide variation of Andean and Chilean-type cultivars on the Canary Islands (Ríos et al., 2007). The potato is now one of the world's largest food crops and production continues to increase throughout the world (Harris, 1992). Behind wheat, barley and sugar beet, potatoes had the greatest annual production in the UK during 2016 (Nations, 2014).

The early dispersion and later breeding processes have provided a large source of genetic diversity. Globally there are now more than 4000 potato varieties (Glendinning, 1983, Lehesranta et al., 2005). Many cultivars have had genes introgressed from wild and cultivated species to promote desired characteristics, such as disease and pest resistance (Howard, 1970). In Europe, seed tubers are planted from March to May and harvested between July and October. Different varieties influence the time to maturity and are therefore classified into four maturity types: first early, second early, early maincrop and late maincrop. These characterise the variety by how long the crop is left to grow until they are harvested; 10-12, 13-15, 20 and 26 weeks respectively (Harris, 1992). In general tubers are then classified by their skin colour; white, red, yellow or purple (Burton, 1966).

1.1.2 Factors Affecting Yield and Dry Matter Content

Potato tubers are a storage organ that originate from underground shoots, called stolon's, which are formed by cell expansion, cell division and a large depositing of carbon and nitrogen-based compounds such as starch and storage proteins (Visser et al., 1994, Appeldoorn et al., 2002). Starch is the major component of dry matter and is the product of a secondary reaction, following photosynthesis, called starch synthesis (Harris, 1992). It is formed by the condensation of sugar in the tuber and then stored to provide the energy and structural materials for future growth (Burton, 1966). Starch is a carbohydrate made up of the polymer chains amylose and amylopectin which exists in the form of granules (Vansoest et al., 1994). The variation in the granule shape and size, and the proportions of the two polymers depend mainly on the plant variety but also on the growing conditions (Debon et al., 1998, Haase and Plate, 1996, Tester et al., 2004). The amount of food produced is dependent on the abundance and composition of dry matter within each tuber and the yield of the crop (Allen and Scott, 1980). Both depend on many environmental, agricultural and genetic factors.

Environmental factors influencing production include: the length of day, light intensity, soil type, temperature, carbon dioxide, nitrogen and water supply (Cottrell et al., 1995, Tester and Karkalas, 2001, Yusuph et al., 2003) . A simple experiment conducted by Burstall et al. (1987) showed that three different production sites of the same tuber cultivar, Maris Piper, caused a change in the average size and yield of each harvest. As most of the influencing environmental factors are interconnected, it has proved difficult for researchers to analyse the effect of each independently. However, tuber development has been shown to be controlled by phytohormones including gibberellins, auxin and strigolactones (Roumeliotis et al., 2012, Kloosterman et al., 2007).

The rate of photosynthesis is strongly controlled by light intensity. Length of day and weather conditions, such as cloud cover and the time of the year, have a direct effect on the productivity of tuber formation (Sibma, 1970). Gray and Holmes (1970) investigated the effect of shading potato plants for a period of 12 days at the beginning of tuber growth. They found that this had no effect on the total tuber number or survival, but it did have a negative effect on the final yield. A number of studies have also shown that soil water is very important for high yield and tuber quality (Dalla Costa et al., 1997, Onder et al., 2005, Yuan et al., 2003). Karafyllidis et al. (1996) found limited soil moisture decreased crop yield, shortened growing period by 1 – 4 weeks and dormancy (in subsequent storage) period by 2 – 8 weeks.

Factors dependent on the methods of agriculture, such as manuring, times of planting, time of lifting and length of growing season, also influence the crop productivity (Burton, 1966). Artificial fertilisation is important in agriculture as it can provide essential minerals needed for growth. Nitrogen, phosphorous and potassium generally have the largest effects, while other minerals have specific biochemical roles and relatively small effects within a narrow range of supply (Harris, 1992). Most soil provides too little of these elements to maximise yield, so growers add fertilisers to provide a steady and continuous supply of plant nutrients (Watson, 1963). Holliday et al. (1963) found that there was an optimum rate for applying fertiliser; exceeding this optimal rate caused a decrease in production yield.

Finally, the nature of the mother tuber seed will also have a direct effect on the crop productivity; the main factor being the cultivar, as well as the age, source and size of the tuber (Gillison et al., 1987, Caldiz et al., 2001, Jenkins et al., 1993). Iritani et al. (1972) found a positive correlation of 0.98 between the weight of the seed tuber and the total yield.

This long list of influencing factors alone illustrates that obtaining a high crop yield can be challenging. A large amount of preparation, knowledge and organisation must be undertaken to maintain the ideal conditions for tuber growth. Nevertheless, certain conditions are still uncontrollable such as the weather or outbreaks of disease. The well-known historical event of the blight (*Phytophthora infestans*) epidemic during the 1840s is the most extreme example of this. This disease spread from the United States, across the Atlantic sea, to Europe (Donnelly, 2002). The effects of blight caused over one million people to starve to death and another two million to emigrate from their countries, devastating Ireland the most (O'Neill, 2009).

1.1.3 Post-Harvest Physiology

Once a potato tuber has been harvested, and is no longer attached to the parent plant, there is a prompt change from storage metabolism to reserve mobilisation, as the tuber shifts from a sink to a source (Viola et al., 2007a). Once independent, the tuber will tend towards a state of equilibrium with its environment. Compositional changes occurring in potato tubers after harvest involve; sugar concentrations, hormone levels, membrane permeability and electrolyte leakage (Knowles and Knowles, 1989, Spychalla and Desborough, 1990).

Starch within a tuber provides the energy and substrate for respiration; sugar metabolism supports future tuber growth (Sergeeva et al., 2012). A review written by Schippers (1977) highlighted an agreement within studies regarding the general trend of respiration rate during storage. Immediately after harvest, tubers will have a fast respiration rate that then decreases after 3-6 weeks and will not increase again until accompanying sprout growth. The rate of respiration for different cultivars under the same conditions is, however, varied (Appleman, 1916). This could be due to the finding that immature tubers (those harvested early) respire more rapidly when placed in stores than more mature tubers (Appleman and Miller, 1926a). Temperature is known to influence the respiration rate of tubers: when the crop is transferred to high temperatures the rates increase (Appleman and Miller, 1926b). From the range of 5 – 25 °C, respiration rates increase two-fold for every 10 °C rise (Burton, 1966). This is true for short term storage periods; during long-term storage these rates can be influenced by other factors. For example, Barker (1933) found a positive correlation between the respiration rates of individual tubers and their content of sugar.

Bailey et al. (1978) found that during an eight-month storage period, the levels of reducing sugars in a tuber increased up to eight-fold. Again, this is influenced by environmental factors but in particular the storage temperature. Barker (1932) found that a low storage temperature caused an increased amount of reducing sugars to accumulate in a tuber. Temperatures below 10 °C induce potato starch to break down into sucrose, which in turn can be split into reducing sugars (Cottrell et al., 1995, Spychalla and Desborough, 1990). This is known as low-temperature sweetening. Hill et al. (1996) concluded this phenomenon is initiated by a change in the kinetic properties of sucrose phosphate synthase and the appearance of a new amylolytic activity. Higher levels of these sugars lead to an undesired sweetened taste, nutritional changes and can cause browning when crisps or fries are fried for consumption. (Wiltshire and Cobb, 1996). Sowokinos et al. (2018) showed that it is possible to screen genetically diverse

potato clones to find the level of cold induced sweetening resistance within different species. This could become a method used in the future to source out those species which are better suited for processed products.

Exposure to light after harvest leads to surface greening due to the stimulation of chlorophyll (Chl) biosynthesis (Dao and Friedman, 1994, Grunenfelder et al., 2006b). The length of exposure necessary for a tuber to become visibly green varies and is affected by many pre- and post-harvest factors: cultivar, light quality and intensity, temperature and crop maturity (Gull and Isenberg, 1958, Edwards and Cobb, 1997). Amyloplasts are responsible for the synthesis and storage of starch granules present in a potato tuber (Wise, 2006). These non-pigmented organelles remain constant when a tuber is found in its natural environment (i.e. underground); however, when exposed to light, the amyloplasts slowly turn into chloroplasts (Anstis and Northcot, 1973). The chloroplasts, used in photosynthesis, then produce Chl under light conditions.

Light exposure also causes an increase in production of glycoalkaloids (GA) and solanine (Dao and Friedman, 1994). An increase in GA and solanine content can both lead to a bitter taste and high levels of GA are also toxic to humans (Friedman et al., 1997, Smith et al., 1996). The guideline for the upper limit of GA content for human consumption is 20 mg / 100g (Omayio et al., 2016). Dao and Friedman (1994) found that there was a 300% increase in GA content which occurred during the greening of cv White Rose tubers, from 2 mg to 6 mg /100g fresh weight. This may still be low in terms of the guideline but different cultivars have shown significant differences in their ability to produce greening-related GA (Griffiths et al., 1998, Percival, 1999, Grunenfelder et al., 2006b). Chl alone does not have a negative effect on the quality of a tuber, however this is invariably used as an indicator that GA may be present in a greater quantity than that safe for human consumption.

1.1.4 Tuber Dormancy

A potato tuber is said to be dormant immediately after harvest. Tuber dormancy is defined as the physiological state in which sprout growth does not occur (Hartmann et al., 2011). Even if a tuber is placed under ideal growing conditions it will not sprout during its dormancy period (Vanderzaag and Vanloon, 1987). The buds, more commonly known as the *eyes*, of a tuber are the locations at which growth occurs. Once the break of dormancy occurs, mobilising energy reserves are transported to and utilised by each developing eye (Coleman, 1987). Viola et al. (2007b) found that once sprouts started to emerge and grow, a sharp increase in both starch and soluble sugars, particularly sucrose

was seen around the eye. As sprouts developed further, the starch and sucrose declined. Once sprouts reached a length of 10 mm starch was undetectable throughout the sprout and glucose became the most abundant sugar. Often the first eye to be released from dormancy is the apical eye. This is usually the largest bud found on the top of the tuber, central to where the eyes are most concentrated. The eyes develop in a spiral arrangement, with increased spacing, moving towards the base of the tuber. The lateral buds are released from dormancy in succession from top to bottom (Harris, 1992). The number and depth of the eyes on the tuber vary depending on the variety (Burton, 1966). Cline (1996) found that the rate of growth per sprout was an inverse function of the number of growing sprouts per tuber and a positive function of tuber weight.

Some researchers have even questioned the concept of tuber dormancy, doubting that there is a period without growth. Burton (1966) stated that whether or not there is growth occurring, the potential for future growth still exists. Davidson (1958) suggested that from the moment of harvest there is never a period where a tuber apical bud is not growing. FIGURE 1:2 shows cross-section images of a sprouted eye and of non-eye location, stained with an iodine solution and observed under optic microscopy.
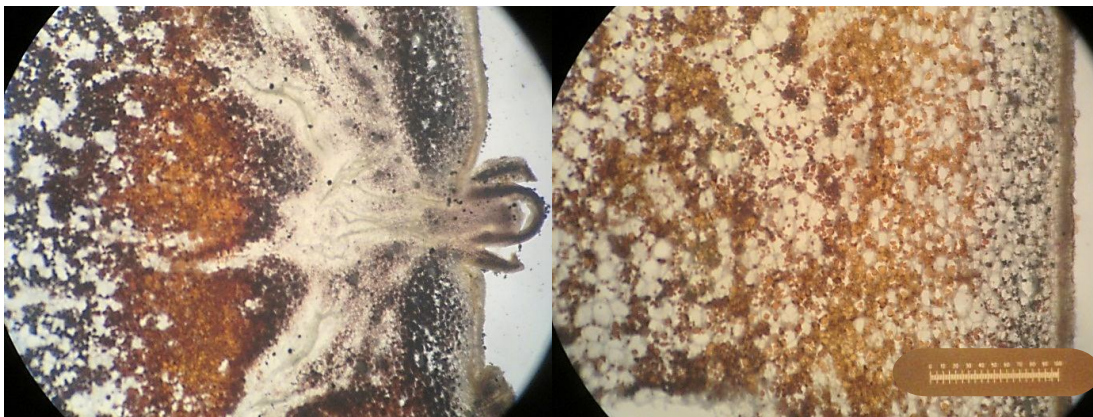
Figure 1:2 Cross sections of a sprouted eye (leftmost) and a non-eye location (rightmost) from a cv Mozart tuber, stained with an iodine solution, viewed under a light microscope. Line gauge is 1 mm in length.

Other researchers have tried to define the end of dormancy. For example, Vanittersum et al. (1992) found that the duration between harvest and visible sprouting was different between two cultivars (Diamant and Desiree), although the estimated time between the onset of sprouting and the sprout growing to 2 mm long was 20 days for both cultivars. Vanittersum suggested that if this period is always similar then it would be good criterion for the end of dormancy.

It is not known what precisely influences dormancy break (Coleman, 1987). A number of research papers have analysed different compositional changes occurring within a tuber during this time, to find their effect on dormancy break (Bailey et al., 1978, Hartmann et al., 2011, Sergeeva et al., 2012, Viola et al., 2007a). For example, De Weerd et al. (1995) found a positive link between electrolyte leakage of a potato tuber and sprouting capacity and suggested a connection between membrane integrity and the onset of sprouting. A review written by Suttle (2004) illustrated that the synthesis and action of hormones such as abscisic acid (ABA) and indole-3-Acetic acid (IAA) are important in the regulation of dormancy within a tuber. Sorce et al. (1996) found that the levels of ABA in extracts taken from a tuber's eyes increased as dormancy ended and sprouting commenced. Sorce et al. (2000) later studied the changing levels of IAA. They found that the highest concentrations were present in the eyes of a tuber and had substantial increases from harvest to the end of dormancy, independent of the storage temperature. Friedman and McDonald (1997) conducted a study investigating the levels of GA within tubers during sprouting; they found that, with the onset of sprouting, GA production was concentrated at the growing portion of the sprout.

More recent studies have investigated transcriptomic changes from tuber dormancy to tuber growth by RNA sequencing. Liu et al. (2015) showed that the changes in gene expression induced, and ceased, several mechanisms during the dormancy progression. For example, they found that genes encoding for key enzymes of starch and sucrose synthase were highly expressed before sprout growth, however after dormancy release genes for sucrose provisions and starch degradation were overexpressed. It was also seen that from early dormancy breaking to sprout growth, genes of Chl a/b binding proteins were highly activated, with more than a 10-fold change. They stated that these overexpressed plastids genes were prerequisites further eye photosynthesis when a tuber was exposed to light.

1.1.5 Potato Storage

The length of dormancy can be affected by several factors including tuber variety, season, growing conditions, and infection (Burton, 1966). Predominantly however, this period is influenced by the postharvest storage conditions. Since British potatoes are only harvested between the months of June and October, a large percentage of tubers must be stored efficiently to ensure there are enough provisions to last until the next harvest. Deterioration, such as premature sprouting or the outbreak of disease, must be minimised to provide seed tubers for the following year's crop; as well as for commercial sales all year round (Lu et al., 2012).

Insulation, ventilation, crate stacking, refrigeration and store monitoring are all storage conditions that must be considered (Cunnington and Pringle, 2008). Overall, the storage conditions are mostly generic; the temperature and application of sprout inhibitors are usually the only factors that are varied depending on the intended purpose and storage length of the crop. The Potato Council have published a Store Managers Guide, written by Cunnington and Pringle (2008), which outlies the important requirements and considerations when setting up and maintaining a storage unit. The following is largely a summary of the key factors.

Storage ventilation is important for maintaining a dry and cool environment. Improper sized spacing between tubers, incorrect placement, unstable conditions, diseases or excess dirt restricts air movement (Kleinkopf et al., 2003). This can cause fluctuations or a non-uniform temperature throughout the tuber store, which in turn leads to "hot spots". Hot spots can rapidly lead to a large pile of tubers spoiling within storage (Olsen et al., 2006). Fans, in conjunction with the crate positioning and designs, are positioned to allow air flow through the crop. This removes crop respiration heat and eliminates temperature variation. Good insulation further aids the aim for a stable environment. It reduces the impact from the outside weather (wind, heat, frost etc).

Potato tubers are made up of approximately 80% water, meaning evaporation from the tuber surface is a major source of water loss (Qiao et al., 2005b). It has been established that a relative humidity of 98% is needed to maintain an equilibrium in moisture exchange between the surrounding air and the tuber at 4 °C (Cunnington and Pringle, 2008). Water loss means a decrease in marketable weight; maintaining a high humidity is therefore important in a commercial store. The only time the relative humidity may be adjusted is immediately after harvest. Hide and Boorer (1991) found that by drying the tubers at a relative humidity of 80%, compared to 95%, the severity of several diseases was reduced. Dark storage is also important for maintaining the quality of the crop. As previously discussed, the presence of light stimulates the production of Chl and accelerated that of GA (Dao and Friedman, 1994, Kozukue et al., 2001).

During the harvest, tubers can suffer mechanical damage. Bruising, wounds and broken skin can be caused by the machinery used and are all a basis for rejection from the commercial markets. Wounds also allow fungi and bacteria to develop in the flesh of the tuber (Hide and Cayley, 1987). To overcome this, the temperature of the storage units is kept at 15-20 °C for the first two weeks. This is done to promote wound healing (Wang

et al., 2015). Following this, the temperature is brought down slowly by 0.5 °C each day, before reaching the desired storage temperature. This procedure is known as 'curing'.

The final temperature largely depends on the intended use for the crop: processed, fresh or seed. For fresh 'table-top' or seed tubers, the temperature tends to be kept below 5 °C, to prevent dormancy break for as long as possible (Knowles and Knowles, 1990). However, tubers intended for processing (in particular, frying) must be kept in a warmer enviroment. As already discussed, temperatures below 10 °C can cause sweetening, and during frying these simple sugars react with amino acids. This in turn causes undesired browning, off-flavours and the formation of harmful compounds such as acrylamide (Amrein et al., 2003). It is important to strike the right balance between the quality of the stored tubers and the eventual safety of the final product. Therefore, other factors such as the tuber variety, length of time in storage, and the application of any sprout suppressant must be taken into account when storing potatoes for this purpose (Burton, 1966).

1.1.6 Inhibiting Sprout Growth

When the period of dormancy ends, the eyes on the tuber start sprouting. The main eye is usually the first to start showing sprout growth, followed by the remaining buds in a downward direction from the top. Premature sprouting causes weight loss and reduced tuber quality, resulting in a reduction in commercial value (Kleinkopf et al., 2003, Lu et al., 2012). Past studies showed that the storage temperature is the most influential factor on the period of tuber dormancy (Sonnewald, 2001, Shin et al., 2002, Davidson, 1958). Vanittersum and Scholte (1992) found that changing the storage temperature from 18 °C to 28 °C reduced the dormancy by up to 45 days.

In addition to low temperatures, many physical and chemical treatments have been tested for the suppression of unwanted sprouting. One of the main methods is post-harvest applications of isopropyl N-(3-chlorophenyl) carbamate (chlorpropham or CIPC), which works by interfering with cell division (Lu et al., 2012). It is applied as a thermal fog which deposits small particles of CIPC on the tuber surface, which then diffuses into the soft sprout tissue as soon as it forms. Today, the application of CIPC can successfully enable potato tubers to be stored for up to 10 months (Kleinkopf et al., 2003). CIPC has been used worldwide for a number of decades; however, concerns regarding the health and safety of the metabolites of this compound have led to the introduction of a legal dose restriction in several countries including the UK (Vijay et al., 2018). Although alternative sprout suppressant treatments are available in the UK, CIPC

is generally used as it is cost-effective and efficient in storage treatment. However, there is a current concern that severe constraints or withdrawal of CIPC could occur if members of the industry do not follow the stewardship guidelines and be CIPC compliant (Storey and Briddon, 2018).

Exogenous ethylene, maleic hydrazide and spearmint oils are alternative sprout inhibitors used in the UK (Storey and Briddon, 2018). Although the hormone ethylene has been shown to initiate dormancy break, it was also found that a continued application of this hormone inhibits sprout growth (Hartmann et al., 2011). Plant oil extracts are still being evaluated today. Gomez-Castillo et al. (2013) analysed the effectiveness of a high concentration treatment of peppermint and coriander essential oils as a replacement for CIPC. The study found that these oils had a control of 65 - 95% for sprout suppression compared to CIPC. Further analysis also revealed that there were no changes in taste and appearance between treated and untreated tubers.

It is worth noting that sprout inhibitors are not guaranteed to work; incorrect or late application can still fail to stop unwanted sprouting (Kleinkopf et al., 2003). Also, due to the nature of CIPC, it prevents wound healing if applied too early in storage. Although there have been many studies carried out to find the dependence and optimal levels for certain conditions in storage and sprout inhibiting compounds, a significant percentage of potato crops are affected by premature sprouting every harvest year (Suttle, 2004).

1.2   FOOD QUALITY AND SAFETY CONTROL

Optimising crop yield is a crucial objective for agriculturalists (Evans, 1996). With recent developments in analytical instrumentation and computer technology, there has been an increasing amount of research in techniques for measuring food quality and safety, and consequently industrial application (Huang et al., 2014).

Food quality can be defined in several ways: physical attributes such as colour, texture and firmness, chemical attributes including moisture, component content and pH, as well as biological attributes such as disease (Huang et al., 2014). Typically, these three components are monitored using analytical techniques. Experimental techniques such as mass spectroscopy and high-performance liquid chromatography have been used previously; however these are expensive, destructive and time-consuming (Gowen et al., 2007). Human visual inspection is often therefore used as an alternative, but although fast and affordable, this method is subjective, laborious and inconsistent. In addition,

human inspection cannot give a chemical assessment of the crop. Due to the drawbacks to both approaches, there is a growing demand for techniques that could perform the required assessments more effectively, non-invasively and at low-cost. Therefore, many researchers have been working to find techniques to meet these needs, for evaluating the internal and external properties of various fruit and vegetables (Hakim et al., 1997).

As previously discussed, if a potato crop sprouts prematurely it must either be discarded or sold for a different and usually less profitable purpose. In recent years, increasing restrictions on the leading sprout suppressant CIPC make unwanted sprouting harder to control (Vijay et al., 2018). In the light of these two concerns, it would be beneficial if an analytical technique could be used to monitor the progression of dormancy within a potato tuber and hence reduce the amount of post-harvest loss. It could provide the means of assessing whether the storage conditions are effective, determine a retail order for the stored tubers or indicate when the use of a sprout suppressant would be most effective. An instrument that could inform store managers the duration of time until the potato crop will start sprouting would be a highly desirable crop management tool. The main aim of this thesis is to confront the unsolved problem of predicting the onset of dormancy break in stored potatoes.

MATERIALS AND METHODS

2.1 THE FUNDAMENTALS OF OPTICAL SPECTROSCOPY

Spectroscopy describes the interactions between radiation and matter. Spectroscopic analytical methods are based on measuring the amount of absorption, reflectance, emission or scattering of radiation by the species of interest (Solé et al., 2005). Different spectroscopic methods are characteristic to a specific region of the electromagnetic spectrum. Optical spectroscopy often refers to methods involving the absorption of Ultraviolet (UV), Visible (Vis) and Infrared (IR) radiation (Svanberg, 2012). The nature of the species of interest in these cases are electrons (in UV and Vis) and molecular bonds (IR), as described in the following section.

At room temperature, most species are found in their lowest energy state, known as the ground state. The stimulus of an absorbed external radiation can cause transitions from the ground state to a higher-energy level (Skoog et al., 2013). The fraction of radiation that is absorbed at a specific wavelength corresponds to the energy change needed for a transition to take place between the two states (Young et al., 2004). Molecules can undergo three types of transitions: electronic, vibrational and rotational, depending on the source of radiation used. An electronic transition involves the promotion of an electron between two energy levels. These transitions can be seen by UV and Vis spectroscopy (Skoog et al., 2013). Whilst IR radiation causes transitions to occur between two discrete vibrational states, rotational transitions involve a sudden change in angular momentum. The energy differences among the rotational states are considerably smaller than those among the vibrational states (Skoog et al., 2013).

Every molecular species can absorb its own characteristic frequencies of radiation, according to specific bonding characteristics within the molecule (Skoog et al., 2013). The transmittance (T) of a species is the fraction of incident (I_0) and transmitted (I) radiation from a sample, $T = I/I_0$. The absorbance (A) is related to the overall transmittance in a logarithmic manner, as shown by the EQUATION 2:1 below (Svanberg, 2012). The amount of light absorbed is dependent on the concentration (c) of the absorbing species and the path length (l) over which the transmission of radiation occurs, as well as the molar absorptivity constant (ε) of the species. This is the Beer-Lambert Law, and it can be used to quantify the concentration of the absorbing molecule (Beer, 1852).

Equation 2:1 Beer-Lambert Law.

$$A = -\log\left(\frac{I}{I_0}\right) = \varepsilon lc$$

The basic instrumentation used for spectrometric measurements includes an appropriate source of radiation, a dispersive element of some kind (e.g. a monochromator) and a detector. Absorption spectrometers require a broadband source that radiates energy over the entire bandwidth of interest, without gaps caused by emission lines or self-absorption (Alpert et al., 2012).

The transmitted radiation, either scattered or reflected, is recorded against wavelength. To do this, the transmitted radiation has to be separated in some manner so that selected frequencies corresponding to particular energy transitions can be examined (Fifield and Kealey, 1995). In dispersive spectrometers, this subunit is referred to as the monochromator. Light entering the monochromator is directed through a thin slit onto a dispersing element, such as a prism or diffraction grating. Rotating the dispersion element causes the incident light of narrow bandwidths to be successively passed through an exit slit, onto the detector (Alpert et al., 2012). The achievable resolution (size of the bandwidths) is dependent on the size of the exit slit (Skoog et al., 2013). The radiation collected by a detector will have a varying intensity of the radiation at different wavelengths (Osborne and Fearn, 1986). The final absorption spectrum can provide both quantitative and qualitative results.

Fibre-optics are an alternative to conventional samplers (such as a sampling table) and are largely used in analytical science due to accessibility. Optical fibre technology is used to transmit electromagnetic radiation to and from a sample (Arnold, 1992). Fibre-optics can enable optical spectroscopy to be performed over longer distance, or even on several spots along the fibre (Wolfbeis, 2008).

2.1.1 Near-Infrared Spectroscopy

Infrared radiation was first discovered by Sir Friedrich Wilhelm Herschel in 1800 (Bauman, 1962). Herschel was measuring the individual temperatures of visible light when passed through a glass prism to produce a spectrum. To his surprise, he found the greatest temperature to be just beyond the red portion of the spectrum (the thermometer was meant to be used as a control to measure room temperature). Additional experiments concluded that an invisible form of light extended beyond the visible spectrum. The development of instrumentation and industrial application of IR spectroscopy did not occur until the 20th century (Scotter, 1990). Newer IR

spectrometers based on Fourier transformation of interferograms contain no dispersive element and are able to detect and measure all wavelengths simultaneously (Skoog et al., 2013).

Near-IR (NIR) describes the portion of the electromagnetic spectrum closest to the visible region, ranging from 780 to 2500 nm. As discussed above, IR can be used to excite molecules into different vibrational states. Specifically, however, NIR causes overtone and combination vibrations to occur within a sample (Bellon-Maurel and McBratney, 2011). Different energy levels are labelled by integers known as quantum numbers: v is the vibration quantum number which can take the value of 0, 1, 2, and so on. According to selection rules, transitions are only allowed when the energy state changes by one ($\Delta v=\pm 1$); these fundamental transitions are detected by Mid-IR (3000 - 5000 nm) (Osborne and Fearn, 1986). However, transitions called overtones, when $\Delta v=\pm 2, \pm 3$, etc., can be observed in NIR spectroscopy. As these transitions are forbidden by the selection rule above, they are observed at a much lower intensity than the fundamental vibrations. Combinations of fundamental bands are also seen, if two or more transitions occur simultaneously (Osborne and Fearn, 1986).

NIR spectroscopy is a low-cost and easy to use analytical technique that does not generally require complicated preparation steps involving chemicals or reagents, it can be performed by an untrained person or automated by a computer to take measurements mechanically. As a consequence, NIR spectroscopy has been applied to a number of different fields, including agriculture, pharmaceutical and material science (Huang et al., 2014, Nicolai et al., 2007). Norris (1964) first used the technology in agricultural application, measuring the moisture in grain. Following this, further application has shown that Visible/Near-Infrared (Vis/NIR) spectroscopy can be used for multi-constituent analysis, such as internal damage of apples (Clark et al., 2003) and colour changes in grapes (Cozzolino et al., 2004). Therefore, the use of NIR spectroscopy in agriculture has increased dramatically in last 50 years, focusing on measuring the composition and developments of food such as fruit, vegetables and meat (De Weerd et al., 1995, Bellon-Maurel and McBratney, 2011). For example, Schmilovitch et al. (2000) used NIR spectroscopy to calibrate a model of the post-harvest relationships between the storage period, firmness, sugar content and acidity of the mango fruit, and Peirs et al. (2001) used NIR spectroscopy to analyse the optimal picking dates of the apple fruit by the correlation between firmness and acidity.

2.1.2 Hyperspectral Imaging

The appearance of food is the primary assessment made by consumers. With advances in computer and optical sensing technology, Red-Green-Blue (RGB) colour vision systems were developed to act as a grading operations in food quality control (Gowen et al., 2007). For instance, Leemans and Destain (2004) found RGB could be used to find segment defects on apples, whilst Sarkar and Wolfe (1985) were able to used colour as an indicator of tomato maturity. However, RGB has a major weakness in that it is not sensitive to wavebands other than RGB. Recognising there was a need for acquiring images over the entire Vis and NIR range, systems of multispectral and hyperspectral imaging were developed.

Multispectral imaging combines images acquired from a few narrow wavebands, sensitive to features of interest. Hyperspectral imaging (HSI) is the latest evolving technique that combines imaging with spectroscopy, such as NIR, to obtain spectral and spatial information from an object over the Vis and NIR regions (Gowen et al., 2007). Hyperspectral images are three-dimensional data cubes that comprise a spectrum (or collection of consecutive wavebands) for each spatial position. The images can be collected by area, point or line scanning. Line scanning is most commonly used in food analysis, due to the fact that lines of pixels can be collected at the same time, similar to what may happen on a conveyer belt (Wang and Zhao, 2016). Reflectance or transmittance data can be collected by HSI systems. To acquire transmittance spectra, samples must be prepared thin enough to allow the light to pass through the sample. Reflectance spectra however, can be collected using thicker samples, meaning food materials may be analysed whole (Huang et al., 2014).

One of the first applications of HSI was by Goetz et al. (1985) in remote sensing of the earth's surface. As the interest and research into HSI increased, it has more recently been demonstrated that it can also be adapted into a multi-constituent analytical technique for food analysis. For example, Arianna et al. (2006a, 2006b) showed that HSI could be used to distinguish apples with surface defects such as bitter pit, black rot and decay, as well as segregating bruised pickling cucumbers from normal cucumbers. Yao et al. (2013) used HSI to detect toxigenic strains in contaminated maize kernels, and more specifically, Qiao et al. (2005a) used HSI to predict the water content of potatoes using the wavelength range 934-997 nm.

2.1.3 Ultraviolet Spectrophotometry

Spectrophotometry is another absorption spectroscopy technique that is used to record the spectral variation of energy transmitted, generally through a sample in solution. As already discussed, UV/Vis incident radiation can cause electronic transitions from the ground to an excited state. UV/Vis spectrometry is highly sensitive; dilute solutions of the analyte are often used for qualitative analysis. An appropriate solvent must be selected by ensuring that the solvent is transparent, able to dissolve a sufficient amount of the analyte and will not interact with the sample (Skoog et al., 2013). A polar solvent for example, may shift the position of the absorption maximum. Therefore, non-polar solvents such as cyclohexane are often used.

UV/Vis photometry are analytical techniques that can also be used in the assessment of food quality. Zalacain et al. (2005) developed a screening method for the detection of artificial colours in saffron, whilst Guimet et al. (2004) were able to use UV/Vis to discriminate between virgin and non-virgin olive oils. This technique can also be used for quantitative analysis by comparing the absorbance of standards and samples at selected wavelengths (Fifield and Kealey, 1995). For example, Belay et al. (2008) showed that UV/Vis spectroscopy could be used to quantify the content of caffeine in coffee beans. Often a wavelength can be found at which the chosen analyte alone absorbs; therefore, the species absorption maxima are often selected for quantitative analysis rather than collection of a full spectrum (Skoog et al., 2013). This also means that it is possible to analyse a specific component in a mixture if another species present is not interfering.

2.2   DATA ANALYSIS

Spectral pre-processing techniques are used to mitigate unnecessary information that will interfere with subsequent data analysis. Spectral averaging, smoothing and normalisation were all used during the data analysis of this project. When the single-beam spectra are referred to as *raw* then the pre-treatment calculations have not yet been performed.

Smoothing can be used to remove random noise from the spectra; if needed, the Savitzky-Golay algorithm was used when handling the data in this thesis. This algorithm fits a polynomial through successive sub sets of neighbouring data points. The resulting smoothed values are moving values of each polynomial (Savitzky and Golay, 1964).

To follow, normalisation is used to reduce the variation in spectra due to unwanted sources of variance, such as physical sample differences (size, colour, shape, texture etc.), light scatter and instrumental factors. There are several methods used for this. Standard Normal Variate (SNV) was often found to be the most effective way of normalising the data and therefore was set as the standardised method of pre-treatment for the data contained in this thesis. SNV, described by Barnes et al. (1989), normalises each spectrum to zero mean and unit variance. The defined equation can be seen in EQUATION 2:2, where x is the row vector containing the original spectrum and z is the SNV - transformed spectrum (Guo et al., 1999). The main difference between SNV and other commonly-used standardisation methods such as multiplicative scatter correction, is that it is carried out on individual samples, instead of the whole data set (Næs et al., 2002). As spectra treated by SNV are mean zeroed before further analysis the spectra were baseline corrected to zero. A mean spectrum, of any replicates, was always calculated after normalisation.

Equation 2:2 Standard Normal Variate (SNV) normalisation.

$$z = [x - \text{mean}(x)]/\text{std}(x)$$

The generalised logistic function, also known as a Richards curve, was used to fit data in this project. Extended from the logistic function, it is a flexible sigmoid function developed for growth modelling (Richards, 1959). The rate of growth first increases from a low value until reaching a maximum after which it decreases towards zero at the upper asymptote of the growth curve (Birch, 1999). See FIGURE 2:1 are an example.
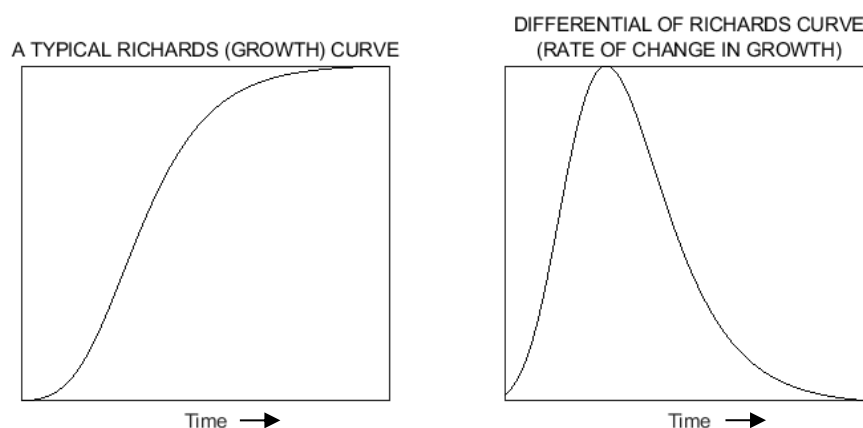
Figure 2:1 Richards growth curve example, and it's differential.

SHORT TERM EXPERIMENTS

3.1 INTRODUCTION

As previously highlighted, Visible/Near-Infrared (Vis/NIR) spectroscopy has been widely used and successfully implemented throughout the agricultural industry. The number of Vis/NIR studies carried out with a focus on the potato (*Solanum* tuberosum) tubers is small; one of the most researched areas within this field are studies investigating certain characteristics of starch. Potato starch is often used for culinary and non-culinary purposes, because it is cheap and readily available (Vansoest et al., 1994, Kizil et al., 2002). At the time of writing, there are no studies that discuss the use of NIR spectroscopy in either monitoring tuber dormancy or investigating differences between the eyes and surrounding surface areas of a tuber. One study was found on the topic of sprouting: Jeong et al. (2008) determined that NIR spectroscopy could be used to find an optimum planting date by predicted the sprouting capacity of potato tubers. This was done by scanning the tubers with NIR spectroscopy and then measuring the sprout weight after 30 days incubation.

One industrial application that has been previously discussed uses machine vision as an alternative to manual sorting in the potato packaging industry. An early study showed that a computer-based vision system could be used to classify tubers regarding their weight, diameter, shape and colour. Combining these four criteria, Zhou et al. (1998) found an overall success rate of 86%. Su et al. (2014) used Vis/NIR hyperspectral imaging and an established online non-destructive testing method to classify tubers with external defects. They achieved a 96% recognition rate of six different defect types found on a tuber surface. Most recently Ming et al. (2018) looked at creating a vision system to detect sprouting in potatoes. They found that their method could achieve an accuracy rate of 90%. The three studies all concluded that machine vision could be used as a useful alternative to manual sorting in the packing industry. However, the issue here is that the detection happens beyond the point where the tuber has changed with the onset of sprouting; that is, the reduction in quality has already begun.

At the start of this project, a series of short-term experiments were conducted to investigate the response of a tuber's eye to Vis/NIR spectroscopy. Subsequently, experiments were undertaken to look at the difference in the profile of a tuber's eye and its surrounding areas. These surrounding areas, i.e. surfaces of the skin that are without an 'Eye', will be referred to as the 'Background'. This comes from the use of these areas

as a reference for the Eye spectra – this will be discussed further in this chapter. Within this thesis, specific eye or background areas used for data collected, can be recognised by its capitalisation. For example, "the buds on tubers may also be referred to as eyes", compared to "the Eye was analysed for 24 hours". Similarly, the analysis methods listed below will also be capitalised for easy identification.

The purpose of these experiments was to investigate issues connected primarily with the measurement process and issues encountered when collecting spectral data from a tuber skin surface. Over the subsequent project years, further and sometimes replicated experiments were conducted to understand the difficulties in the acquisition of data and to ensure the most effective analysis methods were implemented. This chapter focuses on and explains the reasons behind the standard protocol before moving on to investigate implementations of the industrial application in the next chapter.

3.2   EXPERIMENTAL PROCEDURES FOR SHORT TERM EXPERIMENTS

3.2.1 Sample Collection, Harvest and Storage

Tuber samples of different cultivars (cvs), skin types, harvest seasons and suppliers, are all used in this chapter. Tubers that had been in storage for varying lengths of time were also used. Tubers may have either been freshly harvested, kept in cold storage or shop bought. If the tubers were cold stored, they would have been kept in dark, ventilated units at a temperature between 4 – 6 °C ('cold storage') and a relative humidity of 80 – 90%. For the shop bought tubers, their previous storage conditions were unknown. However, it would be expected for them to be stored in a similar environment, at least until transport to the retailer, as this is the common primary method for prolonging tuber lifespan. These details are given in TABLE 3:1 and TABLE 3:3, referencing the figures shown in this chapter. Tubers were cleaned with a brush or air gun to remove excess dirt before analysis. Analysis was conducted at room temperature in an air-conditioned laboratory (nominal 21 °C, 50 – 60% RH) under artificial ambient lighting with fluorescent light tubes (270 Lux). This is true for all experiments conducted in the Norwich Laboratory.

3.2.2 Spectral Acquisition

The spectrometers

Two StellarNet (StellarNet, Inc., Tampa, Florida, USA) spectrometers were used to collect the data shown in this chapter. The EPP2000-NIR-200 and Black-Comet CXR-SR-50

spectrometers had wavelength ranges of 500 – 1100 nm and 200 – 1100 nm respectively. The light source was a Tungsten/Halogen lamp with 200 Watts/m² output, colour temperature 2800 K. Both spectrometers were equipped with a Vis-NIR silica fibre-optic reflectance probe. The light intensity at the tip of the fibre-optic probe (without laboratory lights) was measured as 459, 442, 419 and 401 Lux (J/m²) for 0, 1, 2 and 3 mm distance respectively. Depending on the experiment, each measurement was the average of 50 or 100 scans, collected with an integration time of 20 – 30 ms.

Protocol for Data Collection

The fibre-optic probe and tuber were separately clamped into a position where the probe was oriented perpendicular to the tuber's surface. The distance between the tip of the probe and the tuber's surface was approximately 3 mm. Before each data collection, this distance was adjusted slightly to achieve the best signal, without saturating the detector. A picture of this experimental set up can be seen in FIGURE 3:1. Single time-point spectra and spectra time series were collected using the StellarNet Spectra Wiz software and saved as ASCII files.

3.2.3 Data Analysis

All data processing and visualisation was carried out in MATLAB (The MathWorks, Inc., Natick, MA, U.S.A.) with the Statistics and Machine Learning Toolbox installed. **Unless referred to as 'raw' data, the collected single beam spectra were Standard Normal Variate (SNV) normalised with an offset baseline equal to zero. These spectra are referred to as pre-treated spectra**. Each method of data analysis will be discussed in full throughout this chapter. APPENDIX 1 contains the script written and used to analysis and display the data contain in this chapter. This is an example of the type of scripts that were written for subsequent chapters.

3.3   RESULTS AND DISCUSSION

3.3.1 Single Beam Spectra

The picture in FIGURE 3:1 shows the set-up for data collection. Both the probes and tuber were clamped into a fixed position. Here the probe in the top left corner was set up to interrogate an Eye, whilst the probe in the right of the picture is positioned over an area without an Eye, which is referred to as the Background. This figure shows the typical Eye and Background single beam spectra, after SNV correction and collected from a single white tuber. Williams and Norris (1987) reported that the diffuse thickness relating to

NIR spectroscopy for tuber flesh is 3.7 mm; hence the signal collected by the fibre-optic probe is a measure of the tuber tissue under the skin. Overall the spectra look very similar; the slight difference in signal intensity around 750 nm is known to be due to minor differences between the fibre-optic probes. Although the two probes used throughout this project are made of the same materials, one is simply older and has been handled more than the other; over time this has affected its throughput.

The data were collected as single-beam spectra only, for two main reasons. The first was to simply save time; by not acquiring additional reference spectra (for example a dark current spectrum before each tuber spectrum) it meant that twice the number of measurements could be collected during the same analysis period. Under a certain experimental design, it also meant that movement of the probe was not needed between measurements of the same area. This avoided the introduction of error from changes in the position of the probe with respect to the position on the tuber being analysed. Repositioning errors and handling of the single beam spectra are discussed in more depth later in this chapter.
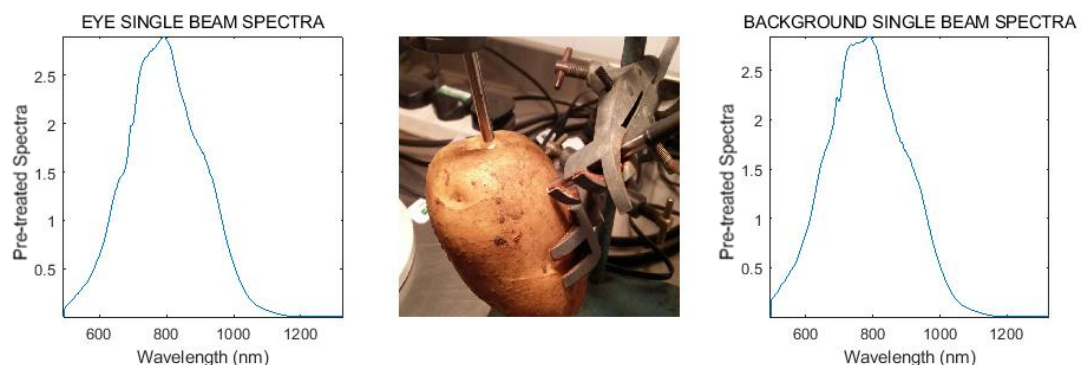
Figure 3:1 Experimental set up and single-beam spectra collected from an Eye and Background area of a tuber. The picture displays how data collection was set up and the plots either side give an example of the spectra collected from the two positions.

3.3.2 Static Series Measurements

The very first and most simple experiment conducted was a time series analysis which monitored a tuber's eye during light exposure. Vis/NIR spectra were recorded at regular time intervals over an extended period while the tuber was exposed continuously to light from the spectrometer source as well as from the laboratory lighting. During this experiment, the probe and tuber were clamped in place throughout, hence the 'Static'

terminology. This experiment has been repeated several times over the four harvest years studied during this project.

FIGURE 3:2 to FIGURE 3:6 show examples of the data collected from several Static Series, collected from different cultivars sampled from different harvest years. During a Static Series, the spectral data were collected every 15 - 60 minutes, over a period of one to four days. The leftmost plot of the figures contains the raw single beam spectra. The overall shape of the single-beam spectra differs for the five tubers, partly because of the different spectrometers and light sources used for the data collection in these experiments. The two Vis/NIR spectrometers can be identified by the wavelength range of the spectra displayed; either 500–1100 nm or 400–1100 nm. Despite the use of different spectrometers, the key feature revealed by all Static Series is a broad absorption band seen between 660 and 700 nm. This can be explained by the production of Chlorophyll (Chl), predominantly Chl-α, which exhibits absorbance peaks at ~475 and ~675 nm (Petermann and Morris, 1985, Friedman and McDonald, 1997). FIGURE 3:2 to FIGURE 3:6 indicate that Chl production has been stimulated in the potato tuber's skin surface and that it can be readily detected using Vis/NIR spectroscopy. Because the 475 nm band is beyond or at the limits of the peak sensitivity region, it is not as useful for identifying the presence of Chl. Therefore, throughout this work, the 675 nm band will be referred to as the Chl band. The colour gradient used in the plot, from dark to light blue, represents the time series from the first to last spectrum recorded. This colour scheme has been used to depict the progression of time throughout this thesis. It should be noted that the single-beam spectra within these plots were pre-treated using SNV normalisation.

To generate an absorbance spectrum, a series of single beam spectra taken from a given position on a tuber's surface are divided by the first spectrum in the series (T_i/T_0). Throughout this thesis these are referred to as 'Kinetic' spectra. The reflectance spectra are then converted to absorbance spectra by taking the $-\log_{10}$. Kinetic Chl Bands refers to the extracted region of the Kinetic spectra between 620 and 720 nm. The region of the Chl Bands could then be integrated to give the corresponding Kinetic Chl Areas. Anchor points either side of the band, at 655 nm and 700 nm, were first used for a baseline correction for the peak before integrating the area. This then highlights the changes manifested by only the Chl peak in the single-beam spectra, over time. A list of the data analysis terms can be found in CHAPTER 10 to be referenced as needed through the remainder of this thesis.

The central plots in FIGURE 3:2 to FIGURE 3:6 show the Kinetic Chl Bands calculated from the single-beam spectra displayed in the first plot. As an example, FIGURE 3:2 shows the results of a Static experiment conducted on a cv Maris Piper tuber from the harvest 2014. The leftmost plot shows the series of single beam spectra collected over the ~30 hours analysis period. The central plot shows the Kinetic Chl Bands calculated by referencing all the spectra collected in the series against the first single beam spectrum. The colour gradient, within the leftmost and central plots of each figure, clearly shows the increases in Chl absorbance as a function of time. Previous studies have shown that tubers exposed to light produce Chl in increments of $\mu g/cm^2$ from several days of irradiation (Petermann and Morris, 1985, Grunenfelder et al., 2006a). The results obtained therefore imply that Vis/NIR spectroscopy is sensitive to small changes in the presence of Chl. Chl is most concentrated in the outermost few millimetres of the tuber; this is why it causes surface greening (Gull and Isenberg, 1960). However, it should be noted that Vis/NIR spectroscopy can detect the presence as well as changes in Chl concentration long before the tuber turns visibly green; according to Grunenfelder (2005) greening scales, these tubers would be graded no higher than a 2.

To reiterate, the tubers analysed for these Static experiments were of various cultivars sampled over the four harvest years. Parameters which also varied were the supplier from which the samples were collected (grower or shop), and the time that had elapsed between the beginning of cold storage and when the tuber was analysed. These details can be found in TABLE 3:1. It should be noted that the cold stored tubers would have been removed from the dark immediately before analysis; the shop bought tuber, however, would have been exposed to light and warmer conditions for an unknown length of time before analysis.

Irrespective of tuber, there is a consistent trend shown by the Kinetic Chl Areas of FIGURE 3:2 to FIGURE 3:6. A 'lag phase' can be seen at the beginning of the analysis, followed by a gradual increase in the rate of change until it reaches a steady state (constant gradient), followed in some cases by a decrease in the gradient towards the end of the analysis period. For example, the rightmost plot of FIGURE 3:2 shows that after an initial lag phase of approximately five hours, the rate of Chl production increased exponentially between measurements until approximately hour 10, by which time it reached a steady state that continued until the end of the 24-hour analysis period. An extremely similar result in other cultivars is seen in FIGURE 3:3 and FIGURE 3:4. This lag phase specific to potato tubers has previously been recorded by Anstis and Northcot (1973) and Morris et al. (1979) who reported lag phases of 23 and 19 hours respectively. It is known that upon

light activation, it is the phytochromes that control many aspects of Chl synthesis occurring in plants (Kaiserli and Chory, 2015). This can explain the delayed response of Chl production after exposure to light. The length of the lag phases differs however, between the five Static experiments shown. FIGURE 3:3 and FIGURE 3:6 display a particularly short lag phase. Arguably this is as expected, since these tubers were purchased from a supermarket and previous exposure to light would have already initiated the production of Chl. FIGURE 3:5 shows a lag phase twice as long as seen by the tubers in FIGURE 3:2 and FIGURE 3:4 (all cold stored tubers). Note that the cv Royal tuber analysed (FIGURE 3:5) was stored for a considerably longer time than the other two.

FIGURE 3:5 and FIGURE 3:6 show the results of Static experiments monitored for almost four days. The Kinetic Chl Areas calculated from these experiments differ from the previous three results due to a decrease in the rate of Chl production after 40 - 50 hours of analysis. A possible explanation for this may be that it is due to stress damage caused by long-term low temperature storage. Bianchi et al. (2014) found that sub-freezing temperatures caused damage to the photosynthetic apparatus of intact potato leaves after only hours of exposure. Gull and Isenberg (1960) found that tuber greening was significantly less after eight months of storage at 4 °C in comparison to tubers stored for 3 months. The Static experiment conducted on a cv Cultra tuber (FIGURE 3:4), which was analysed soon after harvest and therefore had not been exposed to cold storage, did not show signs of this asymptotic phase even after 50 hours. Gull and Isenberg (1960) also saw a decreased rate of Chl production in irradiated tubers after 96 hours. They suggested that this could be explained by an increased respiration rate, rapidly occurring at room temperature after removal from cold storage, which then declined to a relatively low steady rate. However, this would not explain the behaviour of the shop bought tubers, as these tubers would have already equilibrated to room temperature.
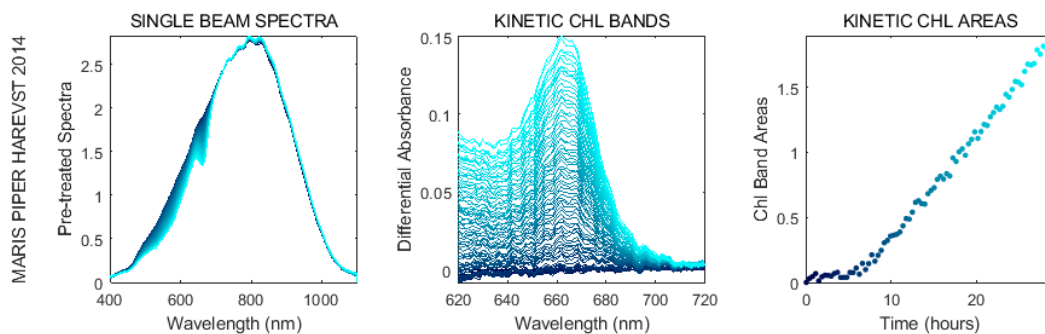
Figure 3:2 Static Series experiment repeat one. cv Maris Piper tuber, harvested 2014.
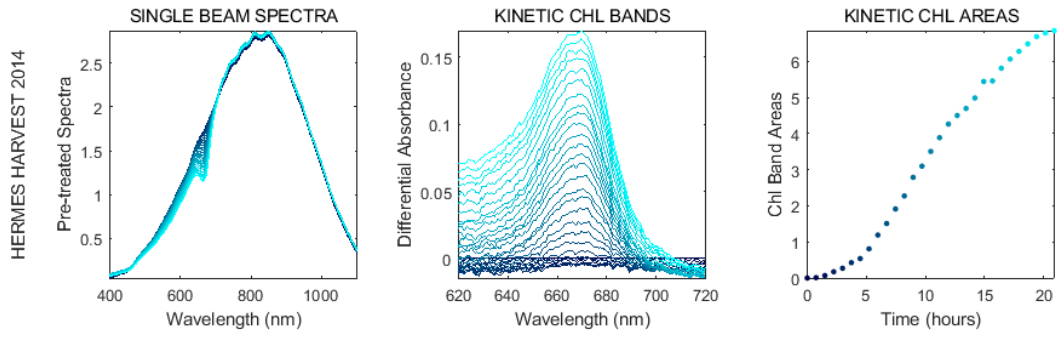
Figure 3:3 Static Series experiment repeat two. cv Hermes tuber, harvested 2014.
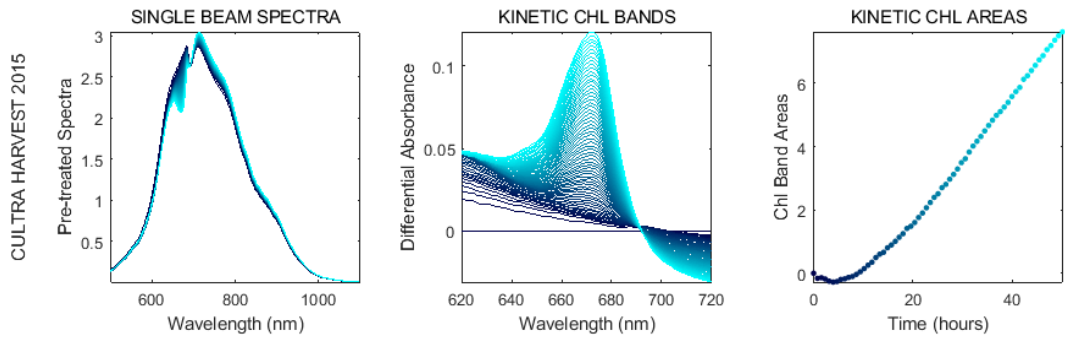
Figure 3:4 Static Series experiment repeat three. cv Cultra tuber, harvested 2015.
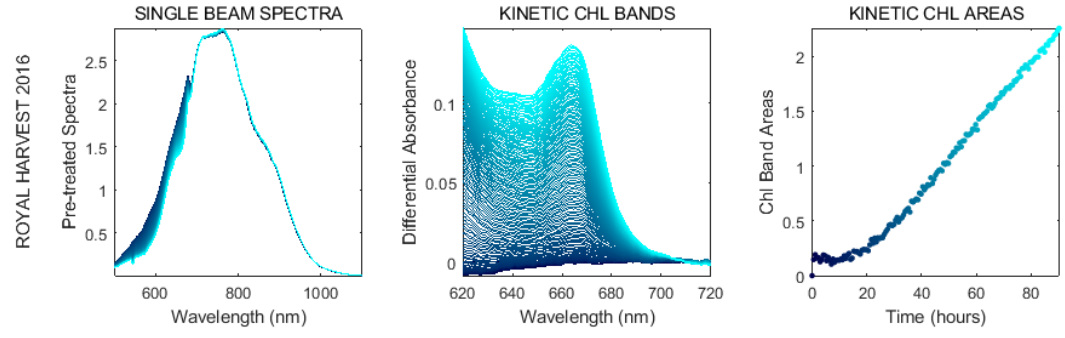
Figure 3:5 Static Series experiment repeat four. cv Royal tuber, harvested 2016.
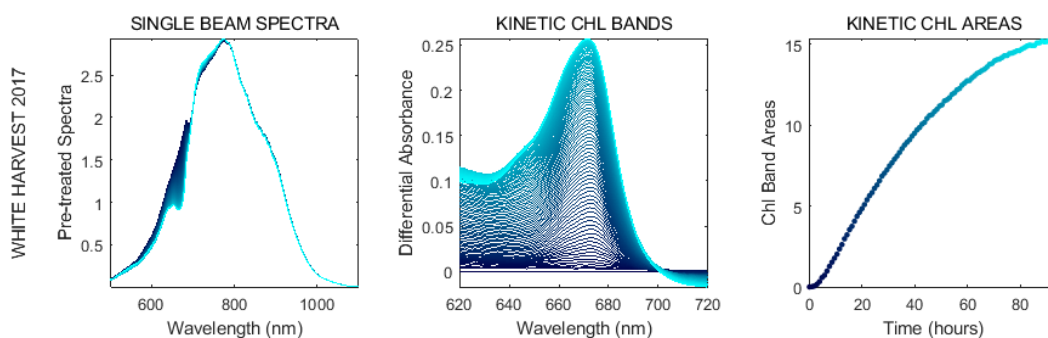
Figure 3:6 Static Series experiment repeat five. White tuber (cv unknown), harvested 2017.

Table 3:1 Details of the Tubers used for the Static Series experiments, Figures 3 – 9.

FIGURE	CULTIVAR	SUPPLIER	HARVEST YEAR	STORAGE TIME
Figure 3:2	Maris Piper	G's Fresh, UK	2014	2 months
Figure 3:3	Hermes	Shop bought, UK	2014	~ 4 months*
Figure 3:4	Cultra	Country Crest, Ireland	2015	N/A
Figure 3:5	Royal	Sutton Bridge, UK	2016	9 months
Figure 3:6	Unknown (white)	Shop bought, UK	2017	~ 5 months*
Figure 3:7	Orchestra	Produce World, UK	2017	5 months
Figure 3:8	Orchestra	Produce World, UK	2017	5 months

* Storage time of the shop bought tubers is a presumption, due to the unknown information of when the tubers were put into storage. It was based on the tubers being lifted during September and put into storage beginning of October. Tubers lifted during this time are known as Maincrop potatoes, this is the most common time for lifting fresh/pre-packed potatoes.

A Static Series experiment was also set up to investigate the Chl production occurring in a tuber when exposed to light and dark cycles. With the tuber and probe clamped throughout, spectra were recorded every 30 minutes for a period of five to six hours, each day for three consecutive days. The spectrometer source was only turned on during spectral measurements. During the analysis periods, the tubers were also illuminated by the laboratory lighting; outside these periods, the lab lights were turned off and the tubers were left in darkness. FIGURE 3:7 shows the results of this experiment as shown by the Kinetic Chl Bands and corresponding Kinetic Chl Areas, for a single cv Orchestra tuber. Once again, the gradient of dark to light colour represents the first to last spectrum

recorded in a single day, but here the three days are displayed in different colours. The Kinetic Chl Areas demonstrate a high sensitivity of the Chl response to the presence of light. After the initial lag phase, the results suggest that some Chl is produced throughout the experiment including when all light sources are removed, although the rate of production is greatest during the periods of illumination. It is established that Chl cannot be produced without the presence of light (Dao and Friedman, 1994, Kozukue et al., 2001). However, this experiment shows that Chl production does not cease immediately after removal of the light source.
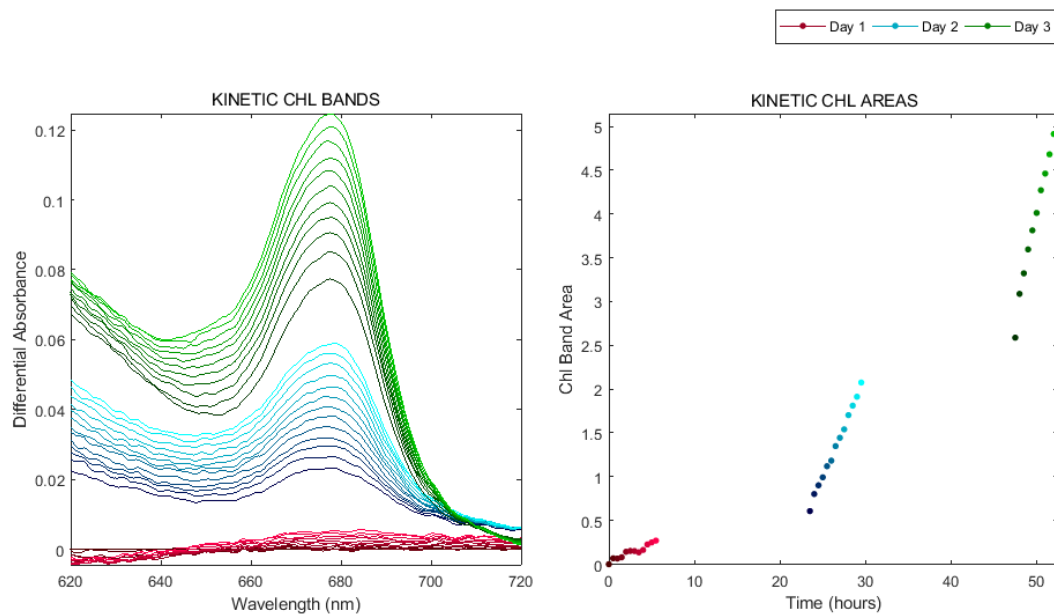
Figure 3:7 Static Series experiment with intermittent light exposure. Harvest 2017, a cv Orchestra tuber was illuminated for periods of 5-6 hours over three consecutive days. The figure contains the data collected during these periods. For the time in-between analysis, the laboratory lighting was switched off. The spectrometer lighting was only turned on for data collection.

A related experiment was conducted to establish the comparative effect of the ambient and spectrometer light sources. The results are shown in FIGURE 3:8. The setup of the spectrometer and sample was the same as the previous experiment except that this time the spectrometer source was left on continuously and the laboratory lights turned on and off. Within this figure the colouring represents periods in which the laboratory lights were either switched on (green) or switched off (blue). Here the Kinetic Chl Areas show that the Chl production increased at a stable rate. These results show that the spectrometer light source is enough stimulus to drive Chl production. In effect, it is the sole driver when there is also ambient lighting, as turning the laboratory lights on and increasing the light intensity did not influence the rate of Chl production.

This is consistent with the finding that the intensity of the spectrometer light source was two to three times greater than the laboratory lighting: TABLE 3:2 shows the parameters of the different light intensities present during experiments, obtained using a digital Lux meter. This agrees with the finding of Gull and Isenberg (1958), who determined that tuber greening was significantly different when exposed to fluorescent lights at intensities of 270 and 540 lux, but that there were no difference in the amount of greening at light intensity greater than 540 lux.
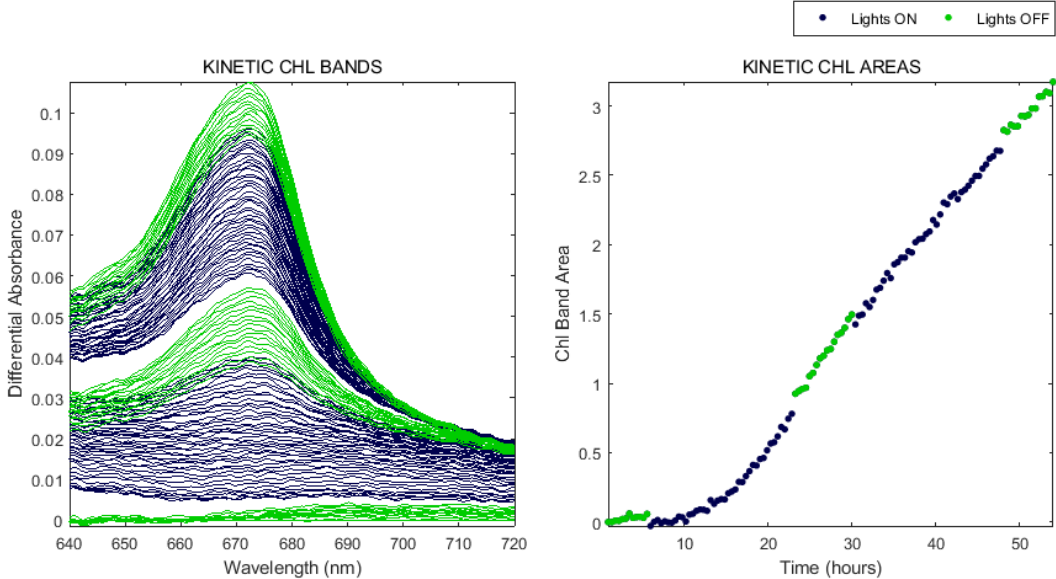
Figure 3:8 Static Series experiment with intermittent laboratory light exposure. Harvest 2017, a cv Orchestra tuber was illuminated constantly with a spectrometer light source. The laboratory lights were switched on and off at different time points, the colouring of the data indicates the two lighting conditions.

Table 3:2 Light intensity (lux) measurements recorded in the laboratory.

| ENVIRONMENT/EQUIPMENT | LIGHT INTENSITY (LUX) | |
| | Laboratory Lighting | |
	ON	OFF
Work Bench	277	-
Light Source	570	460

3.3.3 Repositioning Error

The Static Series experiments show that Vis/NIR spectroscopy can track, in real time, low level changes of Chl concentration in a tuber's skin. It should be noted that tubers

would typically only become visibly green after approximately three days. The Static measurements show excellent signal-to-noise ratios. However, the methodologies used in the Static Series experiments do not translate well into long term experiments due to the limitations on the number of tubers that can be analysed at any one time. For industrial application, it will be crucial for measurements to be taken on multiple tubers to enable a reliable batch representation. In the context of the present project, this means using a single spectrometer to take readings from many tubers in succession. This precludes a static set up, instead requiring movement of either the probe or the tubers to obtain multiple measurements.
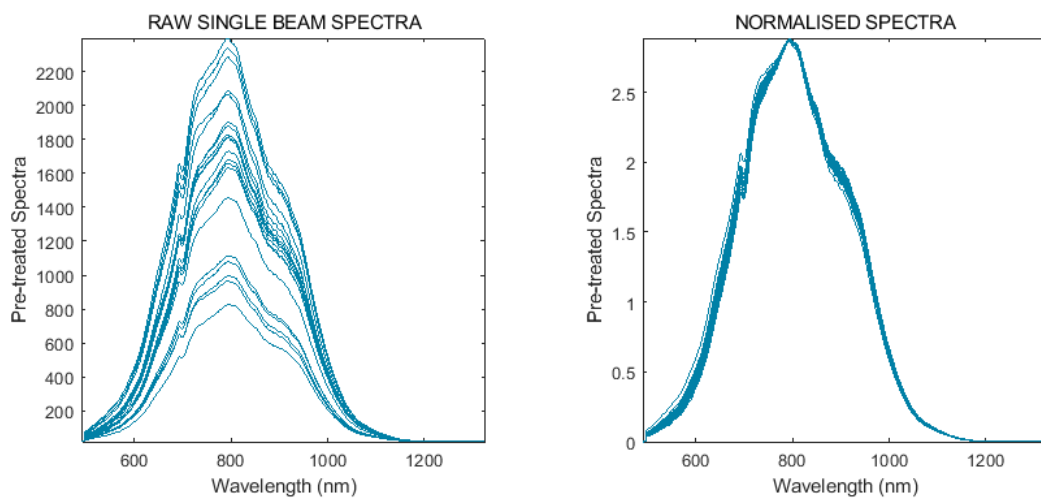
Figure 3:9 Repeated single-beam spectra taken from an Eye of a cv Russet tuber, before and after corrections. Between measurements the tuber and probe were un-clamped and re-aligned.

Multiple studies were devised to explore the variance introduced into spectra due to repositioning of the probe and tuber with respect to one another, and additionally, due to the individual researcher. To start, the Vis/NIR spectrometer was used to record data from a single Eye of a cv Royal tuber. The leftmost plot of FIGURE 3:9 shows the raw single beam spectra of 20 repeats. In between each measurement, the tuber's position was adjusted; the probe was then realigned to the tuber and clamped into its new position. A new dark spectrum was recorded for each measurement. A large variation in the signal intensity, which can only arise from small differences in probe positioning, can be seen between the spectra. The Standard Normal Variate (SNV) method of normalisation was used to remove a large portion of the overall variation. This can be seen by the transformation achieved by SNV in the rightmost plot of FIGURE 3:9.

The spectral data in FIGURE 3:9 indicated that the tuber examined contained minimal Chl as no clear absorbance at 675 nm was seen. The experiment was repeated using a second

cold stored cv Royal tuber, that was exposed to light for 48 hours before analysis began. During this experiment, two Eyes present on the tuber were examined. Ten spectra of one deep-set Eye (sunken into the skin) and one shallow Eye (close to the skin's surface) were measured to further investigate repositioning error. FIGURE 3:10 displays the results: the raw single-beam spectra, the SNV-corrected single-beam spectra and a close-up of the wavelength range containing the Chl band. The corrected spectra show a large reduction of the overall variation seen within the raw single beam spectra; however closer inspection of the Chl band show that considerable variability still exists in this absorption range, particularly for the deep-set Eye. The boxplot demonstrates that the variation is significantly less for the recordings taken from the shallow Eye. Due to this finding, shallow Eyes were used where available for all subsequent experiments.

FIGURE 3:11 displays the results when an Eye and Background area were analysed on a third cv Royal tuber. This time the tuber and probe were not repositioned; instead, the distance of the probe from the tuber was increased with each measurement taken (distance range if approximately 2 – 10 mm). The overall spectral intensity decreased with distance, the illuminated area increased meaning the light intensity per mm² was reduced; this decreased the signal collected by the fibre-optic probe. The Chl band recorded from the Eye still show small variation after pre-treatment. Therefore, to further minimise the variation of the spectral data due to technical reproducibility, a protocol was adopted whereby the probe position was adjusted in setting up each experiment with the aim of achieving a spectral intensity within a range of 500 counts, for example 2000 – 2500. The intensity of the light collected by the probe varied depending on tuber cultivar. The Background data, collected for FIGURE 3:11, show minimal variation between the single beam spectra.

It is clear, then, that non-static experiments will result in considerable irreproducibility in the data. This is especially noticeable once Chl becomes present in the surface layers of a tuber's skin since the specific probe positioning affects how much of the underlying diffuse reflectance is captured. This is clear from the results shown in FIGURE 3:12 of an experiment that followed the response of three Eyes on a single cv Royal tuber, exposed to laboratory conditions with constant ambient lighting for 48 hours. For six hours, two
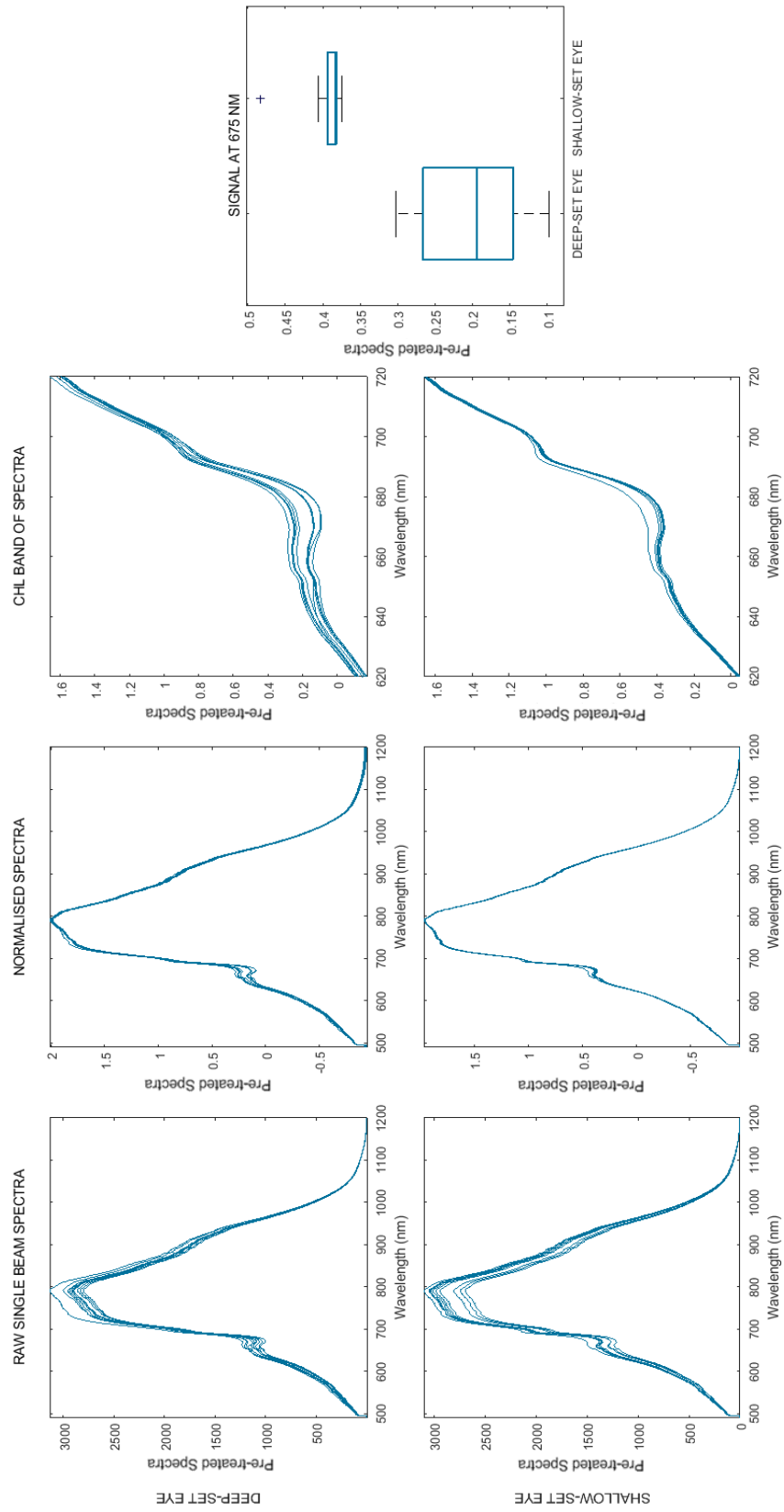
Figure 3:10 Comparision of single-beam spectra repeats of a deep-set and shallow Eye of a cv Royal tuber, before and after corrections. Between measurements the tuber and probe were un-clamped and re-aligned.

Eyes were measured every five minutes. For the following 18 hours a third Eye was monitored as a Static Series. The results of this experiment highlight two key points. The first point builds on the discussion of the outcomes seen in FIGURE 3:9 and FIGURE 3:10, in that the variance of calculated Chl Areas appears to increase with the concentration of Chl. The measurements taken for Eyes 1 and 2 on the second day of analysis demonstrate this alone. Eye 2 has a larger concentration of Chl present and exhibits a greater variance in the measurements. The second point once again highlights the issue of repositioning error. A large reduction is seen in the value of the Chl Area between the end of the first and the beginning of the second measurement series recorded from Eye 3. This can only be due to repositioning error: as previously seen in the Static Series experiments, and well stated in literature, the concentration of Chl present at the tubers skin surface only increases when constantly exposed to light (Dao and Friedman, 1994).
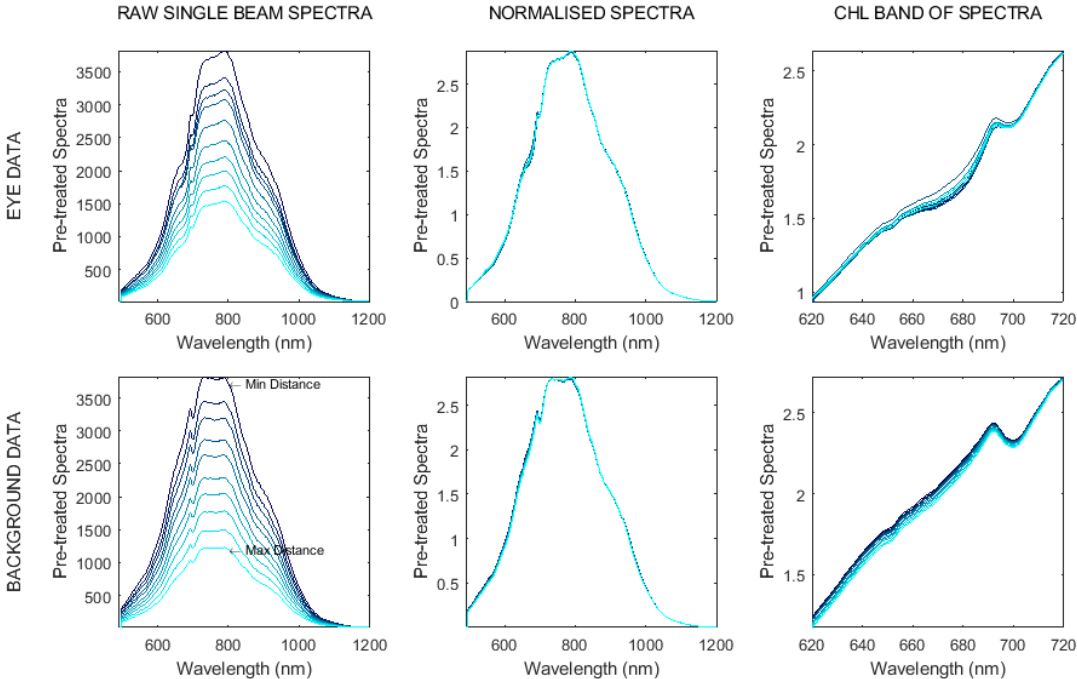
Figure 3:11 Comparision of single-beam spectra of an Eye and Background from a cv Royal tuber, before and after corrections. The left plots show the spectral data recorded at increasing distance, from dark to light blue, between the probe and tuber. The tuber was not repositioned between measurements.
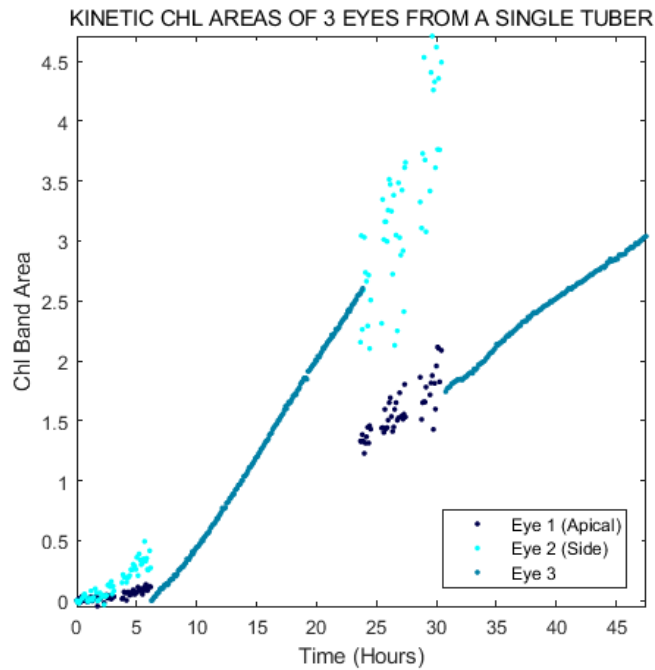
Figure 3:12 Repositioning and Static experiment using three Eyes analysed from the same cv Royal tuber. Eye 1 and 2 were analysed every five minutes for six hours. For the following 18 hours, Eye 3 was set up as a Static Series. This protocol was carried out on two consecutive days. During the experiment the tuber was constantly exposed to ambient lighting and laboratory conditions.

3.3.4 Repeatability of a Line Measurement

The previous section illustrated the variability in the spectral response due to small changes in the positioning of the probe with respect to a tuber's Eye. The results, especially as shown in FIGURE 3:10 and FIGURE 3:12 ,may also suggest a highly localised area of Chl concentration under the eyes. The variance in the calculated area of the Chl region is minimal when Chl is not present, in comparison to when the Chl band is large. This was investigated further by conducting a 'Line experiment', which involved making multiple positionally distinct measurements across a tuber's Eye over a period of three days.

On consecutive days, Vis/NIR spectra were recorded from five positions on a cv King Edward tuber's surface. These are referred as 1 – 5 and are shown by the arrows seen in the picture of FIGURE 3:13. Spectra were recorded at three time points each day, approximately three hours apart. Between measurements, the tubers were left in laboratory conditions with the lights on. The positions went from left to right; the central position corresponds to the tuber's Eye with two positions either side. These were arranged in a straight line with no overlap. The picture shows the probe set up to take a
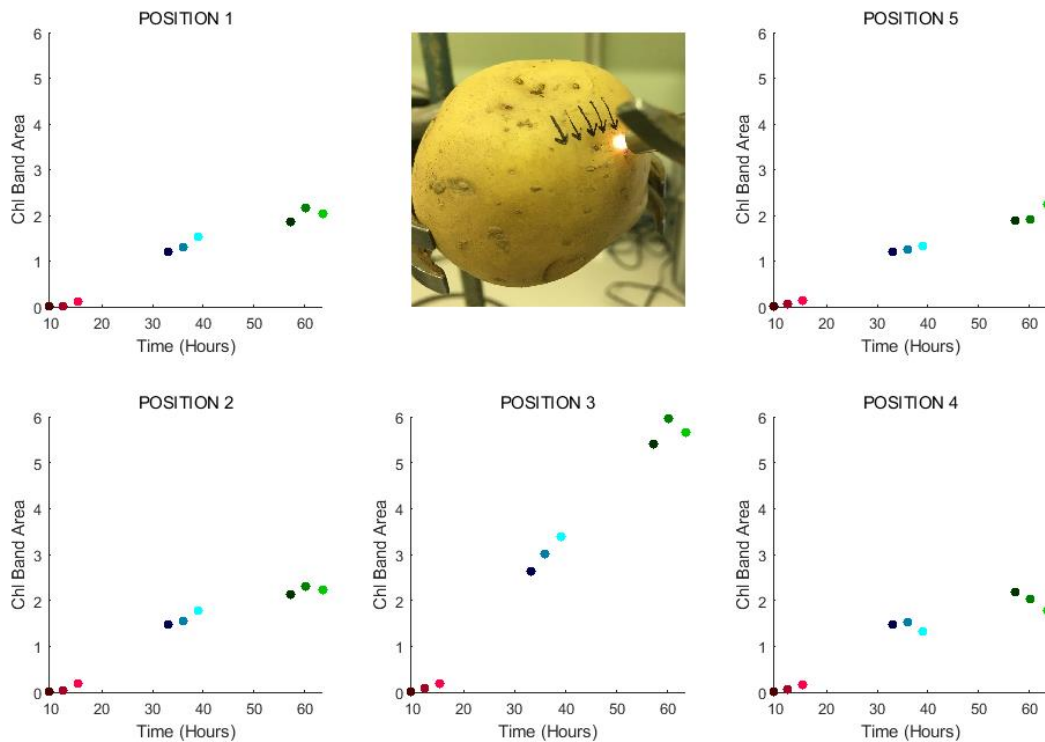
Figure 3:13 Line experiment conducted across the Eye of a cv King Edward tuber.

measurement on position 5. For this short-term experiment, the measurements were performed in triplicate by repositioning the probe beforehand. This was done for every position during each time point. This is in recognition of the results on positioning induced error seen in the previous section. An average spectrum calculated from the triplicates was used in the Kinetic series.

Throughout this thesis, Kinetic spectra will be referred to as 'Kinetic Eye' or 'Kinetic Background' Spectra, allowing differentiation between the two locations. Similarly, Chl Bands and Chl Areas will be referred to in this way. The Kinetic Background series spectra are calculated in the same way as described for the Eye data (shown in the previous figures within this chapter). From this the Background Chl Band and Areas can also be calculated. With exception of position 3, the plots surrounding the picture in FIGURE 3:13 are therefore presented as Kinetic Background Chl Areas.

All five positions show a pattern of increasing Chl absorbance with time. The greatest rate of change and largest Chl presence was seen in the Eye, position 3. Although lower overall, the rate of change was found to be consistent across the remaining four positions. These results show that considerably more Chl is produced at the Eye compared to the adjacent and surrounding tissue. This strongly suggests that the Chl production is

enhanced within a highly localised area directly underneath the Eyes. This might be expected, due to the eyes being the loci of growth and sprouting, although this has not previously been discussed in literature. This experiment has been repeated on cv Royal, Orchestra and Maris Piper tubers, all of which gave comparable results.

Table 3:3 Details of the Tubers used for the Repositioning and Line experiments, Figures 9 - 13.

FIGURE	CULTIVAR	SUPPLIER	HARVEST YEAR	STORAGE TIME
Figure 3:9	Royal	Sutton Bridge, UK	2016	9 months
Figure 3:10	Royal	Sutton Bridge, UK	2016	9 months
Figure 3:11	Royal	Sutton Bridge, UK	2016	9 months
Figure 3:12	Royal	Sutton Bridge, UK	2016	9 months
Figure 3:13	King Edward	Produce World, UK	2017	6 months

3.4   CONCLUSIONS

The often-repeated Static Series experiments show that Vis/NIR spectroscopy, equipped with a fibre-optic probe, can be used to track stimulated Chl production in potato tubers. This can be done at low levels when tuber greening is still not visible. This arrangement, however, means that the spectral response is highly sensitive to the alignment of the probe and tuber. Although best efforts were made to minimise unwanted variance (making sure the probe was perpendicular to the tuber, keeping the intensity of the spectral response within a specified range, taking replica measurements etc.), there will still be a source of error due to experimental procedure.

The measurement uncertainty can therefore be divided into two primary sources. The first is associated with the non-uniform shape of the tuber surface causing small changes in the spectral response (see FIGURE 3:10). The second is due to the highly localised variation in the Chl concentration around a tuber's Eye, which manifests as greater variability in the tubers' responses with increasing concentration (see FIGURE 3:12). If Chl is simply not present under the eye, then the experimental set-up cannot fail to give a response without a Chl peak; however, an eye with Chl present could still give a reduced reading due to mis-alignment.

47

A key finding in this chapter was that the tissue under the Eye can be more biochemically active than elsewhere on the tuber's surface skin (see FIGURE 3:13). Before the recent publication from Garnett et al. (2018), this phenomenon had not previously been suggested in literature.

The following chapters comprise the results of four long term experiments, conducted on tubers from each harvest from 2014 to 2017. These experiments studied several commercial potato varieties under varying conditions and experimental designs to investigate a few different hypotheses. However, the standard protocols of data collection, explained in this chapter were used throughout. This was done to allow the comparison of results from one year to the next.

LONG TERM POINT MEASUREMENT (HARVEST 2014)

4.1. INTRODUCTION

The previous chapter showed that chlorophyll (Chl) can be stimulated and detected by Visible/Near-Infrared (Vis/NIR) spectroscopy during short term experiments conducted over hours or days. The next step was to measure the response of tubers during a long-term experiment, with the aim of further understanding whether the production of Chl could give insight into dormancy breaking and to determine whether Vis/NIR measurements can be used to predict the onset of sprouting within a tuber.

Harvest 2014 was the first long term experiment and was performed on freshly harvested tubers. This meant that the conditions in which the tubers were treated, from the point of harvest onwards, were fully controlled. Storage conditions were devised to closely mimic commercial storage (detailed below). Storing the sample tubers outside commercial stores removed any possibility of influence from sprouting inhibitors. Residue of certain inhibitors, particularly CIPC, have been found in commercial stores even after cleaning: once CIPC has been applied to a crop in a storage unit, accumulation of residues can be found in a number of materials including the concrete walls and flooring (Boyd and Duncan, 1986). As previously discussed, there are many problem with the use of CIPC, but this one especially highlights the issue of cross -contamination of other crops (Douglas et al., 2018).

The experimental protocol used in the Harvest 2014 study involved recording the surface spectra of a tuber before, during and after dormancy break. **The aim was to determine whether the conclusions from the Static experiments discussed in Chapter 3 extended to tubers kept in storage for several months.** In commercial storage table top cvs are invariably kept in the dark, at temperatures below 5 ˚C, as this is the primary means of prolonging dormancy break (Coleman, 2000). Therefore, for the Harvest 2014 study the tubers were stored in conditions to mimic this, but the analysis was conducted in the Norwich laboratory. The same Eyes and Background from the sampled tubers (cvs King Edward, Mozart and Maris Piper) were analysed twice a week for 16 weeks. This experiment was essentially a variation of the experiments shown in FIGURE 3:12. These tubers however, were monitored over several weeks instead of days, meaning that measurements were separated by days rather than hours; and in- between measurements, the tubers were stored in conditions designed to hinder Chl production and dormancy break. To investigate the potential for using longer NIR wavelengths, two

StellarNet spectrometers were employed in tandem, increasing the available wavelength range to 500-2300 nm.

4.2. EXPERIMENTAL PROCEDURE FOR HARVEST 2014

4.2.1. Sample Collection and Storage

Four sacks of tubers of different cultivars and from different UK locations were collected in October 2014. cvs King Edward and Mozart were obtained from Produce World in Cambridge (Cambridgeshire), cv Maris Piper from B & C Farming in Marsham (Norfolk), and cv Maris Piper from G's Fresh in Barway (Cambridgeshire).

The tubers were placed into a storage facility at the Norwich laboratory. The dark storage unit was ventilated so the tubers could be kept at a constant temperature ($\sim$ 5.7 °C) and relative humidity ($\sim$ 80%). This was done to mimic commercial storage.

In turn, the sacks of tubers were removed from the storage room for a short period of time to select and prepare six medium sized tubers from each sample. The tubers were selected randomly although the presence of three suitable, shallow and non-sprouted, eyes was essential. These tubers were washed carefully with mildly warm water to remove any dirt attached to them, blotted dry with tissue paper and put back into storage. Four circles, approximately 2.5 cm in diameter, were then marked out on each of the washed tubers; three around three separate eyes (labelled 'E1', 'E2' and 'E3') and another around an area without any eyes (labelled 'B'). The tubers were also marked with identification labels; K1, K2, K3, K4, K5 and K6 for the six separate cv King Edward tubers, similarly M1 - M6 for the cv Mozart, B1 - B6 for the B&C Farming cv Maris Piper and G1 - G6 for the G's Fresh cv Maris Piper.

The sets of tubers selected for analysis were laid out in storage trays within the storage facility in front of their respective sacks.

4.2.2. Spectral Acquisition

Spectra were recorded using two StellarNet spectrometers; one of the Vis/NIR (Black-Comet CXR-SR-50) described previously in CHAPTER 3 and the Red-Wave NIRX-SR-100 T2 InGaAs StellarNet spectrometer. This spectrometer had a wavelength range of 900 – 2300 nm and is referred to as the Short-wave Infrared (SWIR) spectrometer. Both equipped with a fibre-optic probe and a Tungsten/Halogen light source (with an added colour equalisation filter), these were used to analyse the 24 tubers twice a week for 16

weeks. The sample sets were removed from storage in a polystyrene box containing an ice block and brought into the lab for analysis. The different cultivars were removed in turn. This was done to reduce the temperature change and minimise tubers' exposure to light whilst out of storage.

In turn each tuber was clamped into a position to analyse, firstly, the Background circle. The fibre-optic probe was then positioned perpendicularly to the tuber at the centre of the marked circle, at a distance approximately 3 mm away from the surface. The spectrum was recorded. The position of the probe was then adjusted slightly, remaining within the marked circle, and a second spectrum was recorded. This was repeated a third time giving a total of three spectra for the Background of that tuber. Three spectra, each with a slightly different positioning, were similarly recorded for each Eye labelled on the same tuber. This resulted in a total of 12 spectra being collected. This tuber was then returned to the box and the second tuber was removed to be analysed in the same way as the first, as so on.

During the weeks of analysis, sprout growth was also monitored. The initial visibility of sprout growth from each Eye and then the length of this sprout thereafter, was recorded during analysis. This allowed a 'Sprouting Age' scale to be associated with each tuber according to these observations. The day on which a sprout was first visible was defined as zero on this scale. Analysis days before that would thus have a negative Sprouting Age, and those occurring afterwards a positive value. (See the diagram below to visualise this.) As an example, FIGURE 4:1 indicates that this tuber started sprouting 46 days into the analysis period.
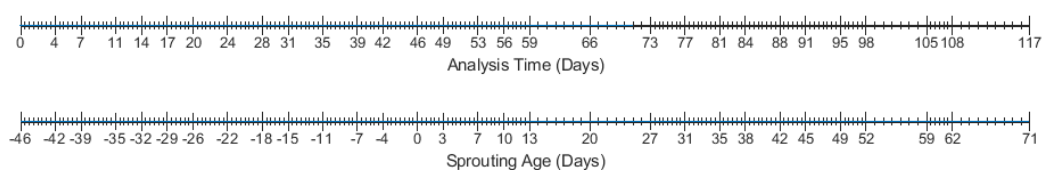
Figure 4:1 Analysis time and sprouting age of Eye 1, G2 from Harvest 2014.

4.2.3. Data Analysis

Pre-treatment methods used on this data set were the same as those conducted on the single beam spectra described in CHAPTER 3. However, in addition, the smoothdata.m MATLAB function was used to smooth the single beam spectra. This was done using the Savitzky-Golay filter method and a window length of 21. Similarly, the methods of data analysis (normalisation, peak integration, etc.) were also used. A quick reference to the

different method terms can be found in CHAPTER 10. These definitions are capitalised for easier identification.

4.3. RESULTS AND DISCUSSION

4.3.1. Kinetic Spectra and Chl Bands

Over 16 weeks, 24 tubers of four cultivars were analysed a total of 30 times. FIGURE 4:2 and FIGURE 4:3 give an example of the data collected by displaying the spectra from a single cv Maris Piper tuber. FIGURE 4:2 contains the data collected from the VIS/NIR spectrometer while FIGURE 4:3 contains the data collected from the SWIR spectrometer. Within both figures, the top row displays the data collected from a single Eye while the bottom row contains the Background data collected from the same tuber.

FIGURE 4:2 displays the pre-treated single beam spectra, the Kinetic spectra and the Kinetic Chl Bands (with removal of any peak offset) of this randomly selected tuber. The shapes of the spectra are slightly different in comparison to the spectra obtained previously using the StellarNet Inc. EPP2000-NIR-200 spectrometer, however this is not unexpected, since the component parts differ (detector, source, etc.). This data was found to be noisier and as a result was smoothed using a Savitzky-Golay polynomial function before further processing.

It is immediately clear that the Kinetic spectra show that the Chl band is responsive during this experiment, exhibiting similar behaviour to results seen in Static Series from CHAPTER 3. Detailed visualisation of the Kinetic Chl Bands shows that the absorbance at 675 nm generally increased from one time point to the next. However, the rate of change in the Chl Bands was greater at the beginning than at the end of analysis. This will be discussed further in the next section, when the Kinetic Chl Areas were plotted against time. The final point that can be made from FIGURE 4:2, again in agreement with previous findings, is that the absorption of the Chl band is greater in the Eye than in the Background. These findings were representative of all the tubers analysed for Harvest 2014. From these results, it can be concluded that Chl production can be stimulated and observed in tubers monitored long term whilst being stored in storage conditions which approximate to those in commercial use.

The SWIR data collected were also pre-treated with spectral smoothing, SNV normalisation and baseline correction. Unlike the data collected from the Vis/NIR
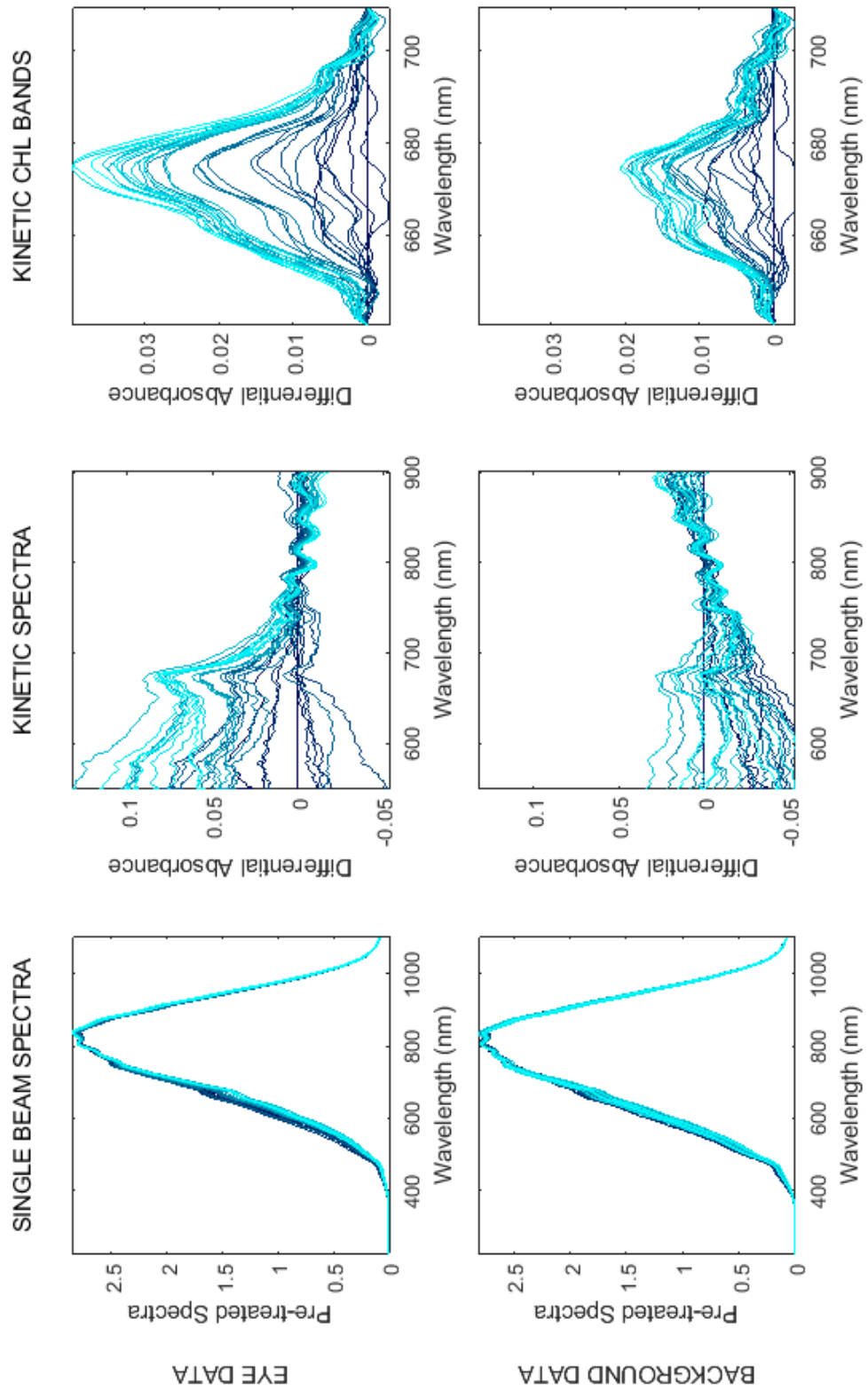
Figure 4:2 Spectra collected from a single B&C Farming cv Maris Piper tuber using the Vis/NIR spectrometer. The gradual colour change from dark to light blue represents the first to last spectra. The Kinetic Chl Bands hear have been corrected for baseline offset. The plots of the three data types are set to have the same limits to allow for visual comparison, between the Eye and Background.

spectrometer, the SWIR showed clear visual differences between the Eye and Background data sets (see the single beam spectra in Figure 4:3). Absent in the Background spectra, a large peak at 1450 nm is observed in the spectra recorded for the Eye. The peak at 1950 nm is also more pronounced for the Eye spectra compared to the Background. It is known that these two broad peaks arise from the absorption of water, and have largely been used to quantify the water content in foods (Büning-Pfaue, 2003). Elbatawi et al. (2008) could accurately predict water content of potato tubers using NIR spectroscopy. The differences seen in Figure 4:3 indicate that water was present at higher concentration under the surface of an Eye compared to areas of Background.

The single beam and Kinetic spectra plotted in Figure 4:3 do not indicate a change in the spectra with time. Nevertheless, the absorbance values at 1450 and 1950 nm were plotted against time to better visualise any trends that might be present (see the rightmost panels of Figure 4:3). The x axis 'Time', corresponds to the number of days since the initial day of data collection. Very little change is seen in these two absorbance bands. This is arguably somewhat surprising. Potatoes are made up ~80% of water: without a condition of high humidity during storage (~95% RH), tubers are known to lose water during long periods of storage (Cunnington and Pringle, 2008). The Eye data at these wavelengths are slightly more variable than the Background data. This is likely another instance of repositioning error; the concave shape of an eye causes greater variance in light scattering than the largely flat Background surface.

The results shown in Figure 4:3 were true for all tubers analysed in Harvest 2014, suggesting that the changes in spectral data at longer wavelengths could not be linked to tuber aging or dormancy break during long storage. Because of this, the focus of all subsequent data analysis was on the data collected from Vis/NIR.

4.3.2. Kinetic Chl Area

Figure 4:4 contains the Kinetic Chl Areas calculated on the data collected from the cv Mozart tubers. The two rows of subplots separate the data collected from the Eyes and Background respectively, whilst the columns separate the six tubers. As three Eyes on each tuber were analysed, the plots on the top row each contain three data points at any one-time point. The three shades of blue highlight the three separate Eyes analysed. It should be noted that the y axis range for the Eye plots is double the value for the Background plots.
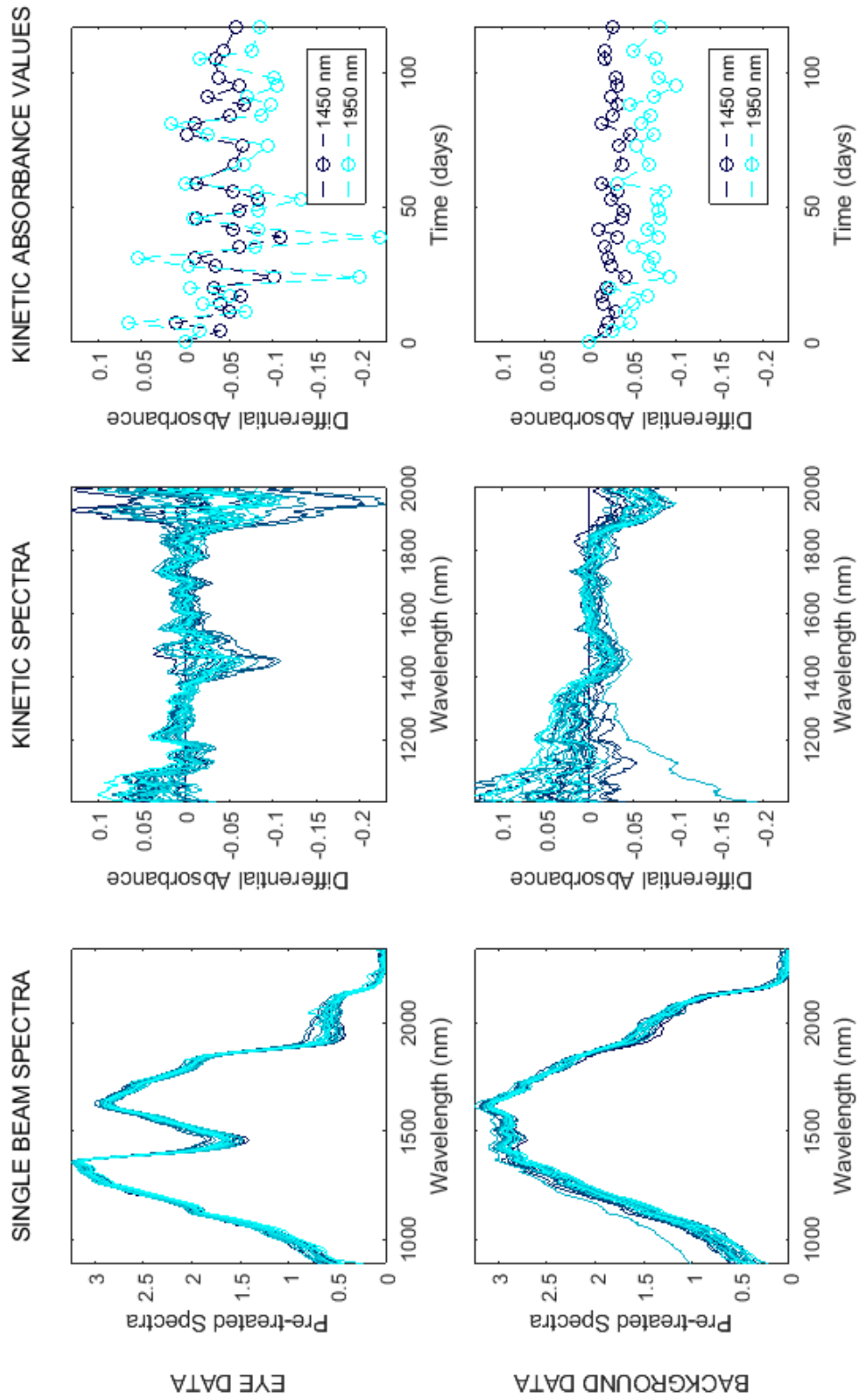
Figure 4:3 Spectra collected from a single B&C Farming cv Maris Piper tuber using the SWIR spectrometer. The gradual colour change from dark to light blue represents the first to last spectra. The right column contains the Kinetic reflectance values at 1450 and 1950 nm against time.

The results from FIGURE 4:4 suggest a sigmoidal-type response in the absorbance of the Chl band as a function of time, for both the Eye and Background data. This can most clearly be seen in tuber 5. Anstis and Northcot (1973) have shown a sigmoidal curve for the changes in Chl concentration for a cv King Edward tuber illuminated for various time periods. In their study, the Chl was extracted and measured by optical density for exposure times of 2 to 24 days. Here the spectroscopic measurements show a small lag phase at the beginning, most clearly in the Eye plots, followed by a period of growth for approximately 50 days, depending on the tuber; and finally, an asymptotic phase seen for the remainder of the analysis period. The lag and growth phases of analysis have been observed previously in FIGURE 3:2 to FIGURE 3:6, with the asymptotic phase also being seen in FIGURE 3:5 and FIGURE 3:6. However, the overall absorption in the Chl band is considerably smaller than in the results shown in FIGURE 3:2 to FIGURE 3:6. This can be explained by considering that the tubers in the long-term study were exposed to intermittent periods of light (each analysis period was ~10 minutes) with a cumulative exposure of approximately 5 hours in total.

The Eye plots show an increased level of 'noise' in the Kinetic Chl Area curves towards the end of the analysis period, from approximately 60 days onwards. Some of this variance can be explained by the previously discussed positional irreproducibility, as well as different concentrations of Chl present in the three Eyes. For example, Tuber 2 shows that one Eye apparently ceased to produce Chl at around the 60-day mark, whilst the remaining two Eyes continued to produce Chl for another couple of weeks. This could be explained by the location of the Eye on the tuber; as previously discussed, eyes closer to the apical bud are known to be more active than eyes found further away (Harris, 1992). On top of the variation between the three Eyes, an increase in the 'noise' is seen for each individual Eye; see Tuber 6 as an example. Eyes 1 and 3 show a reasonably stable response throughout, whereas the responses for Eye 2 become much more variable after approximately 50 days. This could be explained by the presence of a sprout; the reflectance of a sprout is likely to exacerbate repositioning variability: once the sprout has started to show, it has effectively changed the morphology of the Eye. Further growth will cause even greater variance because of increased light scattering.

The Kinetic Chl Areas of the cv Mozart data seen in FIGURE 4:4 were averaged across each tuber to give a clearer overview of the cultivar batch. As three Eyes were analysed from each tuber, the median value for each time point was used. The cv King Edward and two
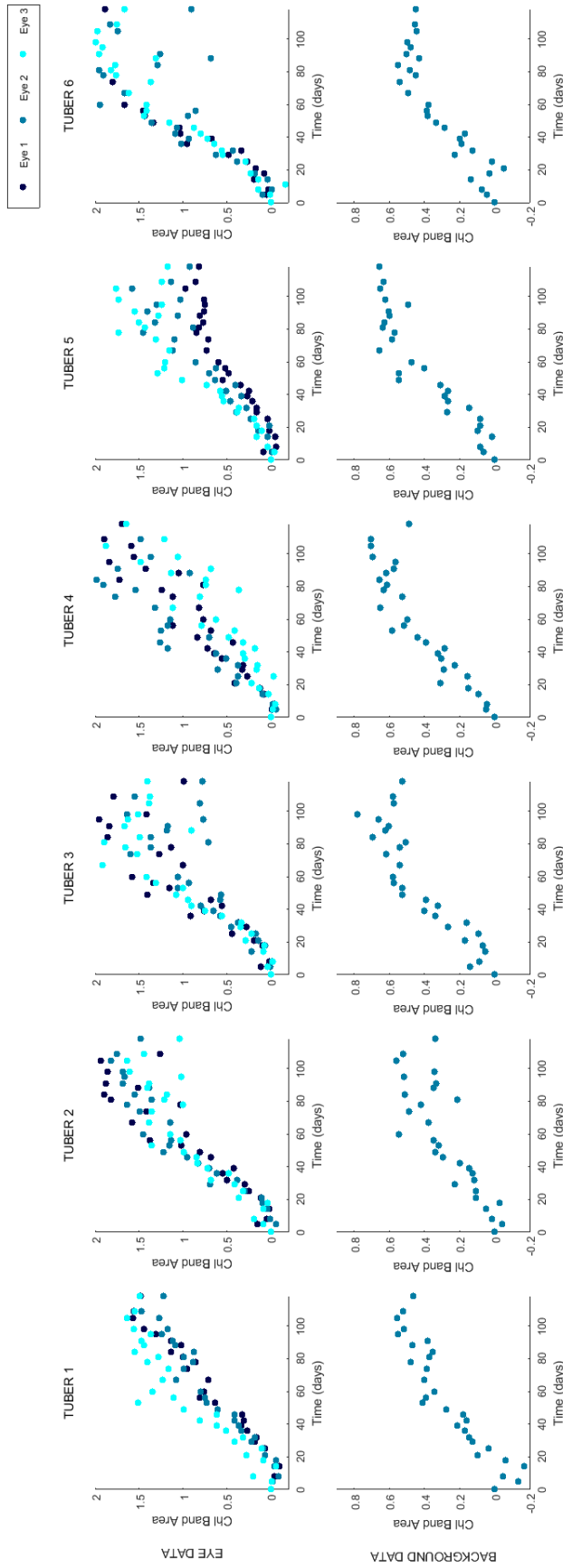
Figure 4:4 Mozart Chl Band Areas plotted against analysis time. The two rows of subplots separate the Eye and Background data, whilst the columns separate the six tubers.

cv Maris Piper sample sets were treated in the same way. FIGURE 4:5 displays these results. Each plot contains six coloured lines representing the average Kinetic Chl Areas from each tuber of the named cv. The median value of the six tubers were then used to calculate an overall batch average value for each time point. These are represented by the black squares. Finally, a generalised logistic function (Richards curve) was fitted to these averages; the result can be seen by the dashed black line. The fit of the curve expressed by R^2 was >0.9 for all cases. The plots in this figure are set to the same axis parameters to aid visual comparison.

In broad terms, the cvs King Edward and Maris Piper tubers show comparable results to those seen with the cv Mozart tubers already presented in FIGURE 4:4. However, there are some differences between the fitted curves for each of the cvs. The cv King Edward curve shows a near absence of the lag phase at the beginning of analysis and the highest rate of Chl production. cv Mozart tubers show a larger absorbance response at the end of analysis compared to the cv Maris Piper tubers. Interestingly, even though the two cv Maris Piper sample sets were collected from two different growers, their batch behaviour is highly similar in both the Eye and Background data.

The two vertical lines in each of the Eye plots of FIGURE 4:5 indicate the average times of different states of dormancy seen for each cultivar batch. The dashed lines in dark blue indicate when the tubers first showed signs of dormancy break, i.e. the average of the times at which the Eyes' Sprouting Ages were defined as zero. The dashed lines in light blue indicate the average time at which the sprouts grown at the assessed Eyes had reached a length of 1 mm. Cunnington and Pringle (2008) define dormancy break to be at the point where 50% of tubers have sprouts of 3 mm or more in length. Though this second marker represents a state in which, according to industry guidelines, the batch would not yet be classed as sprouting, it would allow sufficient time for mitigating action to be taken, such as bringing forward retail sale or starting sprout inhibitor treatment. No further markers were defined, as only a few tubers had reached sprouting lengths of 2 mm by the end of this experiment. It should also be noted that not all the Maris Piper tubers, from both sample sets, even reached sprout lengths of 1 mm, therefore the light blue dormancy line is an underestimation for these batches.

On initial consideration, it may seem like the first of these markers (first appearance of sprouts) should be the main target of any predictive method. However, the idea that by the time a 1 mm sprout has appeared on a tuber there would be no need for an instrument to inform a store manager that the tubers had broken dormancy is simply
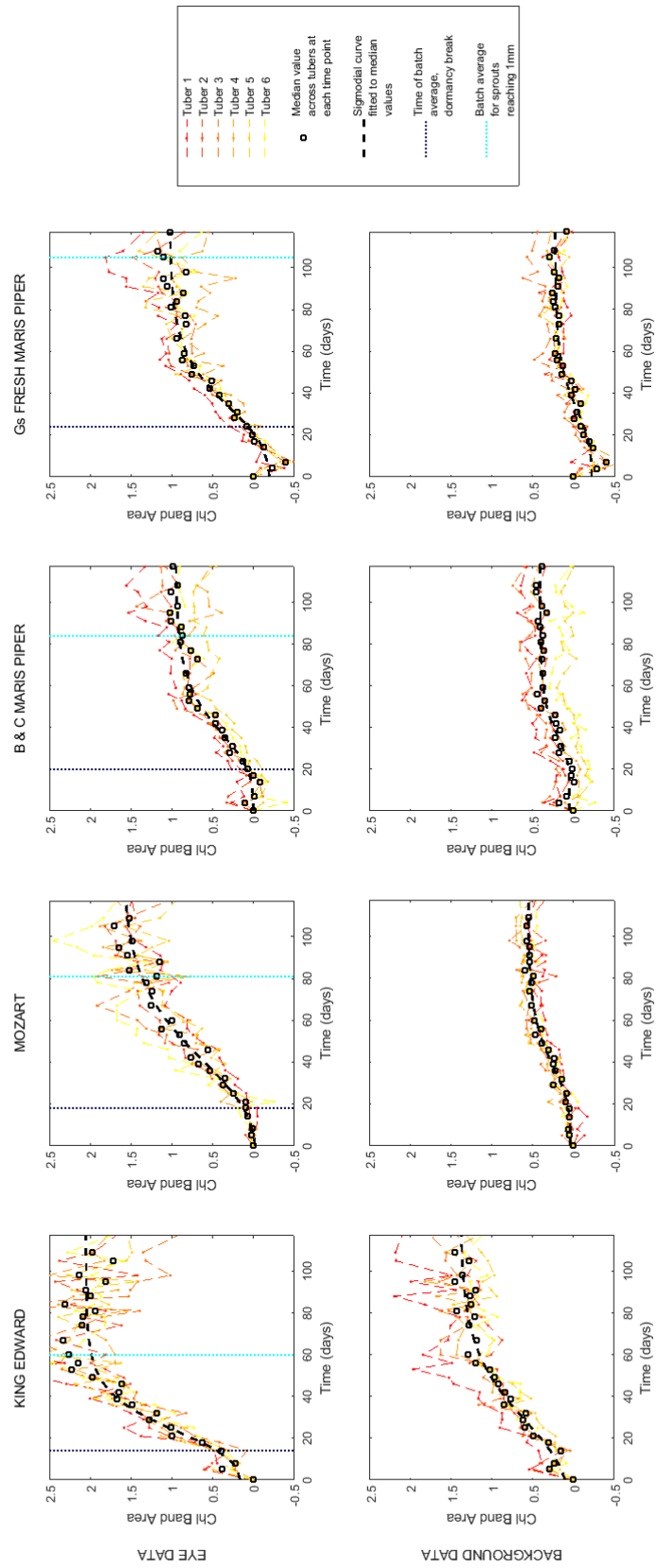
Figure 4:5 Batch cv Chl Band Areas plotted against analysis time. The two rows separate the Eye and Background data, whilst the columns separate the four cultivars. See the text for more details on this figure. Note that the not all the cv Maris Piper tubers had reached 1 mm by the end of the analysis.

not true. Davidson (1958) state that once a sprout reached a length of 0.45 mm it becomes visible to the naked eye. However, from observations made throughout the four harvest experiments reported in this thesis, it was noted that human assessments of the sprouting state of tubers was very subjective, and different for a trained and untrained eye. Having watched hundreds of tubers break dormancy as an individual, it is known what small changes to look for when observing the onset of sprouting. Those who did not have this experience were unable to see the signs so soon. It must be concluded that determining the first appearance of sprouts is highly dependent on the analyst. For this reason, both marker points were believed to have objective value.

The position of the dark blue (Sprouting Age) lines suggests that sprouts begin to grow shortly after Chl production starts, for all cvs studied here. However, this has been contradicted by at least one of the Static Series experiments (e.g. see FIGURE 3:4). This Static Series experiment was conducted on a freshly harvested tuber, and the tuber did not sprout even by the end of the experiment.

Arguably the light blue lines (1 mm sprouts) hold more potential as dependent variables in an eventual predictive approach. For the cvs King Edward, Mozart and Maris Piper (B&C Farming) tubers the light blue line is positioned at the end of the growth phase. For the cv Maris Piper (G's Fresh) tubers this line can be found in the asymptotic phase. Further, the cv King Edward line occurs very much earlier than the other cvs. This may be explained by the characteristic short dormancy of cv King Edward tuber. In contrast, both cvs Mozart and Maris Piper are described as having medium dormancy periods

Finally, the shape of the fitted curves suggests that the Chl production slows down towards the end of the study. As previously noted, this may be because the photosynthetic apparatus becomes damaged when tubers are held in long term cold storage. Note however that the sprouts did continue to grow for the duration of the study, meaning sprout growth is independent of the production of Chl at the surface of the Eye, although most did not reach 2 – 3 mm in length.

4.4. CONCLUSIONS

The Vis/NIR data of Harvest 2014 showed that Chl production can be induced when tubers are kept in cold storage for several months (FIGURE 4:2). The results mimicked what had been seen previously in the Static Series experiments (FIGURE 3:5 and FIGURE 3:6). This experiment also reiterated that the tissue under the Eye has a greater capacity

to produce Chl at the skin surface than anywhere else on the tuber, independent of cultivar (FIGURE 4:4). The use of the NIR spectrometer, at longer wavelengths of 900-2300 nm, did not provide any additional information regarding the changes in a tuber during cold storage (FIGURE 4:3).

It was observed that repositioning error seen by individual tubers can be overcome by taking the average values of multiple tubers (FIGURE 4:5). This means that several tubers would need to be analysed to give a steady reading and reliable result for a batch behaviour. In conjunction with the results seen in FIGURE 3:4 (CHAPTER 3) when Chl production can occur without leading to sprout growth, FIGURE 4:5 also show that sprout growth can continue without surface production of Chl. This is seen by the asympotic phase in this figure.

It has been established that a pattern of increasing Chl as a function of time is seen in the long-term experiments, albeit at Chl levels much lower than those achieved in the continuous exposure Static experiments. It was surprising that the short period of intermittent light exposures was sufficient to act as a stimulus for Chl production especially when considering that the lag phases of the Static Series experiment lasted for as long as 20 hours. Could this absorbance peak be a response to other bioactivities occurring under the tubers skin during cold storage?

The Harvest 2015 study sought to address this question directly. The measurement protocol broadly mimicked that of the 2014 harvest (12 tubers, analysis for 21 weeks etc) but tubers were taken direct from dark storage, analysed (by Vis/NIR and Chl quantification) and then discarded. Over the course of the long-term study, tubers thus differed only by cultivar and how long they had been in storage, not by their cumulative exposure to light.

This study also aimed to move one step closer to a protocol suitable for industry use. Commercial knowledge holds that tubers removed from a storage pile and treated as an analytical subset (as in 2014 harvest study) will not age in storage the same way. A protocol that adopts an 'analyse, discard' model was felt to be ultimately more acceptable to the industry. All subsequent years' studies were based on this approach.

CHLOROPHYLL PRODUCTION IN STORAGE (HARVEST 2015)

5.1. INTRODUCTION

The results from Harvest 2014 suggested that Visible (Vis) spectroscopy may have the potential for predicting the dormancy state of a potato tuber. A key element of the experimental design was that the same collection of tubers was monitored throughout. Although the exposure of individual tubers to light was relatively small during each episode of data collection (approximately 10 minutes per time point), the cumulative exposure over the multiple measuring sessions was sufficient to stimulate the tubers' bioactivity. Chlorophyll (Chl) production clearly varied during the study, with the magnitude of the Chl band generally exhibiting sigmoidal behaviour as a function of time, and with the suggestion that different cultivars had different behaviours potentially related to their dormancy status.

It is possible however, that over the course of the Harvest 2014 study, the physiological status of the measured tubers diverged from that of the rest of the (unmeasured, stored) batch, due to the experimental design. To address this possible shortcoming, the remaining three annual studies adopted "measure then discard" protocols. This ensured that the only difference between the measured tubers and the remainder of the batch at any given time point was the length of time in storage, and not their previous history of light exposure.

The study on Harvest 2015 aimed to answer a fundamental question that could not be addressed by the cumulative-exposure protocol of previous study: is the 675 nm peak being affected by another chemical species produced in tubers during long-term dark storage? As a secondary objective for the Harvest 2015 study, the presence of Chl was also quantified, using wet chemistry and Ultraviolet (UV) spectroscopy, in tubers before and after light exposure. The aim was to verify that the key changes seen within the Vis/NIR spectra were due to Chl production.

UV spectrometry has been previously used to study certain pigments and compounds in potato tubers, including chlorophyll. Dao and Friedman (1994) recorded visible spectra of (White Rose) potato peel that had been exposed to light for 20 days using UV-Vis spectrometry and stated that the green colour was due to an absorbance peak near 670 nm. It has been stated in multiple papers that this reflectance peak is sensitive to low concentrations, up to 5 nmol/cm^2, of chlorophyll (Datt, 1998, Gitelson and Merzlyak, 1998). Gull and Isenberg (1958) monitored the production of chlorophyll in three

different potato cultivars when exposed to various strengths of fluorescent light. Although the cultivars analysed had different susceptibility to chlorophyll formation, the amount of greening increased with light intensity. Kozukue et al. (2001) looked specifically at the chlorophyll production in potato sprouts; a linear relationship was found between chlorophyll concentration and storage time under light. These experiments required destructive methodology.

Many academics have calculated algorithms for chlorophyll assessment using specific wavelengths from the visible range of the electromagnetic spectrum. There are a number of solvents that can be used for extraction of chlorophyll, the most commonly used is N,N-dimethylformamide (DMF), methanol or acetone (Mackinney, 1941). Gitelson and Merzlyak (1996) stated that, in their algorithm, this could be used as an index for the onset, stages and rate of ripening processes within the plants.

Chlorophyllous pigments found in potato tubers include Chlorophyll a (Chl a), Chlorophyll b (Chl b) and Protochlorophyll (Pchl). When Chl or Pchl concentrations are barely measurable within a tuber, it suggests that the tuber has never been exposed to light. For Pchl to be formed, a tuber must be stored in darkness after it has been irradiated long enough for Chl to be produced. Virgin and Sundqvist (1992) found that tubers, which had not previously been exposed to light, had to be irradiated for at least 30 minutes to allow for a detectable amount of Pchl to formed following a subsequent stay in darkness. Pchl exists in different forms and is known to show maximum spectral absorptions at 665, 635 and 628 nm (Böddi et al., 1979).

5.2. EXPERIMENTAL PROCEDURE FOR HARVEST 2015

5.2.1. Sample Collection and Storage

Samples of cvs Cultra and Rooster tubers were collected from Country Crest farm in Ireland on a weekly basis. Both cultivars were stored in commercial storage units, with conditions of 3.5 – 5 °C and ~90% RH. The samples were collected from the same wooden crates each week. Twelve tubers of each cultivar were used for the analysis at each time point. All tubers were cleaned using a dry brush immediately before data collection. The dormancy state of each Eye, non-sprouted or sprouted, was also recorded. After analysis, the tubers were either disposed of or used for Chl quantification.

5.2.2. Spectral Acquisition

Visible/Near-Infrared (Vis/NIR) spectra were recorded using the primary spectrometer, StellarNet Inc. EPP2000-NIR-200, equipped with the fibre-optic reflectance probe and a Tungsten/Halogen light source. An average of 100 scans was recorded with an integration time of 30 ms. Three Eyes and a Background Area were analysed on each tuber using the standard protocol defined in CHAPTER 3. Three repeat measurements (with repositioning) of each location were taken; hence 12 spectra were recorded from every tuber, giving a total of 144 spectra for each cultivar at each time point. The three replicates of each position were always averaged, after normalisation, to find a mean spectrum for that position at a single time point. This data was collected by myself and a visiting worker, Dusan Ristic.

5.2.3. Chlorophyll Extraction and Quantification

Five of the tubers used for Vis/NIR analysis were also used for a Chl quantification experiment. The method for Chl extraction was adapted from the protocol described by Petermann and Morris (1985). An 8 mm diameter cork borer was used to obtain two cores from the exposed surfaces of the Background and first Eye that had been analysed using Vis/NIR. The outer 4 mm of each core was cut into quarters and weighed. Samples were extracted in 15 mL N,N-Dimethylformamide (DMF) in the dark at 4 °C for 48 hours. Each sample was vortexed for 5 minutes immediately before the absorbance of the supernatant was measured at 603, 625, 647, 664 and 703 nm. This was done using a UV/Vis spectrometer, 1700 CE PharmaSpec (Shimadzu, Japan).

5.3.   RESULTS AND DISCUSSION

5.3.1. Visible/NIR Data

The average spectra of various subsets of each week's data were calculated to determine if any clear changes between the spectra, particularly for the Chl band, could be seen. A weekly mean of the 12 tubers was calculated for the single beam Eye and Background spectra, displayed in the leftmost and centre of FIGURE 5:1. From the Harvest 2014 study, it is believed that the sample size of 12 tubers (analysed with a similar 3 replica Eye and Background protocol) gives a reliable representation of the batch at that time point. The gradual colour change from dark to light represents the consecutive analysis weeks. The two rows separate the cv Cultra and Rooster data. Overall, the single beam plots display very little change occurring over the 21 weeks. The most obvious changing feature can be seen in the cv Rooster Background data between 550-650 nm, see FIGURE 5:1.
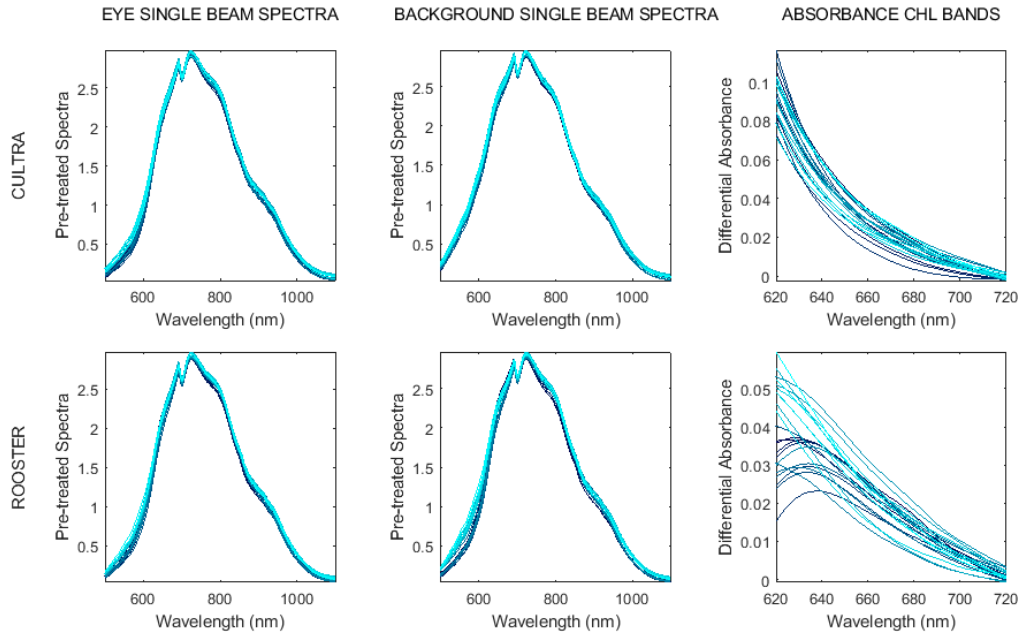
Figure 5:1 Weekly averages of the single beam Eye, Background and Difference spectra. The gradual colour change from dark to light represents the consecutive analysis weeks. The two rows show the separate cultivars.

Protochlorophyll (Pchl) has an absorption maximum at 635 nm and could therefore account for the changes seen here (Moran, 1982).

To further explore if any information could be extracted from this data, an alternative method of acquiring an absorbance spectrum was used. As these tubers were only analysed once, a spectrum could not be referenced to its first (I_0) in a "time series" (see Beer Lambert Law, EQUATION 2:1). The single beam Eye spectrum was instead ratioed to its corresponding Background spectrum taken at the same time point. In the remainder of this thesis, this is referred to as an 'Absorbance' spectrum. It is known not to be a true absorbance spectrum in accordance with the Beer Lambert Law but is a practical approach that enables the useful "Absorbance Units" scale to be used. Twelve Absorbance spectra could therefore be calculated for each cultivar during each analysis week. The rightmost plot of FIGURE 5:1 shows the weekly average Absorbance spectra of the 21 weeks. Again, it only highlights changes seen in the cv Rooster data around 630 nm.

The single beam spectra showed no presence of the Chl band in the Vis/NIR spectra, which had been seen so clearly in the Harvest 2014 study. The Chl Areas were
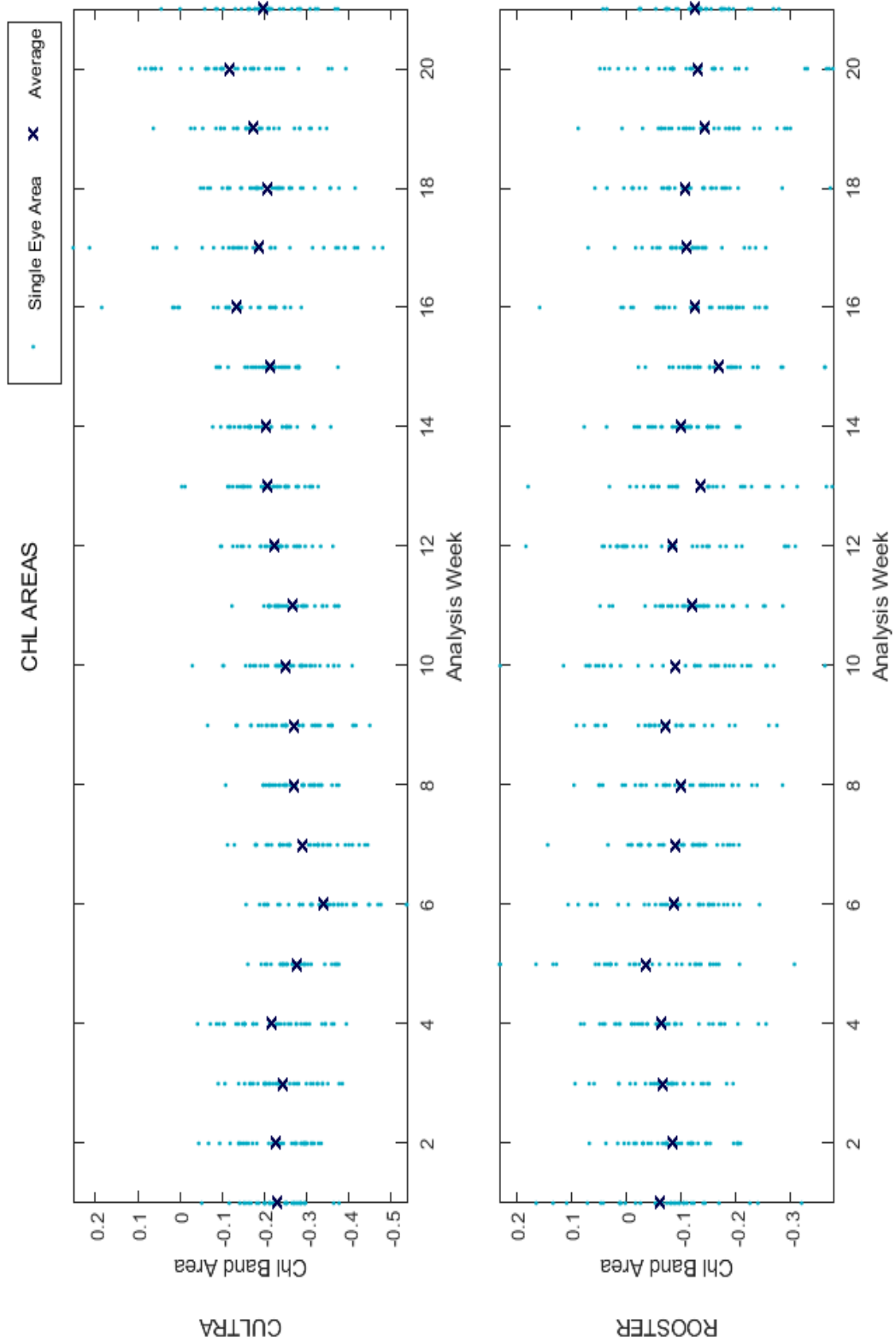
Figure 5:2 Chl Areas of the tubers analysed during the 2015 Harvest. Each dot represents the Chl Areas related to a single Eye analysed during that analysis week, and the crosses show the average value of that week.

nevertheless, calculated and plotted against time, see FIGURE 5:2. Every light blue data point represents the Chl Area calculated from a single Difference spectrum. As three Eyes from each tuber were analysed, there are 36 data points for each analysis week. The mean area value, for each week, was also calculated and is represented by the dark blue crosses. These plots are analogues of FIGURE 4:4 and FIGURE 4:5 from Harvest 2014; however, in the present figure, no trend is seen with time throughout the analysis period. With the hypothesis that the 675 nm peak was due to Chl production, these results confirm that Chl is not produced at levels measurable by Vis/NIR in tubers that are stored, even long term, in the dark (Dao and Friedman, 1994, Edwards and Cobb, 1999).

5.3.2. Chlorophyll Quantification

Several different published methods have been used for the extraction of Chl. The protocol described by Petermann and Morris (1985) was found to be the most suitable. The concentration of Chl was calculated using the formulae determined by Moran (1982):

$C_a = 12.65\ A_{664} - 2.99\ A_{647} - 0.04\ A_{625}$

$C_b = -5.48\ A_{664} + 23.44\ A_{647} - 0.97\ A_{625}$

$C_p = -3.49\ A_{664} - 5.25\ A_{647} + 28.3\ A_{625}$

$C_T = C_a + C_b + C_p$

where A_λ is the absorbance recorded at the individual wavelength λ, and C_a, C_b, C_p, and C_T represent the concentration of Chl a, Chl b, PChl and the total Chl concentration, respectively, in μg/mL. The results for each chlorophyllous pigment exhibited a similar trend across the analysis weeks. FIGURE 5:3 specifically shows the results for the total Chl concentrations. Each dot represents the concentration value of a single Eye minus the Chl concentration of the Background taken from the same tuber. The crosses on the plots show the weekly averages.

The results closely resemble those in FIGURE 5:2, where the absorbance of the Chl band showed no consistent increase during the duration of study, implying that Chl was not produced. FIGURE 5:3 showed no significant trends in the amount of Chl present in the tuber skin over the 21 weeks. Taken together, these results confirm that Chl was not produced under the Eyes in either cultivar during this commercial store. This is not unexpected however, as the prevailing the literature consensus is that Chl is not produced in absence of light.
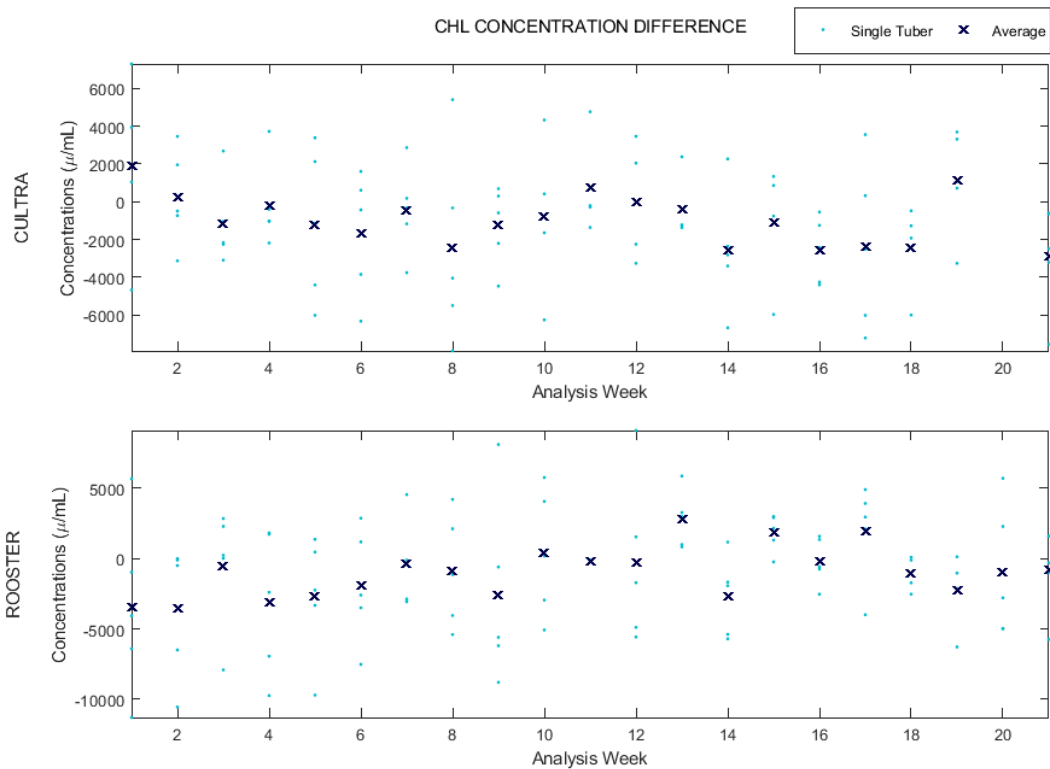
Figure 5:3 Weekly averages of the total Chl concentration calculated of the area under the Eye minus the area under the Background. The graphs show the Chl data point for each tuber analysed (blue dots) as well as the average weekly concentration (black crosses).

5.3.3. Chl Concentration in Tubers after Exposure to Light

A short experiment was completed at the end of the Harvest 2015 study to stimulate Chl production in a collection of tubers. This was done to look for a correlation between the tubers' Vis/NIR spectra and their Chl concentration as measured by wet chemistry.

Ten tubers of cvs Cultra and Rooster were removed from storage and Vis/NIR data recorded for an Eye and Background area on each tuber. The tubers were then randomly split into two groups and exposed to light for several days: the first group was left in laboratory conditions for 7 days, and the second for 14. The tubers were then reanalysed by Vis/NIR spectroscopy, before Chl quantification took place. The same Chl extraction and quantification methods were used as previously discussed.

FIGURE 5:4 shows the average values of the different Chl concentrations calculated from the two sample sets. The plots in this figure also contain the Chl concentration values calculated from the tubers analysed during the last week of the Harvest 2015. This allows comparison to tubers that have not been exposed to any light. The values shown were found by, once again, calculating the difference between the concentration found
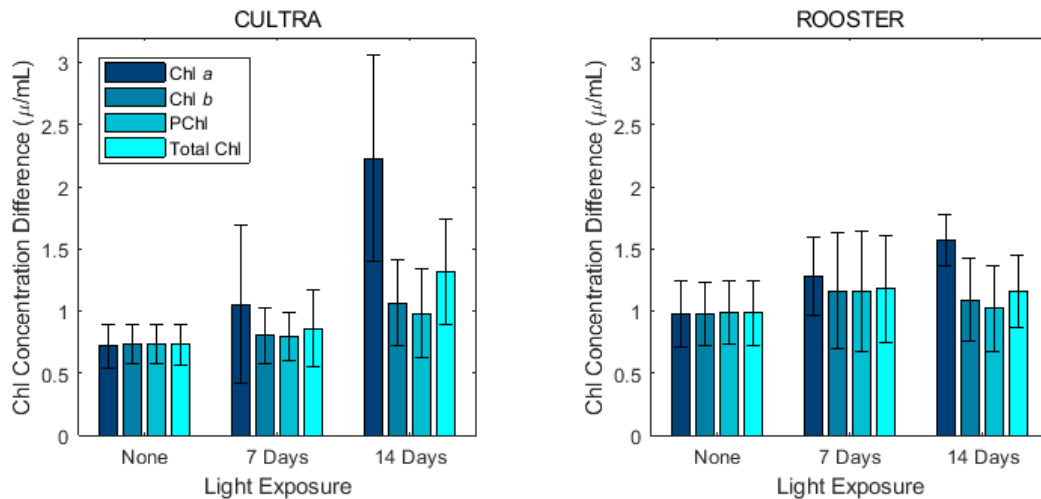
Figure 5:4 Results from an experiment to promote Chl production. Chl concentration difference between the concentration found at the Eye and Background of a tuber. The value shown is the average found from five tubers. The first set of five tubers were exposed to zero light, the second for 7 days and the third for 14 days. The error bars show +/- 1 standard deviation.

at the Eye and Background of the tuber. FIGURE 5:4 suggests that the concentration of Chl in all its forms increases with light exposure. However, the form that shows by far the greatest increase is Chl *a*. This is also consistent with the previous findings that Chl production is greater at the eyes on a tuber in comparison to surface areas without. This figure also shows that the cv Cultra tubers were more active at producing Chl over the two weeks than cv Rooster. The error bars however, show a large variation in the data collected. This could be explained by a couple of reasons; firstly, only four tubers were analysed each week, it has already been seen that tuber from the sample batch can be highly variable, and secondly that these tubers was new each week and therefore the data could not be normalised from week to week. Therefore, this experiment would need to be repeated with a larger batch of tubers for the results to be reliable.

FIGURE 5:5 shows the breakdown of the Chl concentrations for the Eye and Background area separately. This shows the relationships between the Chl concentration present at the two locations. Overall it can be seen that the only significant difference between the two is seen in the Chl a. For Chl *b* and PChl no significant difference is seen between the Eye and Background data.

FIGURE 5:6 contains the complementary Vis/NIR data. The leftmost plots display the Absorbance Chl Bands collected from the ten cvs Cultra and Rooster tubers. Here the two colours represent the varying durations of light exposure. Neither cultivar's Chl Bands show a clear distinction between the differing irradiation durations although Static
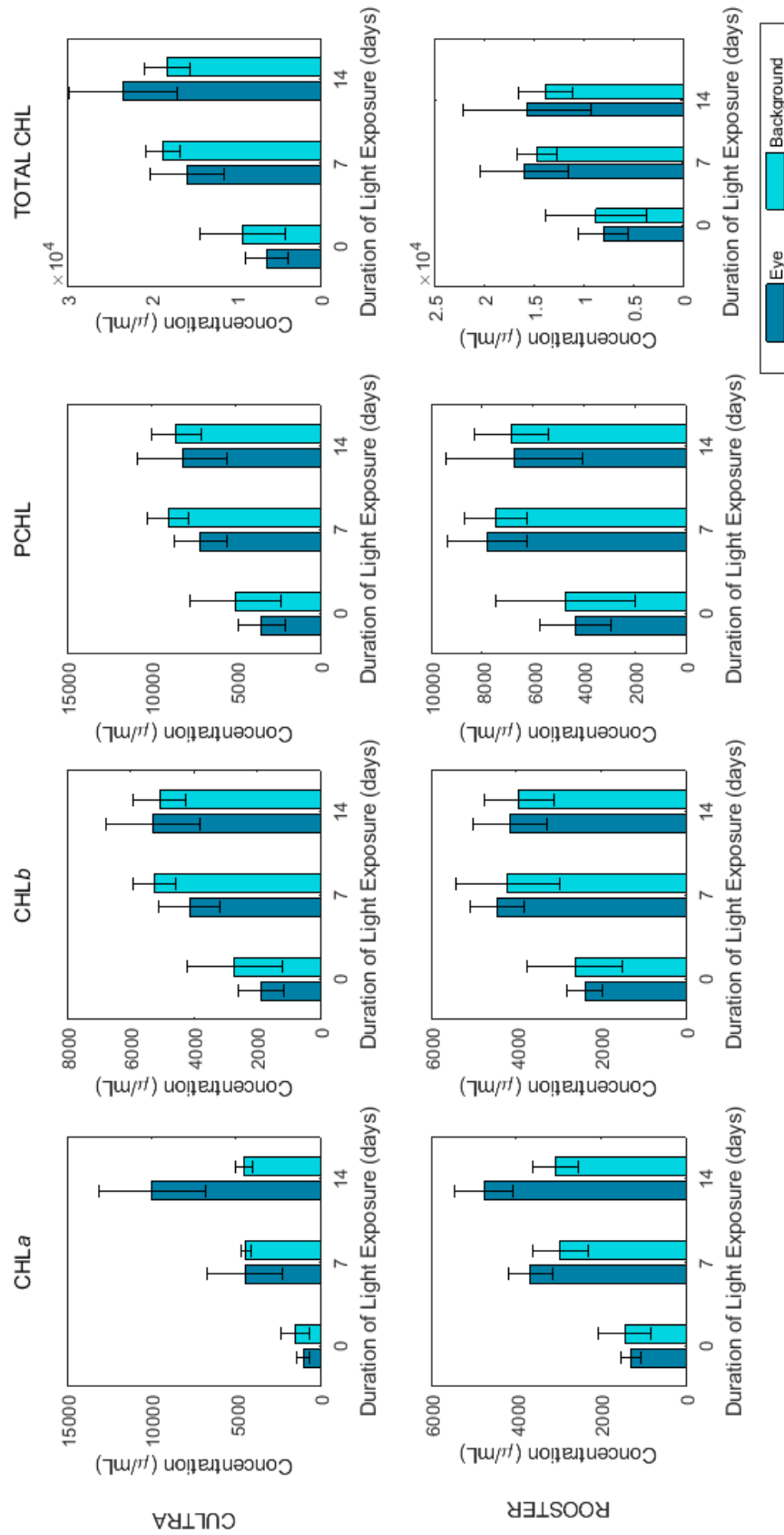
Figure 5:5 Concentration values of the Chlorophyllous species analysed at the Eye and Background. The value shown is the average found from five tubers. Within each plot; the first set of five tubers were exposed to zero light, the second for 7 days and the third for 14 days. The error bars show +/- 1 standard deviation.

Series experiments conducted in 2016 and 2017 showed that the absorbance of the Chl band reached the asymptotic stage of a sigmoidal curve seen in the response of Vis/NIR spectroscopy after ~ 5 days. As these tubers skin did not become deep green in colour, it is reasonable to assume that the saturation points of Chl production had not been met. However, it is possible that the photosynthetic apparatus was subject to cold store damage.

The rightmost plots of FIGURE 5:6 show the quantified Chl *a* concentration against Chl Band Areas of the ten Eyes analysed. A small correlation between the two can be seen for the cv Cultra, but not for the cv Rooster tubers. This may be another example of probe to tuber mis-alignment during the set of up the Vis/NIR spectrometer.
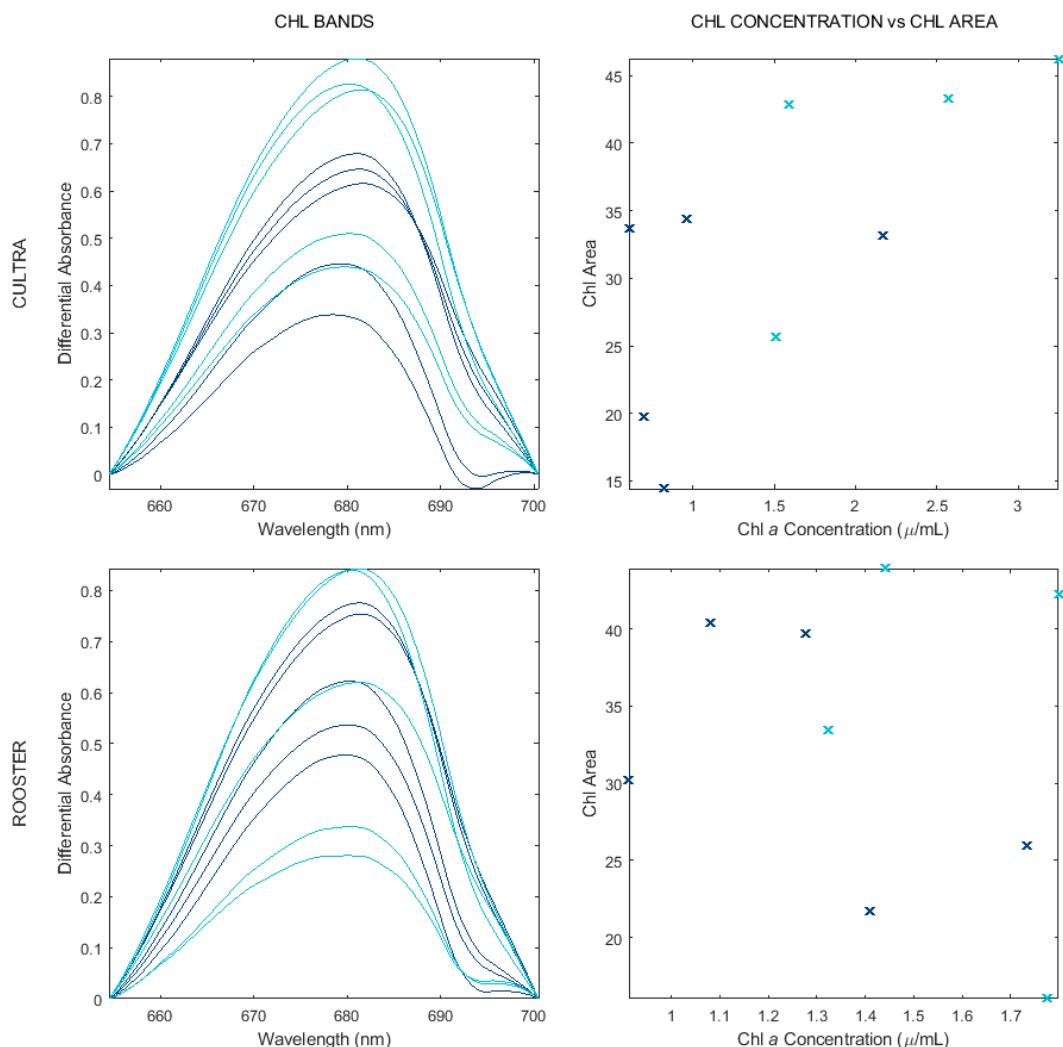
Figure 5:6 Chl Bands and Chl concentration of tubers exposed to either 7 (dark blue) or 14 (light blue) days of light. Both spectroscopic data have been referenced to Background values.

5.4. CONCLUSIONS

The Vis/NIR spectroscopy responses seen from the tubers during Harvest 2015 confirm that tubers stored in the dark do not produce Chl (Grunenfelder et al., 2006b, Gull and Isenberg, 1960, Idelberger et al., 2004, Moran and Porath, 1980). However, they also show that the absorbance band at 675 nm in not influenced by other species of bioactivity occurring in a tuber during cold storage, and can therefore be reliably assigned to the presence of Chl. Furthermore, this confirms that the experimental design of Harvest 2014, involving short intervals of exposure to light under laboratory conditions, was sufficient to stimulate the production of Chl in the tubers analysed.

As the Harvest 2015 tubers nevertheless broke dormancy during the study period, it means that the two biological pathways, formation of Chl and dormancy breaking, are not dependent on one another. Although not previously being suggested in literature, it means that the production of Chl can potentially be indirectly related to dormancy break, although not a direct cause or effect.

RATE OF CHANGE

The two biological pathways, chlorophyll (Chl) production and dormancy break, are believed to be independent to one another. Nevertheless, a link between the two was seen in the data from Harvest 2014. The results from Harvest 2015 confirmed that for this to be investigated further, the tubers must be exposed to light, as otherwise no Chl is produced at all. This goes against the initial idea of developing a passive method of measuring the state of tuber dormancy. Although exposure to light is not physically destructive, it will necessitate the disposal of the test tubers, as the stimulation of Chl production may cause surface greening and this is discriminated against by both consumers and processors (Grunenfelder et al., 2006a).

However, after discussion with the Agronomy manager at Produce World (C. Williams, personal communication, September 14th, 2017) it was learned that tests are regularly conducted in which tubers are removed from storage and put into a "hot box" for 24 hours. The tubers are placed in a container which creates warm (~30 °C), damp conditions. This is done to check for defects on the tuber, such as bruising, soft rot and blight (Pieterse, 2012). The prospect of having to sacrifice a dozen of tubers to give a reliable batch prediction is thus familiar to, and already practiced in, the industry.

The hypothesis to be investigated in the Harvest 2016 and 2017 studies was that the rate of Chl production, and therefore the *Kinetic Rate* of the Chl Band, may change systematically as a tuber approaches dormancy break. This was investigated by exposing tubers to light for several hours during Visible/Near-Infrared (Vis/NIR) analysis and measuring the rate of change of the Chl band area.

Note that the Harvest 2016 analysis was carried out at Sutton Bridge Crop Storage Research (SBCSR) centre; a primary focus of this year was application in industry, which will be discussed further in CHAPTER 7. The static measurements made during this year could only be acquired once or twice a week on each sampled cultivar. The sampling scheme is outlined below. Although large numbers of tubers could not be analysed, the Harvest 2016 study introduced the idea of the rate of change measurement and served as exploratory work in advance of Harvest 2017.

6.1. HARVEST 2016

6.1.1. Introduction

The analysis of Harvest 2016 was carried out at the SBCSR premises. The storage facilities mimicked very closely those used for commercially cold-stored tubers. The SBCSR conducts applied research on the post-harvest behaviour of potato tubers, including pathology and sprout suppression. A cold store unit, built for such research, was assigned to this project. The SBCSR also supplied the tubers (of four different cvs) used during Harvest 2016. One (or two for cv Challenger) tuber was analysed weekly in a Static Series measurement. This was conducted in a second 15 °C storage unit exposed to a halogen lamp for 8 hours. The dormancy state of each tuber was also assessed visually before and after every analysis.

6.1.2. Experimental Procedures for Harvest 2016

Sample Collection and Storage

Samples of cvs Challenger, Lady Claire, Shelford and Maris Piper were obtained and stored at the SBCSR facility from September 2016 to April 2017. The cultivars were cold stored in the dark, at 4°C and 90% RH. Before analysis, each tuber was cleaned of loose mud and dirt using an air compressor.

Spectral Acquisition

The Vis/NIR spectra were recorded using the EPP2000-NIR-200 and the Black-Comet CXR-SR-50 spectrometers, both equipped with a Vis-NIR silica fibre-optic reflectance probe and connected to the same Tungsten/Halogen light source (StellarNet, Inc., Tampa, Florida, USA). A Static Series measurement of each cultivar was analysed once (or twice for cv Challenger) a week, using a fresh tuber removed from cold storage. The standard protocol for this measurement is described fully in CHAPTER 3. An average of 100 scans with an integration time of 50 ms was used for all measurements. For each tuber analysed, 280 spectra were recorded at equal time intervals, over 8 hours. The Static Series seen in CHAPTER 3 (FIGURE 3:2 and FIGURE 3:3) indicated that 8 hours would provide enough time for a response in the Chl band to be seen in the tuber.

The Eye spectra were collected using the first spectrometer listed above whilst the second was used to collect the Background data from the same tuber. Using the same technique as in previous measurements, the probe and tuber were clamped into position to enable the data collection from the same positions for the duration of the data

analysis. The measurements were carried out in a storage unit kept at ∼ 15°C, using a desk lamp to irradiate the tuber during analysis in addition to the spectrometer source. The dormancy state of the tuber was also recorded at the beginning and end of each Static Series, i.e. whether the tuber showed visible sprouting. The measurements at SBCSR facility were carried out by several individuals: Myself (QIB), Lana Head (SBCSR), Stephen Ferrett (SBCSR) and Marion Tout (The University of Sheffield) depending on analysis time and to cover absences.

6.1.3. Results and Discussion

FIGURE 6:1 displays the Kinetic Eye and Background Chl Band Areas against light exposure time for the cv Shelford tubers monitored during Harvest 2016; each plot corresponds to one tuber analysed during a single week. The plots display every seventh area value calculated, 40 in total, to reduce overcrowding and allow a better visualisation of the data. The results suggest that Chl was able to be produced predominantly in the early weeks (up to 17) of the analysis period. The remaining weeks' tubers showed little absorbance change over the 8-hour measurement time. The lag phases in these tubers appeared to last for most of the analysis period. The cv Shelford batch sprouted by week 23.

The cvs Maris Piper and Lady Claire showed similar trends in the Chl Areas (data not shown), in that the capacity to produce Chl appeared greatest in the early (7 ∼ 9) weeks of data analysis. Thereafter only the occasional tuber showed significant change in the Kinetic Chl Areas. These cultivars broke dormancy by weeks 8 and 24 respectively. A tentative explanation for the lack of Chl production seen in the later weeks may be the lower environmental temperatures of 15 °C, compared to the 21 °C of the Norwich laboratory. Low temperatures have been suggested to damage the ability to photosynthesize (Sundbom et al., 1982). Out of trend, the cv Challenger tubers fluctuated between inactivity and activity in the Chl absorbance throughout the 26 weeks.

The Kinetic Background Chl Areas of the cv Shelford tubers are also displayed in FIGURE 6:1. The activities of the Eye and Background broadly have the same pattern over the course of the study. However, there are some differences, and these are most obvious for cv Shelford. Specifically, a few tubers showed a Chl absorbance change only at the Eye, and a couple showed more activity in the Background in comparison to the Eye. This can be observed by comparing the two rows in FIGURE 6:1.
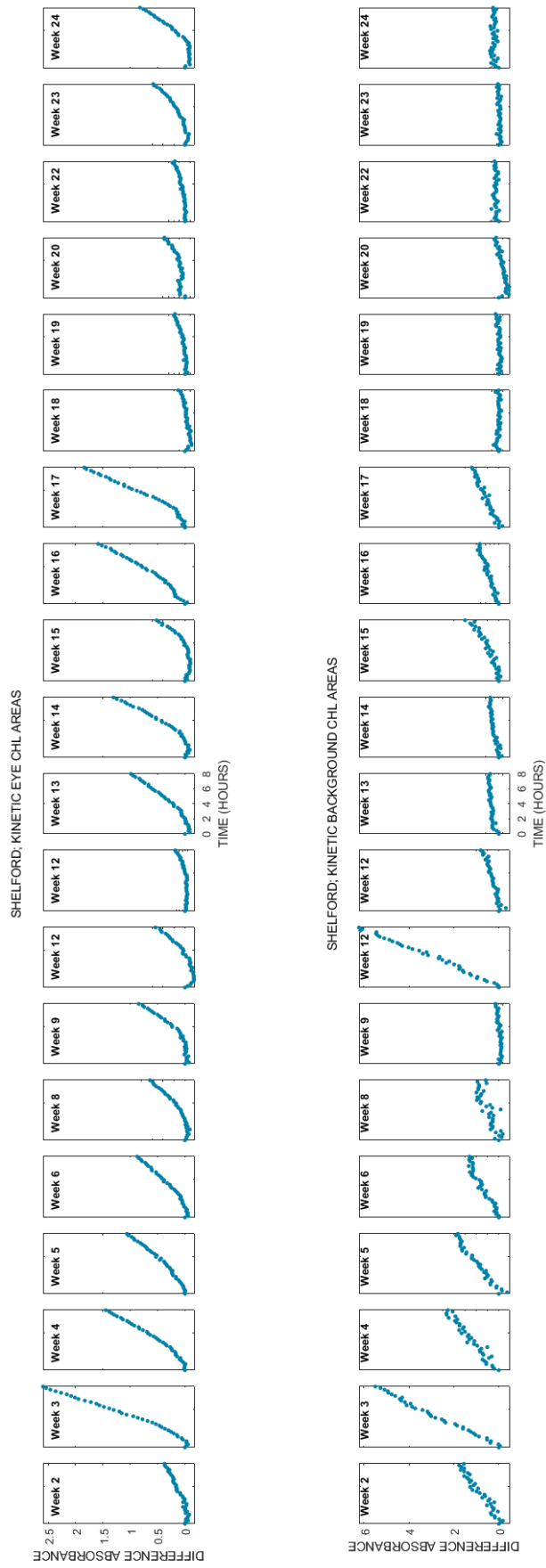
Figure 6:1 Kinetic Chl Areas of the cv Shelford tubers sampled in Harvest 2016. Each plot contains 40 spectra collected over 8 hours. The rows separate the Eye and Background data.

As for the Eye measurements, the cvs Shelford, Maris Piper and Lady Claire tubers also showed greater Chl activity at the beginning of analysis for the Background. Once again out of trend, the cv Challenger data showed very little activity in the Chl production in the Background areas of the tubers throughout the experiment.

In summary then, three out of four cvs, showed generally greater Chl activity at the beginning of the experiment compared to the end, for both the Eye and Background. This is consistent with the hypothesis, arrived at in CHAPTER 4, that dormancy break occurs at some time after the period when the tubers are most able to generate Chl under stimulation. However, there are other potential explanations for this finding: as well as cold temperature damage, it could be due to the increased respiration rate seen in tubers immediately after harvest, suggesting the tuber has not yet entered a dormant state (Schippers, 1977).

To visualise this further, the 'Chl Rate' of each kinetic series was calculated. The polyfit.m MATLAB function was used to find the linear regression of each kinetic series. Due to the initial lag phase seen in most of the data, the gradient was extracted using the Chl Area value from the final two hours only. The linear regression was used to assign a Chl Rate (i.e. the absorbance change over a time) to each measurement. The upper row of FIGURE 6:2 displays the Eye Chl Rates of the four cultivars, plotted against analysis week. It is seen that the Chl Rates in general decrease over the analysis period of Harvest 2016.

The lower row of plots shows the 'Chl Difference Rate' calculated by finding the difference between the Chl Rates of the Eye and Background series measurements, taken at the same time point on the same tuber. Generally, the Eye locations are more active than the Background (evidenced by positive values on the y axes). This is consistent with previous indications of greater bioactivity under the eye. However, these plots are quite noisy, and no firm conclusions can be drawn on any trends in the relative activities of the Eye and Background locations over this study. Note also that the Background raw data are also generally noisier than the Eye and were collected with a different spectrometer. Overall, it seems likely that the Chl production under the Eye after 8 hours follows the same pattern over the course of the study as than that of the Background. This would be in keeping with the results of Harvest 2014 (FIGURE 4:5).

In the Harvest 2014 study, the same tubers were analysed each week; this meant that the tubers were exposed to intermittent light over the analysis period, hence it was logical and straightforward to plot the cumulative value of the Chl Areas against time. To compare Harvest 2016 in a similar way, the cumulative Chl Rates of each cv were
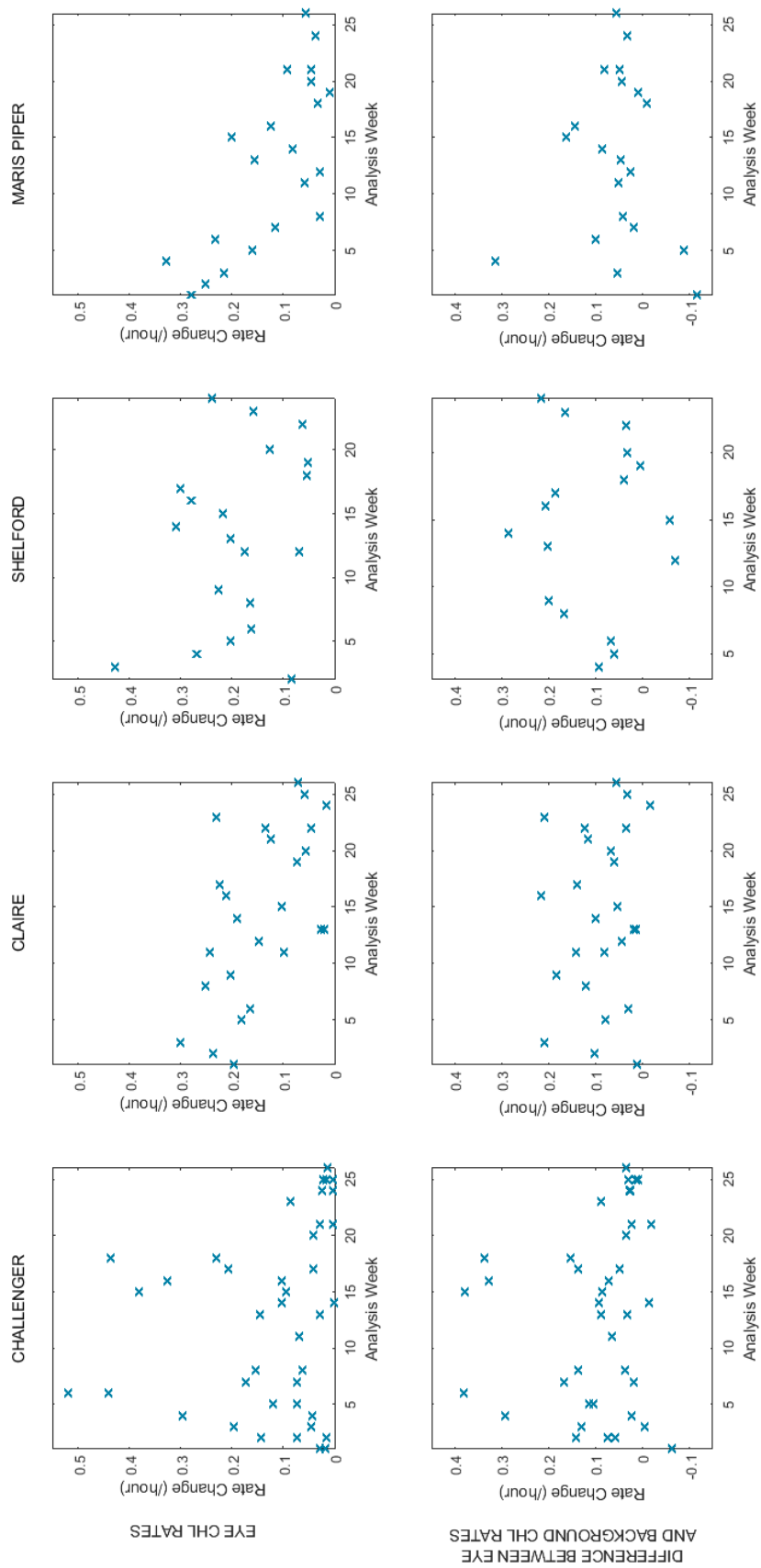
Figure 6:2 Chl Rates of the tubers analysed from Harvest 2016. The upper row displays the Eye Chl Rates, whilst the lower row shows the Difference Chl Rates. The columns separate the four (titled) cvs analysed.
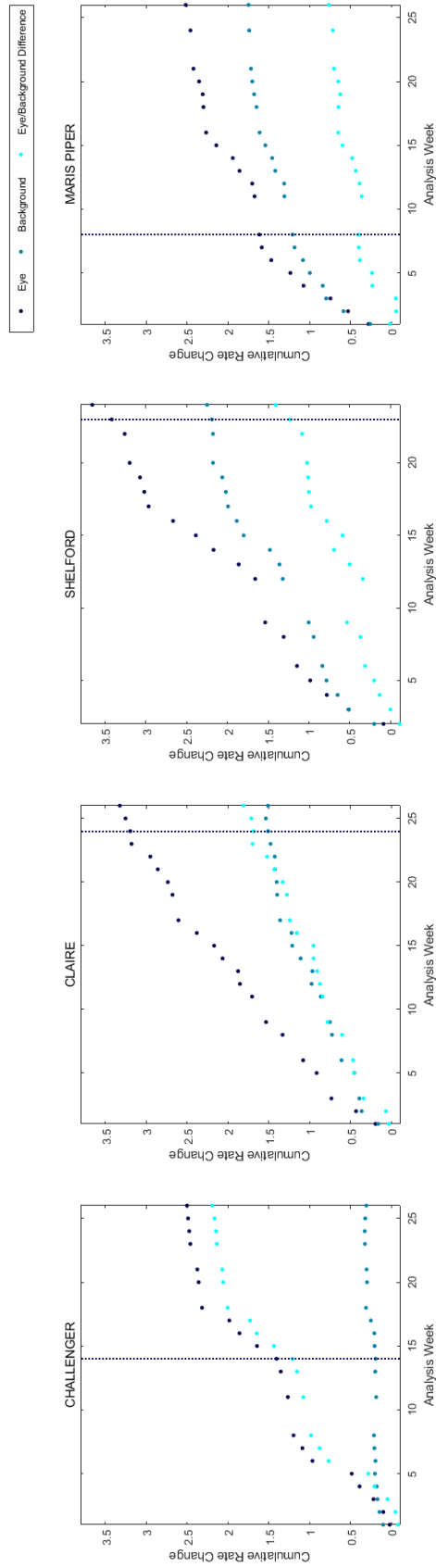
Figure 6:3 The cumulative Eye Chl Rates of the four (titled) cvs analysed for Harvest 2016. Each plot contains the values for the Eye. Background and Difference Chl Rates, as well as a vertical line indicating the batches time of dormancy break.
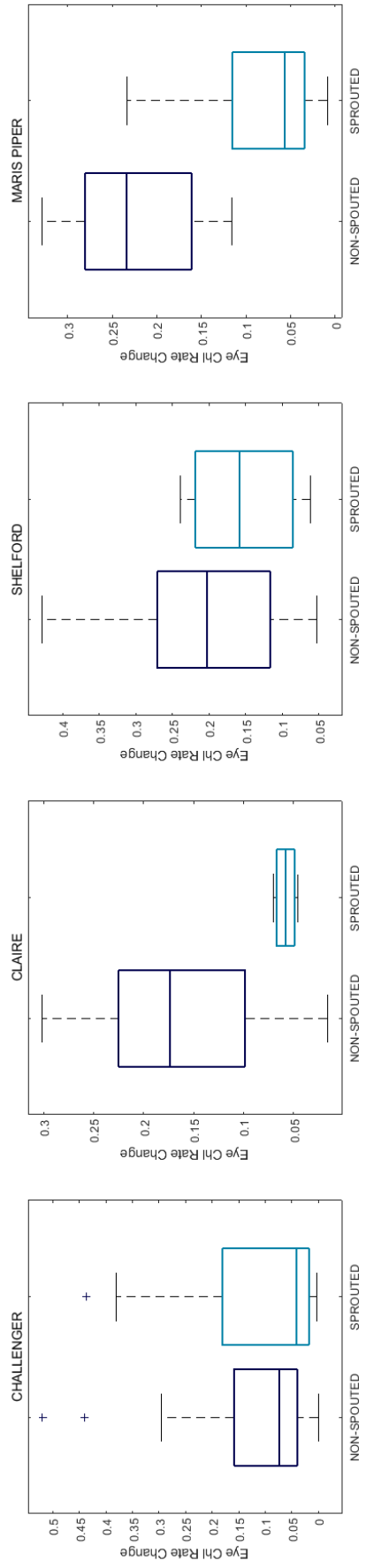
Figure 6:4 Eye Chl Rates of Non-sprouted and Sprouted tubers of the four (titled) cvs from Harvest 2016.

calculated from the weekly Chl rate data and plotted against analysis week. These plots can be considered as growth curves for essentially a batch-wise "virtual tuber". Effectively, each tuber analysed is used as a representation of the current state of the cv batch remaining in store at that time. This was done for the Eye, Background and Difference (Eye minus Background) Rates. Outcomes are displayed in FIGURE 6:3.

The growth and asymptotic phases, like those identified in CHAPTER 3, can be seen in FIGURE 6:3. cvs Challenger, Shelford and Maris Piper show a growth phase up to weeks 18, 16 and 8 respectively, and asymptotic phases thereafter. The cv Lady Claire tubers appear to show a steady growth throughout the analysis period. This cv was the last to break dormancy; had the analysis continued the asymptotic stage may have been reached.

Each cv batch sprouting date is indicated by the vertical line within each plot. For the Harvest 2014 data, the location of dormancy break was found to occur just before the asymptotic stage. However here in FIGURE 6:3, the line locations relative to the sigmoidal growth curves show no consistency between cultivar. It is not clear why, although since only one tuber was analysed per week, the cumulative curves are therefore highly influenced by the state of individual tubers. This is a primary motivation for the revised sampling scheme adopted for the subsequent Harvest 2017 study.

The dormancy lines on FIGURE 6:3 indicate when the batch majority (>75%) had started sprouting, but do not indicate the specific dormancy states of the individual tubers analysed. The dormancy state of all tubers analysed, non-sprouted and sprouted, was recorded at the start of their measurement. The boxplots within FIGURE 6:4 summarise the Eye Chl Rates in each case. Disregarding the cv Challenger tubers, which are again out of trend, the boxplots show that the Chl Rates are substantially reduced once the tubers have sprouted. This agrees with the results seen in FIGURE 4:5 (harvest 2014) where the Chl growth curves reached an asymptotic stage after the tubers had begun to sprout.

6.1.4. Conclusions

The Harvest 2016 study saw a change in the experimental approach, from point measurements of the Chl band to Chl rates of change over a period (hours) of exposure to light. Broadly, the responses of tubers were consistent with those seen in previous, comparable Static measurements. However, detailed examination of the results revealed

somewhat different behaviours from those hypothesised at the start of the Harvest 2016 experiments.

The treatment and conditions to which the tubers were exposed to immediately after harvest may have influenced the outcomes. Although the SBCSR facility in Sutton Bridge is predominantly allocated to potato research, the vast number of different cultivars and tuber samples coming into the facility during the harvest season affects the treatment these tubers received at the beginning of storage. Indeed, the curing stage is sometimes curtailed, and samples placed direct into cold storage (in preference to leaving them outside storage). These tubers are then shocked into cold storage, rather than brought down gradually until they can become truly dormant with little bioactivity occurring. Farmers cannot predict exact dates for harvest, which then means samples are just brought into the facility when ready – with limited space this makes it difficult to treat the incoming tubers with optimum conditions for curing. The absence of a curing stage may be the cause for the unseen lag phase within these tubers.

The results from Harvest 2014 showed that an average measurement was needed to show a stable reading of the tubers' behaviours, and in these results the point of batch dormancy break was seen just before the asymptotic stage of the Chl growth curves. However, in the comparable results from Harvest 2016 (FIGURE 6:3), the batch dormancy break lines did not show similar placement across cvs, or to the placements seen in Harvest 2014. Although the protocol of Static Series measurements used in Harvest 2016 removes the repositioning error arising from the changing alignment of the probe and tuber, it must be questionable whether analysis of a single tuber per week is sufficient to deliver a batch reading of the crops' dormancy state. This shortcoming provided the motivation for the revised sampling scheme adopted in the next section.

6.2. HARVEST 2017

6.2.1. Introduction

Issues around sample storage and data collection in Harvest 2016, which will be discussed in full in CHAPTER 7, meant that full control of the environment and data collection was desirable for the final harvest experiment. The facilities became available at the Quadram Institute, where a storage unit could be assigned to this project alone. It was also evident by this time that a larger sample of tubers, even for Static Series experiments, needed to be analysed to overcome tuber to tuber variance. Finally, a

suspicion arose that eight-hour analysis/light exposure periods were not long enough to allow the linear phase in the response of Chl to be reached. Several tubers analysed during Harvest 2016, showed a lag phase of similar duration to that of the analysis period, meaning a steady growth rate of Chl production may have not been met for all the tubers within the 8 hours. With these in mind, Harvest 2017 was designed to monitor a significant number of tubers, for a longer analysis period that would allow all tubers enough time to start producing Chl at a constant rate.

6.2.2. Experimental Procedures for Harvest 2017

Sample Collection and Storage

A large sample of each of cvs King Edward, Maris Piper and Orchestra were obtained from Produce World Group (Sutton Bridge, Lincolnshire), at the end of September 2017. The tubers were placed into cold storage at 12 °C. The storage room lights were permanently turned off and the room contained a humidifier to ensure a relative humidity of between 85 – 95%. A curtain was also added between the entrance door and the tubers, to ensure the tubers were not exposed to outside light when entering and exiting the room. The tubers were transferred from the sacks in which they had been delivered to plastic crates. This was to allow air flow through the tuber piles to reduce "hot spots" during the storage period. Finally, the room was locked so it could not be entered by others accidentally.

For the first few weeks the tubers were cured by reducing the room temperature slowly by 2°C each week, until a temperature of ~6 °C was reached, as a curing phase for these tubers (Kim and Lee, 1992). At this point the relative humidity within the store had stabilised to ~91%. Although the normal storage temperature for prolonged storage is 4 °C, this temperature was chosen to accelerate the biological processes somewhat. The aim was to limit the overall study time to around 3-4 months, by which time it was anticipated that even the long-dormancy cvs would have sprouted.

Sample Preparation

The afternoon before analysis, a sample of 15 – 20 tubers from each cultivar was randomly taken from the plastic containers kept in cold storage. Still inside the storage unit, excess dirt was removed from the tubers using a soft brush. Each tuber was then labelled with its cultivar identity ("K", "M" or "O") and placed into a large cool box. This process was done under green light to ensure that Chlorophyll production was not

stimulated during cold storage. These tubers remained in the storage room overnight, with the lid of the cool box open.

The following morning, these tubers were transported to the lab in the cool box for the start of analysis. For each cv, 10 suitable cv tubers were selected and analysed (this number was chosen for simple pragmatic reasons – it was the most that was feasible in the timescale, collecting data for each tuber three times per day, with approximately four mins per setting up/acquisition etc.). Tubers were removed from the cool box one at a time to ensure every tuber was exposed to as little light as possible before the initial measurement was recorded. A larger sample group than needed was taken from the cold storage to allow unsuitable tubers to be discarded. A tuber was deemed unsuitable due to the presence of deep set eyes, skin damage, signs of disease or large sprouts (> 2 mm). The analysis order by cv was King Edward, Maris Piper, Orchestra. Harvest 2017 saw more than 300 tubers analysed in total.

Spectral Acquisition

The Vis/NIR spectra were recorded using the StellarNet Inc. EPP2000-NIR-200 spectrometer, equipped with the fibre-optic reflectance probe and a Tungsten/Halogen light source. The spectra were collected using the standard protocol described in CHAPTER 3. Over three consecutive days, the same tubers were analysed nine times. The spectra from the same Eye and Background areas on each tuber were recorded in three replicas at each time point. Spectral measurements were recorded in the morning, at midday and during the afternoon of each day, all approximately three hours apart. Between analyses the tuber was left at room temperature and exposed to constant ambient lab lighting.

Visual Dormancy Monitoring

The sprouting activity of each tuber was monitored throughout the period of Vis/NIR analysis. This was to enable the definition of a post-harvest "Sprouting Age" for each tuber. Before the initial Vis/NIR data was recorded, the intended Eye was examined for the presence of a sprout. The dormancy state of this Eye was recorded as 0 for non-sprouting and 1 for sprouted. A non-sprouting Eye was then re-inspected each subsequent day for the appearance of an emerging sprout. If a tuber was not showing visible sprouting by the last time point of analysis, then the tubers remained in the Norwich laboratory (room temperature with constant ambient lighting) until the growth of a sprout could be seen. In this case, the date was recorded on the day on which a sprout was first observed.

6.2.3. Results and Discussion

The Kinetic Chl Bands were calculated for each tuber analysed during Harvest 2017. To allow visualisation of data from all tubers, FIGURE 6:5 displays only the final Chl Band from each Kinetic series, shown by the ten light blue Chl Bands within each plot, for each analysis week as indicated by the title, arranged by week (columns) and cultivar (rows). This immediately highlights the considerable variation across the measurements of the ten tubers. Even though the tubers were kept in the same cold storage and sampled for analysis at the same time, there was large tuber to tuber variation in the activity of Chl production seen during the same analysis week throughout.

In contrast to the Harvest 2016, these Kinetic Chl Bands show that Chl was produced throughout the study, in both the Eye (FIGURE 6:5) and Background (data not shown). The majority (~80%) showed a greater change in the Chl absorbance for the Eye in comparison to the Background, consistent with previous findings. The remaining tubers either showed an increased response in the Background area, or similar absorbance in both. These three behaviours are another example of tuber to tuber variation. This reiterates that a larger sample size is needed to reduce the influence of irregular tubers on a batch prediction.

The dark blue Chl Band, shown in every subplot of FIGURE 6:5, shows the median band measured that week. Some subtle trends can be observed in the changes in the median Chl Band from week to week (also the case when using the mean). A small decrease, from the start to the end of the study, is seen in the kinetic absorbance of the cv King Edward tubers. The cv Orchestra show a small opposing trend of increasing kinetic absorbance, whilst the cv Maris Piper tubers show a slight increase from the beginning to middle, followed by a decrease from middle to the end of the study. These trends may be explained by the varying dormancy lengths attributed to each cultivar. Specifically, cv King Edward is known to have a short dormancy, cv Maris Piper a medium and cv Orchestra a long dormancy. These results illustrate that the three cultivars behaved differently. Trends of the same nature were seen in the Background Chl Bands for each cultivar.

A second source of tuber to tuber variation is the inherent state of dormancy at the time of analysis. When a tuber was selected for data analysis this variable was unknown, i.e. was the tuber due to sprout in hours, days or weeks? Of course, if sprouts were already present on the eyes then it was known that dormancy had broken in storage. TABLE 6:1 displays the number of tubers that had already broken dormancy when removed from
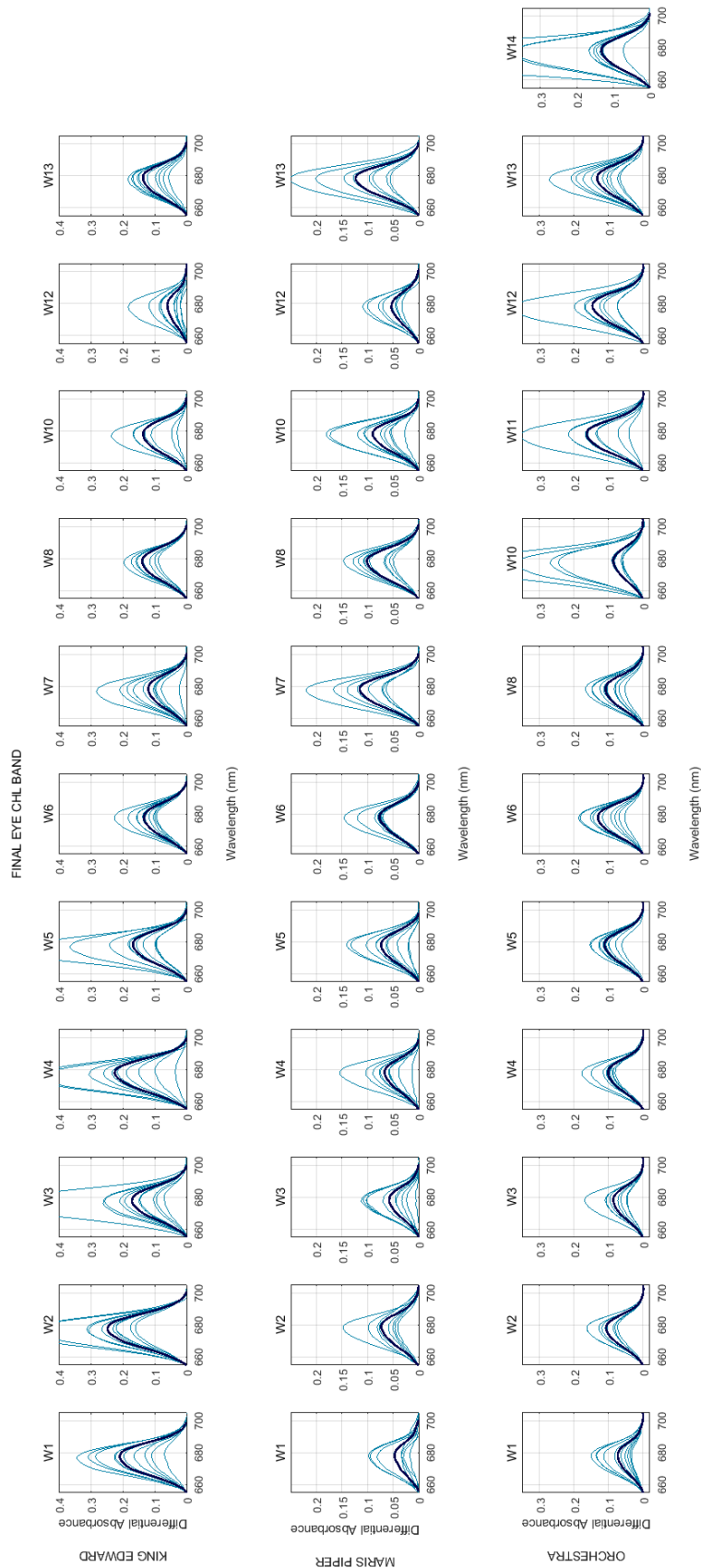
Figure 6:5 The final Chl Bands taken from the ten Kinetic Eye Chl Bands collected in each week. The rows separate the cultivars, whilst the columns separate analysis weeks. The averages (medians) are plotted in dark blue.

cold storage, during each analysis week. This data was used to give an indication of the three cvs batch dormancy state. The majority of the cv King Edward tubers had sprouted by analysis week 10; the cv Maris Piper by week 13; and the cv Orchestra by week 16.

During and after analysis, dormant Eyes were examined daily to look for the onset of sprouting. This was done to characterise each tuber with a "Sprouting Age" and provide a quantitative variable describing the tubers' dormancy state at the point it was removed from storage. Essentially the age indicates the number of days, counting from the initial day of analysis, until the Eye (used for analysis) first showed visible signs of sprouting.

Table 6:1 The number of tubers that were characterised as having broken dormancy on removal from cold storage before analysis had begun.

ANALYSIS WEEK		NUMBER OF TUBERS SPROUTED (/10)		
Date	No.	King Edward	Maris Piper	Orchestra
18.10.17	1	2	1	-
25.10.17	2	3	1	-
31.10.17	3	3	1	0
07.11.17	4	4	2	0
14.11.17	5	2	0	0
21.11.17	6	1	0	0
28.11.17	7	6	0	0
05.12.17	8	3	0	0
13.12.17	9*	-	-	-
19.12.17	10	9	2	0
26.12.17	11*	-	-	-
03.01.18	12	10	4	3
09.01.18	13	10	10	4
17.01.18	14	-	-	5
24.01.18	15	-	-	7
31.01.18	16	-	-	10

* Week 9 is absent due to illness and week 11 due to the Christmas break. Sampling ceased once all tubers had started to sprout.

For tubers selected in the random sample that were found to have started sprouting in storage, an accurate measurement of a (negative) Sprouting Age was not possible. Instead, the length of the sprouts was used as a proxy, to give an indication of time passed since dormancy break had occurred. The Sprouting Ages and sprout lengths were then used to categorise the tubers into different states of dormancy. TABLE 6:2 shows the

classification for this. Group 1 defines the tubers that had the longest post-analysis time until dormancy break, whilst Group 7 defines the tubers that had the largest sprouts and were therefore the longest out of dormancy. This was used to explore whether the inherent physiological state of dormancy at the time of removal from storage influenced the tubers Chl response as recorded during the subsequent two days of data collection.

Table 6:2 Sprouting Age Groups - dormancy classification according to the sprout length or the number of days until tuber sprouting occurs.

GROUP	SPROUT LENGTH (mm)	SPROUTING AGE (DAYS)
1	N/A	22+
2	N/A	15-21
3	N/A	8-14
4	N/A	4 – 7
5	N/A	0-3
6	< 1	N/A
7	> 1	N/A

The Kinetic Chl Areas, plotted against analysis time in elapsed hours from the initial measurement, were used to calculate Chl rates for the data analysis of Harvest 2017. The typical nominal hours at which spectra were recorded were 0, 3 and 6 hours on day 1; 24, 27 and 30 on day 2; and 48, 51 and 54 on day 3. The Kinetic Eye Chl Areas and Sprouting Age Groups were used to see if the tubers close to breaking dormancy had a characteristic behaviour with regards to the Kinetic Chl Area or Chl rate, compared to tubers in a deeper state of dormancy. FIGURE 6:6 shows the kinetic series of each cv Maris Piper tuber analysed for Harvest 2017, separated by analysis week and coloured according to its dormancy grouping. The bluest dots represent the tubers with the longest time until dormancy break, whilst the greenest dots represent tubers that have already broken dormancy. Results from Harvest 2014 suggested that the Chl absorbance change would be greatest for Groups 4-5, when the tubers were close to, but had not yet, broken dormancy. Groups 1 and 7 would be expected to show little change in the Chl Band according to the sigmoidal behaviour seen in Harvest 2014, and the latter for Harvest 2016.

However, it is difficult to see trends in the data with many points on a single plot, therefore the Chl Rate was calculated for each tuber to aid data exploration. An important observation made from FIGURE 6:6 nevertheless is that outlier values appear to be present within some kinetic series. The isoutlier.m MATLAB function was therefore
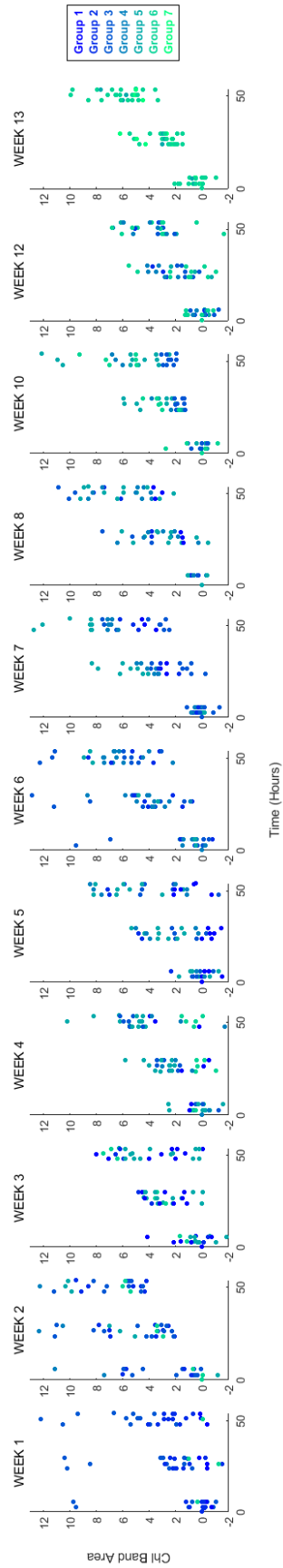
Figure 6:6 The Kinetic Eye Chl Areas, plotted again analysis week, for all cv Maris Piper tubers. The plots separate the analysis weeks. The colour from blue to green represents the 7 Sprouting Age Groups used to classify a tuber's dormancy state.
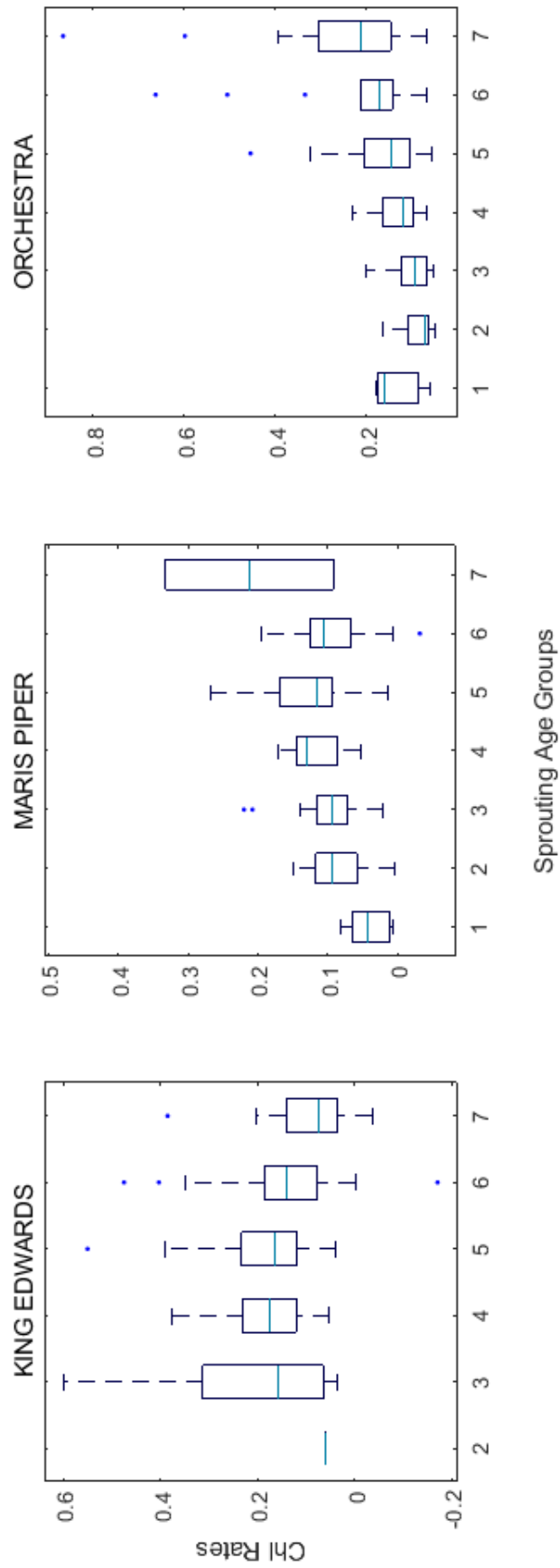
Figure 6:7 The Eye Chl Rates of the three (titled) cvs from Harvest 2017, plotted according to Sprouting Age Groups.
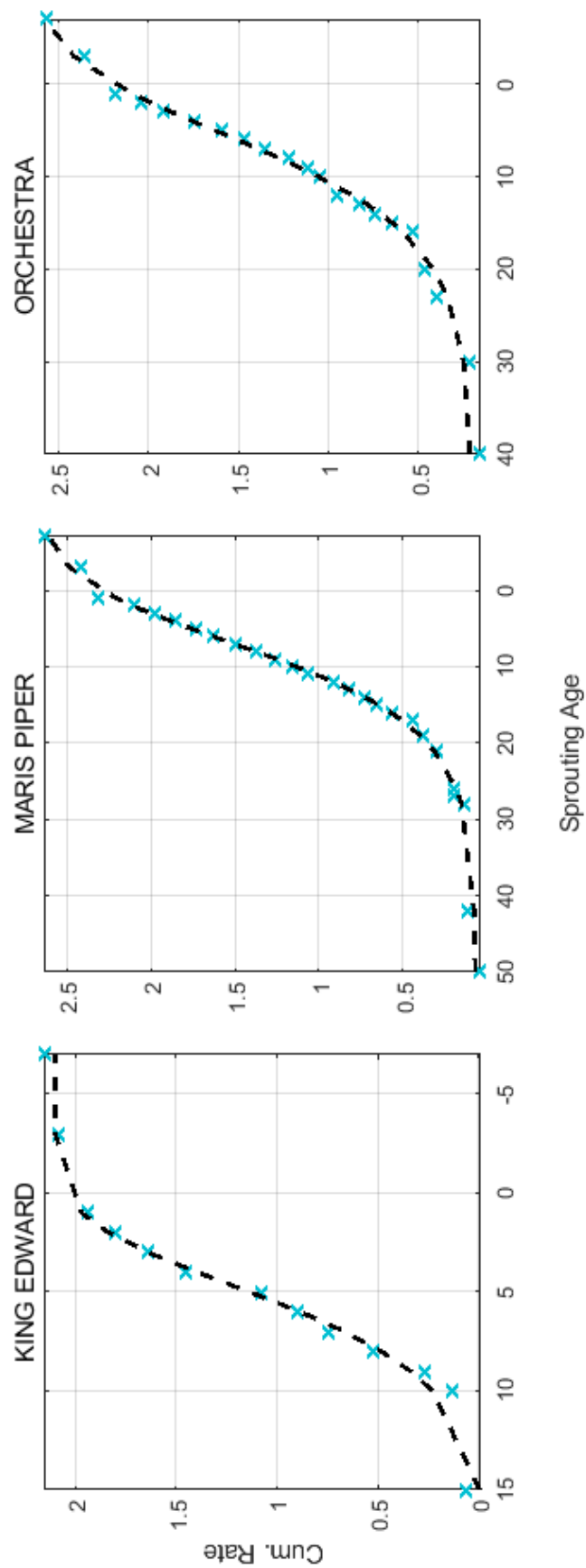
Figure 6:8 The cumulative Eye Chl Rates of the three cvs analysed for Harvest 2017. The blue crosses show the cumulative rate up to that sprouting age, whilst the black dashed line shows a fitted Richards curve.

used to reject any clear outliers when calculating the Chl Rates for each tuber. FIGURE 6:7 shows the Eye Chl Rates plotted against Sprouting Age Groups.

By tracking the median value in the boxplots grouped by Sprouting Age, and referring to the explanatory figure in CHAPTER 2 (rightmost of FIGURE 2:1), the Chl Rates show the potential for a similar sigmoidal behaviour to that in the growth curves in FIGURE 4:5 (Harvest 2014) and cumulative rate plot in FIGURE 6:4 (Harvest 2016). The plots showed similar trends for cvs Kind Edward and Maris Piper; disregarding Group 7 (already sprouted) for cv Maris Piper, the greatest Chl Rates were seen in tubers with 4-7 days before dormancy break. Groups either side either show a slightly lower Chl Rate. The cv Orchestra tubers however show an increasing Chl Rate from Group 2 – 7, suggesting that Chl activity did not reach a maximum close to dormancy break.

To try and replicate the result seen by Harvest 2014 and 2016, the cumulative Chl Rates were plotted against Sprouting Age (not Groups). Tubers with the same Sprouting Age were used to calculate a median Chl Rate for that age. For example, nine cv King Edward tubers were assigned with a Sprouting Age of 5, the Chl Rates calculated for each tuber were pulled together to find a median. The median values were then used to find the cumulative Chl Rate, FIGURE 6:8 shows the results plotted against Sprouting Age. This plot shows great likeness to FIGURE 4:5 for Harvest 2014, for all three cvs. Note that the asymptotic phase is only just seen by the cvs Maris Piper and Orchestra, this may be due to the cease of analysis shortly after the batch had sprouted. The positioning of the sigmoidal curve also shows that the when the Sprouting Age is at zero, the tubers have entered the asymptotic stage of their behaviour in Chl production.

6.2.4. Conclusion

Results from Harvest 2016 suggested that measuring stimulated Chl rates holds the potential for making predictions about the instantaneous dormancy state of the tuber. A longer measurement time of ~60 hours irradiation allowed all tubers to produce a changing response at the Chl band. However, not only does the large tuber to tuber variation need to be accommodated, this study has also shown clear inter-cultivar differences in behaviour. For cv King Edward, the Chl absorbance change was greatest at the beginning of storage. However, the cvs Maris Piper and Orchestra did not show the same behaviour; their Chl activity increased during the analysis period.

Although it has been previously shown that the stimulation of the Chl absorbance at 675 nm happens for all cultivars, the trends of its response are different in storage dependent on cultivar. Although the results from Harvest 2016 also hinted at this, the small sample sets made it unclear whether this was due to tuber or cultivar variation. However, as analysis was carried out on a larger sample numbers for Harvest 2017, it shows a cultivar variation in addition to the tuber to tuber variation. These factors will make it difficult to outline a single analysis method that will give a batch dormancy prediction for different cultivars stored commercially; cultivar-specific models may be required.

Most importantly, this Harvest study was able to replicate the behaviours seen in Harvest 2014, even though completely different tubers were analysed each week. These tubers will much more accurately represent the contemporaneous state of the stored batch, considering the sampled tubers will have been treated in the same way up to the point of removal from storage for analysis.

In this harvest study, the post analysis progress to dormancy break was accelerated by exposing the tubers to more optimal conditions for biological activity. Under these experimental conditions, cvs King Edwards and Maris Piper were seen to be most active with regards to the Chl rates at around 3-4 days before dormancy break. (For cv Orchestra, a rate threshold would be a better route for predicting dormancy break.) Although this seems like a small-time frame for store manager to act upon, the conditions of cold storage mean that this will not occur quite so quickly in practice in commercial storage.

SPUD

7.1. INTRODUCTION

Early in the project a patent for this technology was filed through Plant Bioscience Limited, UK (Wellner and Kemsley, 2017). This patent outlines the use of optical reflectance in predicting when a potato tuber will sprout. The idea is that using a wavelength range of 600 – 750 nm, and specifically the Chlorophyll (Chl) band, to measure both the Eye and a reference spectrum from the same tuber, a prediction on tuber dormancy can be calculated. This patent was filed in September 2016 and published in March 2017. During the process of finalising the patent, an award was secured from the Norwich Research Park Translational Fund to design and build a piece of equipment that would be suitable for the commercial market. Initially a brain storming meeting was arranged with Cambridge Design Partnership, who were commissioned to engineer the prototype, in October 2015, to outline the key components needed for the technology. The following specifications and requirements were discussed:

- The device must be able to differentiate the 680 nm absorbance band from neighbouring non-responsive wavelengths.
- Must work on multiple cultivars, that is, with wide range of shapes/colours
- Must be simple to use by unskilled users.
- Must be robust, and able to work in cold, wet, and dusty environments.
- The devices should be retailed at less than ~£1000.
- Capable of having driver and analysis software easily modified and updated.

It was agreed that the equipment would consist of two measurement concepts. The first was based upon a Hamamatsu C12666MA Micro Spectrometer Head (Hamamatsu Photonics K. K., Japan) due to its suitable operating wavelength range of 300 – 800 nm, small size, and low cost. In volume this spectrometer component is ~£100 each. A white LED broadband illumination was placed around the spectrometer as the source. The second concept was to place three red LEDs emitting at the wavelengths of 630, 650 and 690 nm close together to illuminate the tuber in sequence, and to measure the reflectance using a single element photodiode detector. The idea behind these LEDs was to measure specifically the Chl band as well as two wavelengths to the sides of the peak to provide a baseline.
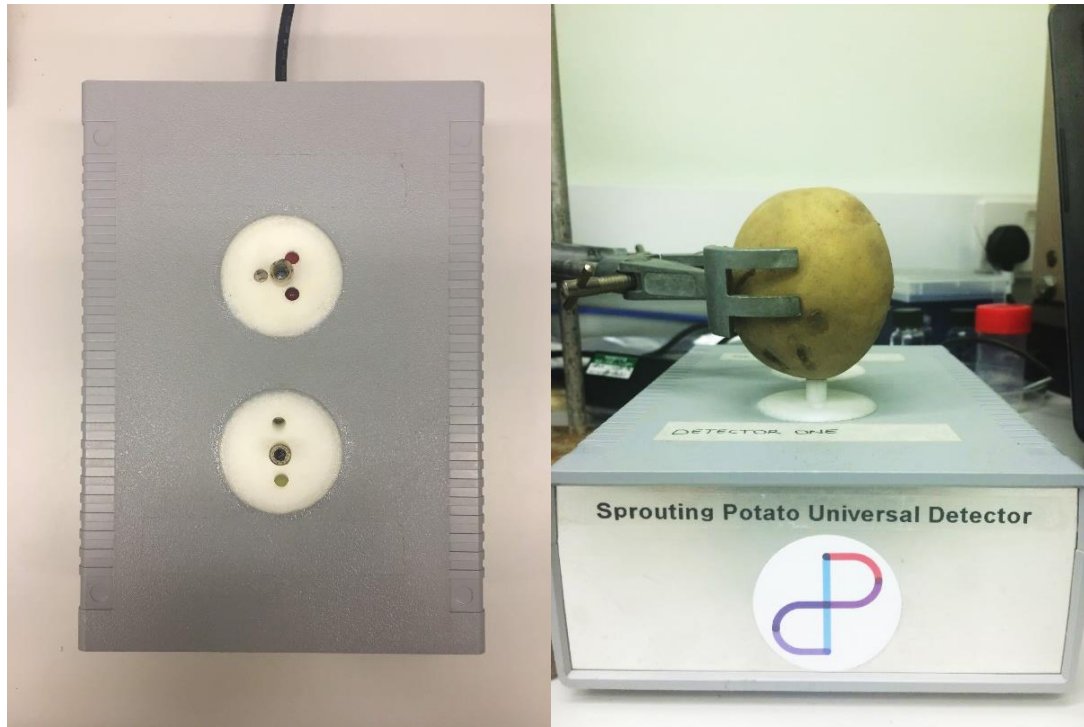
Figure 7:1 Photos of the SPUD equipment. Photo 1 (left): Aerial view, LED analysis is located at the top and Hamamatsu spectrometer at the bottom. Photo 2 (right): a tuber set up for analysis on the SPUD, by clamping the tuber over the Hamamatsu spectrometer situated within the grey box.

Both concepts were integrated into one prototype unit; therefore, the two could be assessed separately and against one another to see if either could be used as an effective measurement method in the future. This piece of equipment was named the Sprouting Potato Universal Detector; or SPUD. FIGURE 7:1 is a photograph of the final prototype. The left photo shows the aerial view of the system whilst the right photo shows a tuber set up for analysis. The aerial view shows the Hamamatsu spectrometer at the bottom of the picture whilst the LEDs are seen at the top.

FIGURE 7:2 shows a comparison of the optical paths taken during Vis/NIR analysis with a fibre-optic probe (left) and the layout of the LED and detectors in the SPUD (right). Ultimately the transmitted light paths are similar for both methods, however the SPUD diagram shows that the light reflected from the surface skin will not be present (as it is in Vis/NIR) and further, the contribution from ambient light cannot affect the measurements taken since the tuber surface skin is in complete contact with the detector cylinder.

Harvest 2016's experiments were completed at Sutton Bridge Crop Storage Research (SBCSR) and were planned with an industrial focus. The outcome of results, outlined below, from the SPUD were broadly comparable to the Vis/Near-infrared (Vis/NIR)

data collected in the same year (see CHAPTER 6.1). The same general experimental protocols (sample numbers, tuber storage and preparation, etc) were used here, and will therefore not be discussed in length. This Chapter focuses on the practicality of the SPUD equipment and the application of tuber assessment in commercial stores.

Figure 7:2 Optical light path of the spectral measurements using the fibre-optic probe (left) and the SPUD equipment (right). The thick arrows represent the transmitted light from the sources, whilst the thinner arrows represent the reflected light travelling towards the detector.

7.2. EXPERIMENTAL PROCEDURE FOR SPUD

7.2.1. Short Term Experiments

Samples of cv Russet tubers, acquired from the SBCSR facility, were used for some preliminary Static Series measurements to test the prototype equipment. Unlike the standard protocol used in CHAPTER 3 however, here no fibre-optics were used. Two tubers were simply clamped into position with an Eye directly over the two sensors of the SPUD. The tubers were positioned to maximise contact of the tubers skin around the sensor. The Static Series shown here were run for 48 (Exp1) and 72 (Exp2) hours. Spectra were collected every five minutes. These experiments were conducted in the Norwich Laboratory under ambient lighting at room temperature.

7.2.2. Long Term Experiment (Harvest 2016)

Sample Collection and Storage

Samples of cvs Challenger, Lady Claire and Shelford were obtained and stored at SBCSR from September 2016 to April 2017. The cultivars were cold stored at 4°C and a 90% relative humidity.

Spectral Acquisition

The evening before analysis three tubers were removed from the cold storage, moved to the 15 °C storage room and placed under a halogen lamp to stimulate Chl production in advance of analysis. In turn these tubers were set up for a Static Series measurement using the SPUD Hamamatsu spectrometer. Measurements were thereafter taken once in the morning, midday and afternoon. The same protocol as described in 7.2.1 above was followed to interrogate a single Eye from each tuber. The selected Eyes were cleaned of lose mud and dirt using an air compressor before analysis began. Spectra were recorded every minute for three hours. Each measurement was an average of 600 scans, each with an exposure time of 100 ms. The dormancy state (sprouted or non-sprouted) of the tuber was also recorded at the beginning and end of a series. Once analysis had finished these tubers were disposed of.

7.3. RESULTS AND DISCUSSION

7.3.1. Short Term Measurements

An important aim of these experiments was to understand and gauge the practicality and effectiveness of the SPUD equipment. It was quickly apparent that the LED diode station was not able to differentiate changes seen between the three wavelengths during static measurements. The idea was that the 690 nm diode would monitor the changes in the Chl band, whilst the other two diodes would provide measurements of a baseline away from the Chl band. However, this was not the case (an example of the data collected using the three-diode component can be seen in APPENDIX 2). The stability of the 630 and/or 650 nm wavelengths was poor, and they did not function as useful baseline readings; no consistent behaviour could be seen in the response of the 690 nm diode, either relative to the baseline diodes, or intrinsically. The first issue is thought to be because the LED system suffers from poor stability with respect to temperature or time; further, the dynamic range of the A/D is low (8bit) and typically readings will only span a small proportion of this, and with relatively large noise. The second is likely due to the 690 nm diode being approximately 10 nm away from the centre of the Chl peak. The three diodes were chosen however, due to commercial availability and their guarantee of ongoing supply, in case this method was to be developed further.

The upside of the LED method would have been cost. The use of additional or different LEDs may provide better spectral information that can follow the changes in the Chl absorbance. This may still warrant further investigation. It should also be noted that the
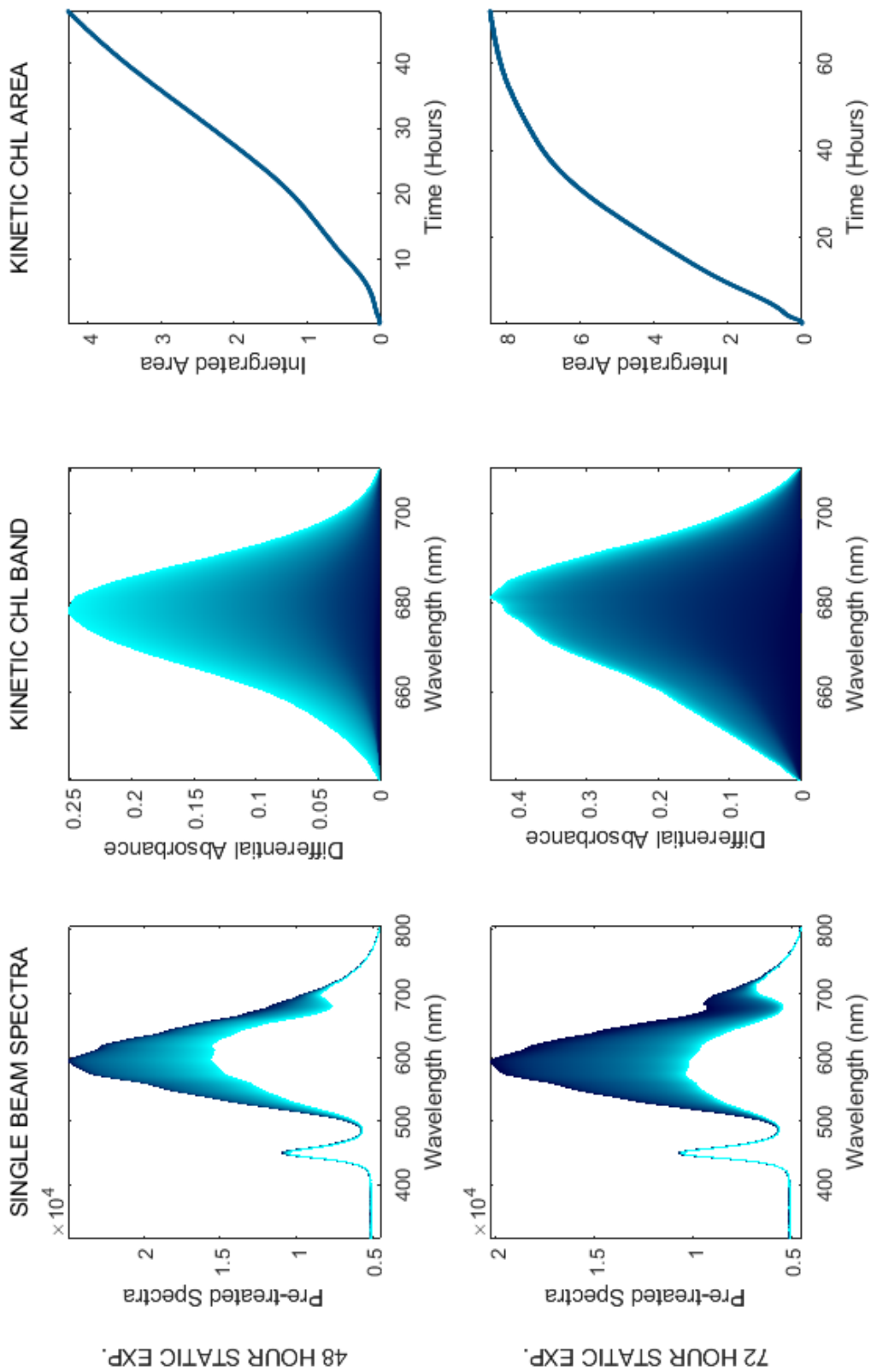
Figure 7:3 Static Series experiments of two cv Russet tubers, using the Hamamatsu spectrometer. The two experiments (split by rows) were run for 48 and 72 hours, respectively. The gradual colour from dark to light represent the initial to final spectrum recorded.

light exposure during data analysis may not be sufficient in the three LED analysis. Without additional light present, these diodes alone may not be strong enough to provide sufficient stimulation. Considering the tuber is placed on top of the SPUD equipment, exposure of the Eye to ambient light during analysis is limited.

In sharp contrast, the results from the SPUD Hamamatsu spectrometer proved entirely able to detect the changes seen in the Chl band during a Static Series measurement. FIGURE 7:3 shows the single beam spectra Kinetic Chl Band (with baseline correction) and Kinetic Chl Areas (see Chapter X for more details) of two Static Series measurements. The plots show a graduated colour change dark to light blue, representing the initial to final spectra recorded. The rows separate the two experimental repeats. The single beam spectra recorded from both static experiments show good stability between measurements taken by the Hamamatsu spectrometer. The Kinetic Chl Bands highlight the change in absorbance at 675 nm in both experiments. This result corresponds to that seen in the static experiments when conducted with the StellarNet spectrometers in CHAPTER 3. The integrated area curve for Exp1 shows the lag and growth phases, whilst Exp2 shows the growth and asymptotic phases. The absence of the asymptotic phase in Exp1 is what prompted Exp2 to be conducted for a longer analysis period. The single beam spectra show that Chl was already present at the Eye at the start of Exp2, explaining the absence of a lag phase in this experiment.

The results here provided an optimistic view on using this equipment for the Harvest 2016 data collection. In the laboratory it was every bit as sensitive as the much more expensive StellarNet spectrometers. The question was, how would it fare in the commercial environment?

7.3.2. Long Term Experiment – Harvest 2016

The experimental protocol was to analyse the kinetic behaviour of the Chl band of new tubers taken out of storage periodically, in an analogous plan to that used for the StellarNet measurements. Every week, up to three cvs Challenger, Lady Claire and Shelford tubers were analysed using the Hamamatsu spectrometer. A set of tubers of the same cv were removed from storage the evening before analysis. These tubers were left in a 15 °C store under a halogen lamp. On the analysis day, a tuber was set up for measurements at ∼ 9 am, 12pm and 3pm. As multiple tubers could not be analysed at any one time, this meant that the tubers were exposed to light and warmer conditions for different periods of time; 15, 18 and 21 hours respectively, before analysis began.
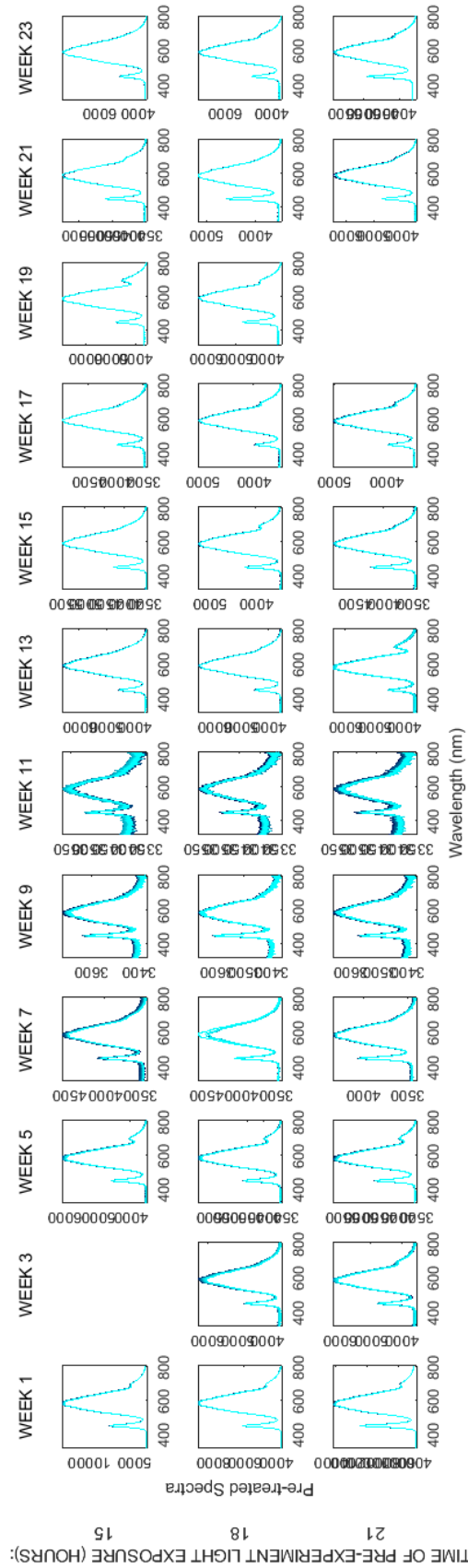
Figure 7:4 Single beam spectra of cv Lady Claire analysed by the Hamamatsu Spectrometer. This figure shows the data collected in the odd analysis weeks. The three rows correspond to the different time periods of irradiation (morning, midday, afternoon).

FIGURE 7:4 shows series of single beam spectra collected from cv Lady Claire tubers. Due to the number of measurements undertaken, this figure displays the result collected during the odd analysis week numbers only. The rows separate the three-time points at which the measurements were started, i.e. at 9am (morning), 12pm (midday) or 3pm (afternoon). Any missing data was due to human or experimental error. Little information on changing absorbance can be seen when looking at the whole wavelength range of the single beam spectra in FIGURE 7:4. The data shows that the Hamamatsu spectrometer was able to determine that a large percentage of the tubers have Chl already present at the Eye at the start of analysis. Considering the results of the Static Series conducted in CHAPTER 3, this was expected. 15 hours of irradiation proved long enough for the tubers to produce Chl after cold storage. This was also true for the cvs Challenger and Shelford tubers.

FIGURE 7:5 to FIGURE 7:7 show the Chl Band Areas for the data sets collected from cvs Challenger, Lady Claire and Shelford respectively. Each plot contains a maximum of three kinetic series taken at one of the three-time points; am, midday or pm. Although these tubers were irradiated for subsequently longer periods, it was assumed that 15 - 21 hours of irradiation would mean that the tubers were into the growth phase of the sigmoidal behaviour of Chl production. Not only was 15 hours long enough to stimulate the tubers into this phase, but 21 hours was not long enough for the tuber to reach the asymptotic phase. Seen by the Static Series from FIGURE 7:3 (as well as previous Static Series experiments in CHAPTER 3) it is known that the growth phase is linear, therefore the three measurements could be thought of as repeats for each cultivar for the week. These repeats were expected to show similar changes in the Kinetic Chl Areas, which was true within reason, although there is inevitably tuber to tuber variations.

A clear observation made from the Kinetic Chl Band plots was of the large amount of noise seen in the measurements from week 11. For FIGURE 7:5 to FIGURE 7:7 the spectra were treated with the smoothdata.m in Matlab; nevertheless an increase in noise can be seen from week 7. This issue was investigated. It was found to be the result of small particles of dirt and mud collecting on top of the Hamamatsu source and detector point. As the tuber sits on top of a cylinder surrounding the source, the equipment design easily allowed dirt that had not been fully removed from the tubers surface to fall into this hole (refer back to FIGURE 7:1). Once the equipment had been cleaned out at the beginning of week 12, the response from the spectrometer returned to recording smooth spectra, see FIGURE 7:7. The build-up of dirt was monitored from here on, to avoid this occurring again. Unfortunately, this looks to have also been the case between weeks 20 to 22, the
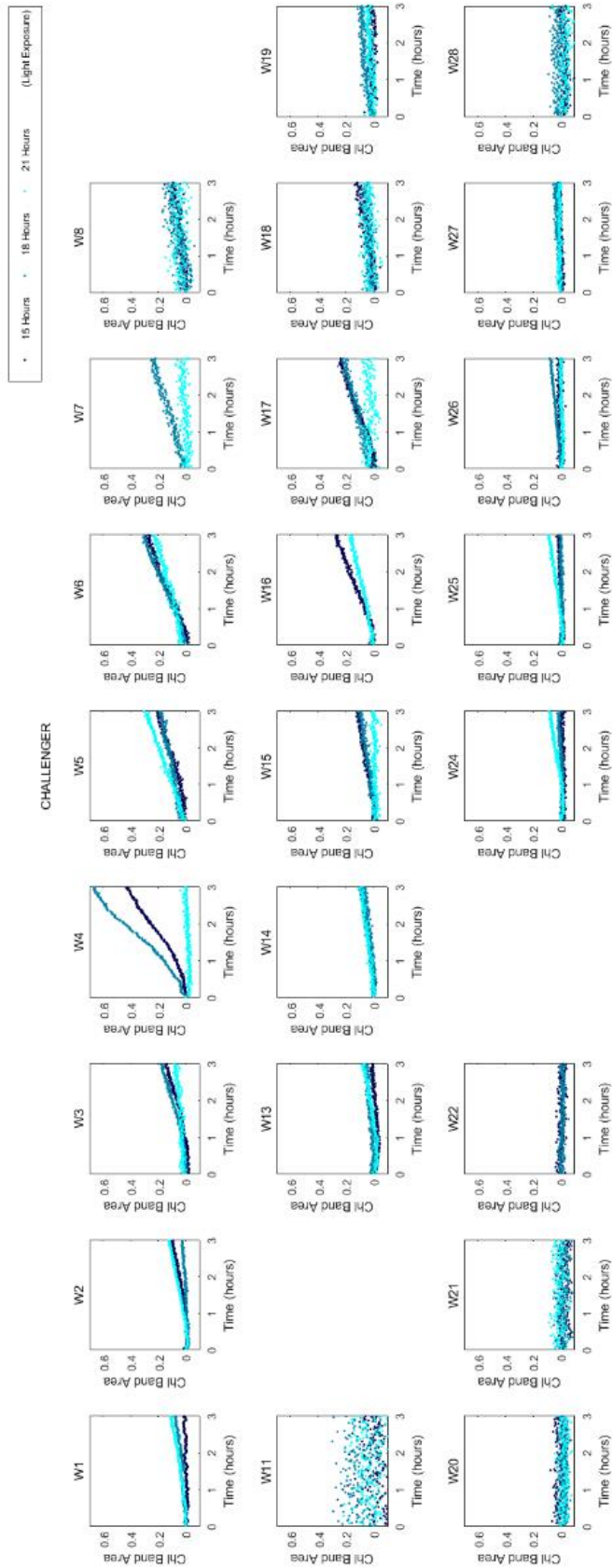
Figure 7:5 Kinetic Chl Areas of cv Challenger analysed by the Hamamatsu Spectrometer. Each plot corresponds to a single analysis week and contains a maximum of three kinetic values. The three colours represent the length of irradiation period for the tubers before analysis period.
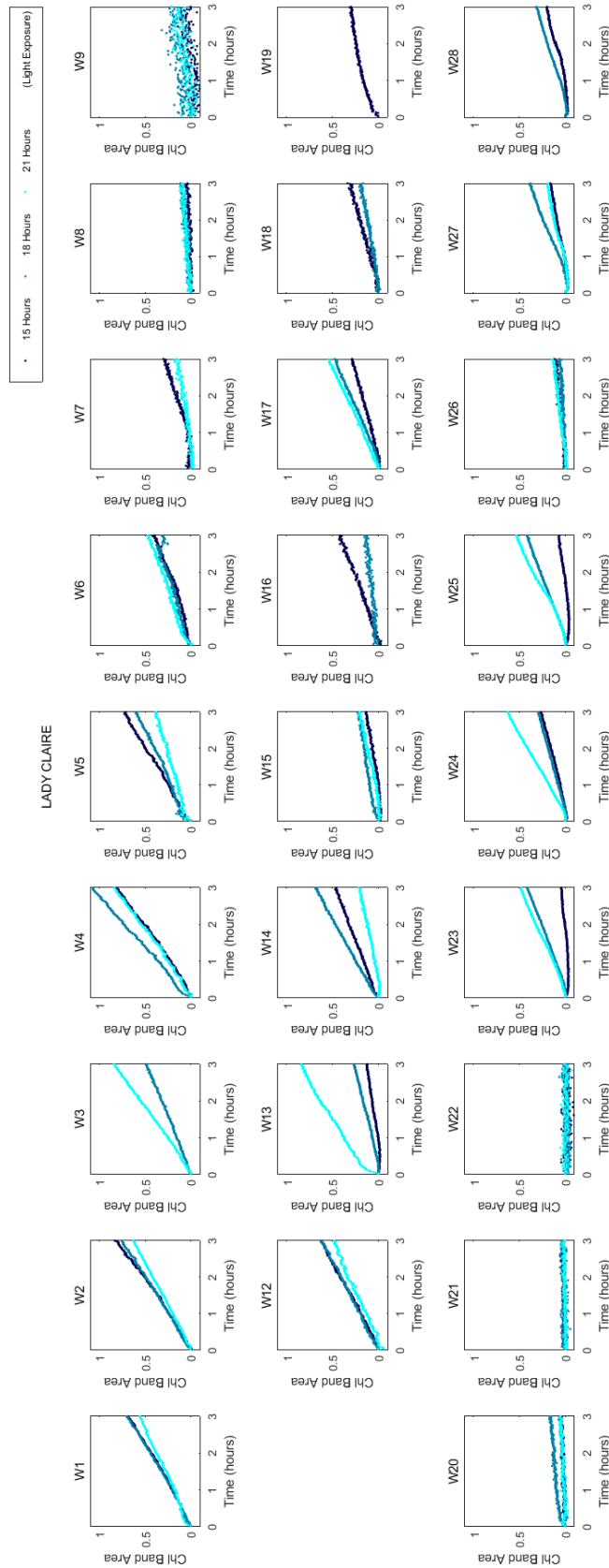
Figure 7:6 Kinetic Chl Areas of cv Lady Claire analysed by the Hamamatsu Spectrometer. Each plot corresponds to a single analysis week and contains a maximum of three kinetic values. The three colours represent the length of irradiation period for the tubers before analysis period.
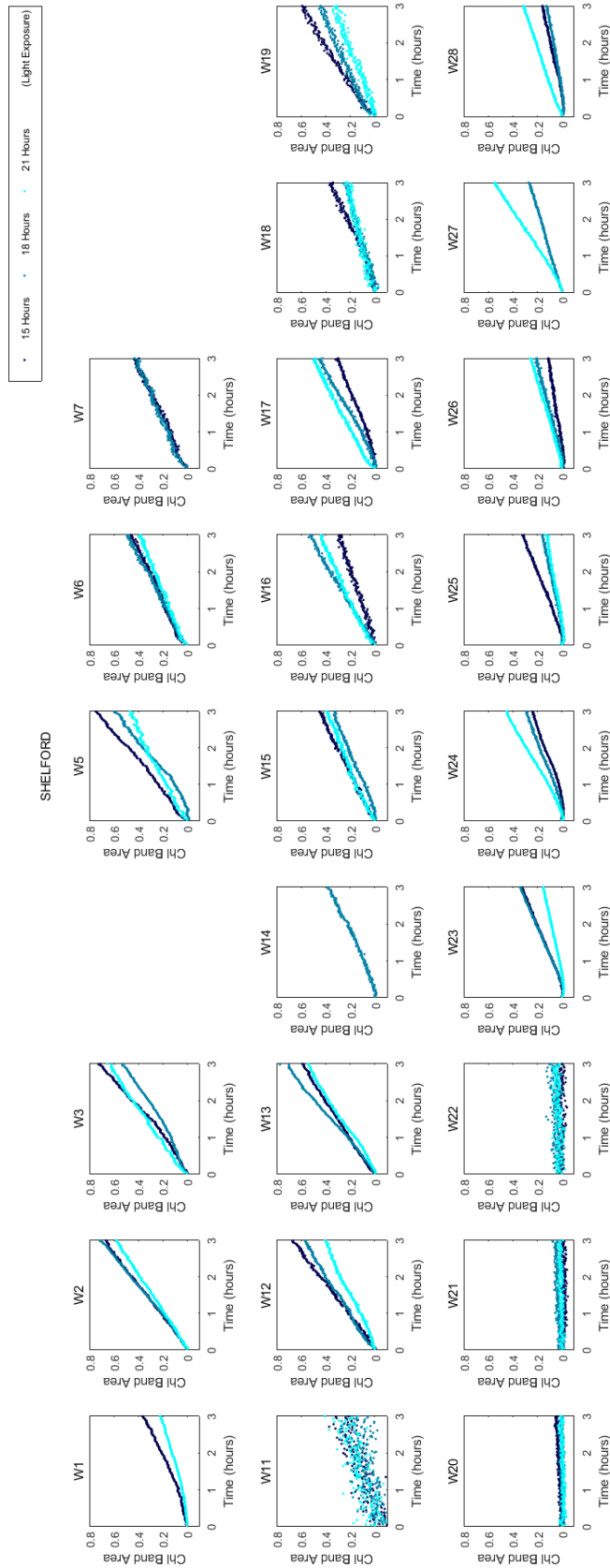
Figure 7:7 Kinetic Chl Areas of cv Shelford analysed by the Hamamatsu Spectrometer. Each plot corresponds to a single analysis week and contains a maximum of three kinetic values. The three colours represent the length of irradiation period for the tubers before analysis period.
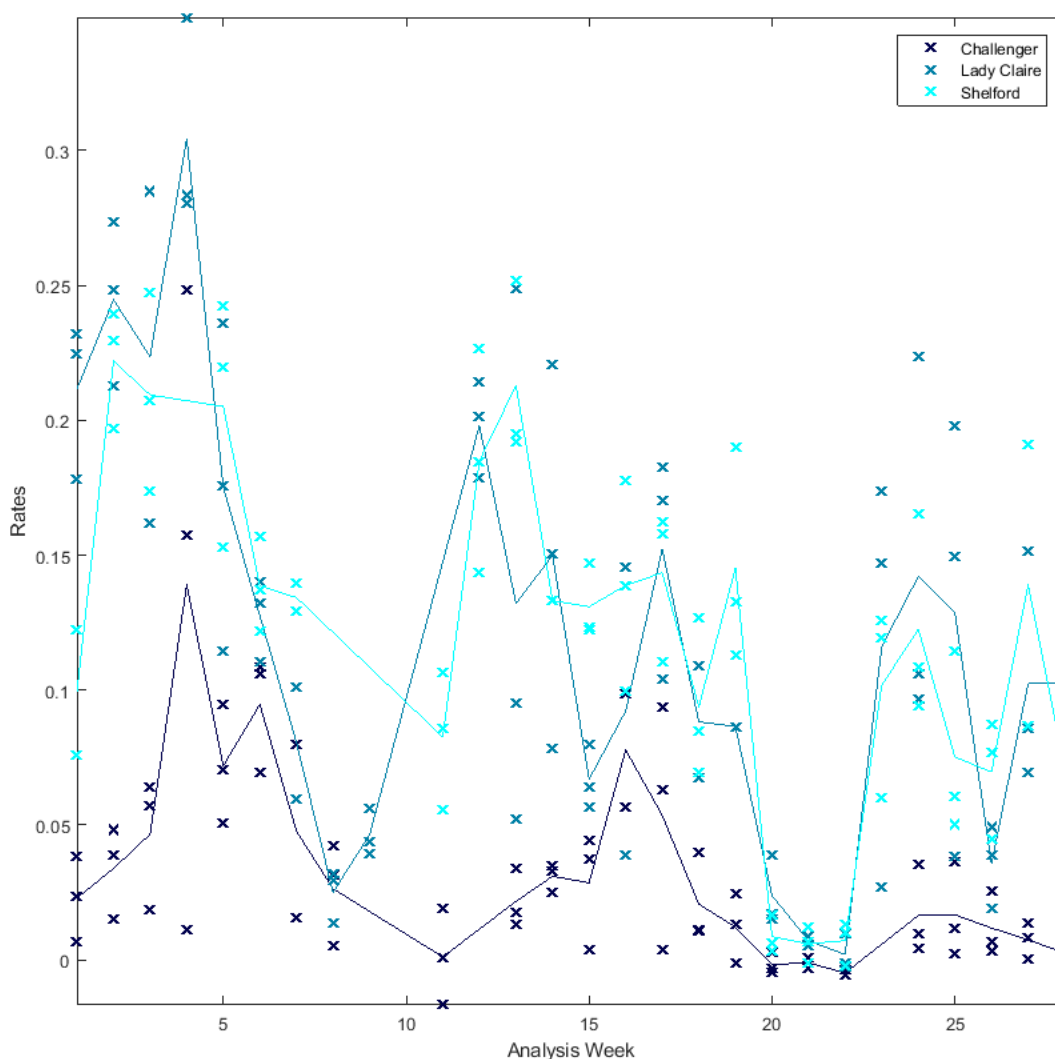
Figure 7:8 Chl Rates of data collected using SPUD for Harvest 2016. Plotted against analysis week; each point represents a single measurement taken, whilst the line shows the mean values.

design of the sampling location makes it difficult to see this happening.

Just as in the data analysis and results seen in FIGURE 6:3 from the measurements collected by Vis/NIR for Harvest 2016, the cumulative Chl Rates did not show the sigmoidal growth curve seen in Harvest 2014, and the data could not be related to the batch dormancy date. FIGURE 7:8 shows the Chl Rates plotted against analysis week. Each cross represents a single measurement, whilst the line shows the mean value calculated for each week. This figure appears to indicate that the drop in spectral intensity measured in weeks 7-11 and 20-22 is reflected in the measured Chl rates of change. In the worst cases, the spectrometer is not measuring the tuber surface at all, but merely a layer of dirt. This reiterates the flaw in equipment design, and the interference the

presence of loose dirt has on the spectrometer readings. Ignoring the weeks of 7–11 and 20-22, a small exponential decline can be seen.

As discussed for the Vis/NIR data of Harvest 2016, the experimental design is the reason a batch dormancy prediction could not be made. The variance in an individual tuber's dormancy state was too great with the protocol of analysing only three tubers per week. However, the protocol of pre-illumination for these tubers proved useful in removing the varying lag phases seen in the Chl production.

7.3.3. Performance of SPUD (versus StellarNet)

The signal to noise ratio (SNR) was calculated for the two StellarNet spectrometers and the Hamamatsu spectrometer used for Harvest 2016. A SNR was calculated for the first spectrum in each Kinetic Series collected from the cvs Challenger, Lady Claire and Shelford tubers. A mean value was then found for each machine. For the EPP2000-NIR-200 (StellarNet Eye measurements), the Black-Comet CXR-SR-50 (StellarNet Background measurements) and the Hamamatsu (Eye measurement), the SNR were respectively 79.2 dB, 42.5 dB and 45.2 dB. It should be noted that for the Hamamatsu, calculations were made with the exclusion of the weeks (7-11 and 20 – 22) with little signal intensity due to the build of up mud on the detector point. These values give an indication of the quality of a single measurement recorded by the different spectrometers, taken under their specific experimental conditions. It must be considered that the two StellarNet spectrometer were taking measurement from different locations on the same tuber (i.e. Eye and Background), however the EPP2000-NIR-200 gives a much larger SNR. Again, the different light sources and tuber positioning must be considered when comparing the StellarNet and the SPUD SNR, however a similar result can be seen between the expensive Black Comet StellarNet spectrometer and the much cheaper Visible Hamamatsu spectrometer. Considering that a signal of 1000 times stronger than the noise has a SNR of approximately 30 dB, these values show that all three spectrometers can produce spectra with a good SNR.

7.3.4. Commercial Data Collection

As previously stated, the facilities to keep the sample tubers in a commercial-like environment were unavailable at the Norwich centre for Harvest 2016. A collaboration with the SBCSR facility allowed the analysis of tubers to be conducted in a desired manner. Data collected for this harvest was made by myself and three employees of this facility: Lana Head, Stephen Ferrett and Marion Tout. For several weeks, the execution of analysis was closely monitored for those conducted by the SBCSR employees. This was

done until it was felt that the methodology was being carried out correctly. However, several issues still arose with the practicality of collecting data in a commercial setting.

Although those who were involved in the study were instructed that the tubers needed to be stored in constant darkness, it transpired that this was not always the case. The facility has numerous research projects going on at the same time, spread over a vast number of different storage units, all with varying storage requirements. Understandably, this can make it difficult to organise and keep track of the different studies beginning conducted by different people. In the early weeks of the Harvest 2016 study, it was found that the lights in the storage unit had been turned on and off, due to people having to access another study kept in the same unit. Once aware of this problem, it was addressed by covering the shelves where the sample tubers were kept in black cloth. This was the best solution for a non-ideal situation; however, the black cloths reduce air movement around the tubers, meaning their overall temperature increases slightly and hot spots may be caused in the crates of tubers. Once maintenance on a separate store had been completed, the tubers were moved into a storage unit of their own. The storage unit was equilibrated to the required conditions before transfer. The transfer itself only took a few minutes; it is unknown if this may have induced a change in the tubers.

If this technology were to be transferred into commercial settings in the future, it might be carried out by unskilled workers. Even with the training supplied to the operators in the present study, multiple mistakes were made through Harvest 2016 for the SPUD and Vis/NIR data collected. The issue regarding the build of dirt in the SPUD was discussed above. Although this issue was made known to all involved in the project in week 12, it can be seen in the Kinetic Chl Area data that this may have occurred again in the fortnight up to week 22.

Regarding the Vis/NIR data seen in CHAPTER 6 further issues can be raised. Although this is known to be a simple technology, a recurring problem was that the probe and/or tuber were not clamped tightly enough to hold them securely in place. This can be seen in the data when a sudden jump in the data occurs. The movement of either the probe or tuber shifts the position of the analysis area and therefore gives a different response in the spectra. Therefore these Kinetic Series were removed from data analysis. This issue was flagged up and highlighted to those who needed to know; however, it was still occasionally seen in subsequent data. Several of the measurements have been removed

due to this, as it is unknown whether the probe was still in the correct position to interrogate the Eye of the tuber.

Another issue was that occasionally the spectrometer light source was left off after the dark reference was collected, and therefore remained off for the period of analysis. Finally, occasionally the whole scheduled analysis was forgotten completely, for both SPUD and Vis/NIR, leading to entire episodes of missing data.

Assignment of a tuber's dormancy state was another issue highlighted during this harvest year. There did not seem to be a general agreement of the length of sprouts needed to classify a tuber as breaking dormancy. This was also similar for the identification of whether an Eye was showing any sprouts or not. This is a crucially important issue, as it is very challenging to develop a method for predicting an event ("dormancy break") if there is no consensus on what it looks like or when it has occurred.

7.4. CONCLUSION

This Chapter has focused on evaluating the effectiveness of the SPUD equipment within difficult environmental conditions, and comparison of its performance with the StellarNet. Overall the output of the Hamamatsu spectrometer was impressive, and ideal for the use of monitoring the chlorophyll production within a tuber. Relative to the data recorded by the StellarNet spectrometers, the Hamamatsu shows an equal if not slightly greater stability within the spectral measurement. With further design development, the Hamamatsu spectrometer could be a highly desirable alternative due to the stability and reliability of the system, as well as the large difference in cost between this and a NIR spectrometer.

However, issues arose due to the flaws in the design of the SPUD prototype. A re-design would need to remove the concern of dirt interfering with the reflectance measurements taken. A closed system would need to be designed where dirt and dust could not enter the machine. What is beneficial about the design of SPUD, however, is that the tuber can be partially rested on the equipment and is therefore in a more stable position compared with just being clamped. In comparison, the experimental procedure of the Vis/NIR data analysis meant that a few measurements had to be discarded due to the shift in alignment of probe and tuber during Static analysis. The clamped position of the probe and tuber allows the potential for this to happen much more readily, especially once the tuber begins to dry out.

Conducting Harvest 2016 in a separate, semi-industrial facility highlighted a lot of issues that may arise if this research became implemented into a commercial setting. The design of the technology would need to address multiple issues. Firstly, physical constancy between the tubers and reflectance system is essential. Movement of either would hinder the calculation of Kinetic spectra seen in a series measurement. Ideally the measurements would take place within a container (like the idea of a "Hot Box" (Pieterse, 2012)) where the conditions inside do not change throughout the analysis and could be set automatically. For example, operating the lights (on for stimulation, say, or off) cannot be forgotten. Furthermore, the current set of up of both the spectrometer systems (StellarNet and SPUD) only allows for a single tuber to be analysed at a time. This would not be sufficient as a procedure to give a batch measurement.

HYPERSPECTRAL IMAGING

8.1 INTRODUCTION

Hyperspectral imaging (HSI) is a technique that can be used as a real-time detection tool for food quality and safety assessment. Maintenance of food quality and produce safety is essential in the food industry. Brosnan and Sun (2002) summarised the advantages of computer vision; precise descriptive data, cost effective, reduction in human involvement, automated processes, quick and objective. As outlined in CHAPTER 2 this technique combines imaging and spectroscopic technology to obtain large amounts of spectral and spatial information from an object's surface. Research in this area has become increasingly popular in the last ten years (Huang et al., 2014). From this, applications translated into the food sector have included detection of contamination, quantification of constituents and identification of defects (Da Wen Sun 2002).

Industrial application of machine vision has been suggested as an alternative to manual sorting in the potato packing industry. Several studies have focused on the grading and inspecting of potatoes using machine vision techniques (Rady and Guyer, 2015). A study by Toa et al. (1995a) investigated separating tubers depending on their shape and the presence of greening using a Fourier based separation technique. Respectively, the two criteria resulted in an 89% and 90% agreement between the vision system and human system, for 120 potato samples. Machine vision has also proven able at detecting surface blemishes (due to various defects such as greening, black dot, silver scurf and common scab) with an accuracy of 90 % (Barnes et al., 2010). A later study found that the presence of the internal disorder 'hollow heart' in intact tubers could also be detected using HSI with an accuracy of 89 % (Dacal-Nieto et al., 2011).

Visible/Near-Infrared Hyperspectral imaging is not without its disadvantages. The foremost issue is the initial purchase cost of the system; on the market today, these systems can cost tenfold to that of a Visible/Near-Infrared spectrometer, or more if a device such as a Hamamatsu spectrometer is used. Secondly, computer vision is dependent on the quality of the images captured. Due to the ambiguity in the shape and biological variation of agricultural produce, object identification may be difficult in these applications (Brosnan and Sun, 2002). Thirdly, HSI requires a vast amount of data processing that needs high performance computers with large data capacity and a skilled programmer; this is even more apparent when real-time online measurements are taken.

8.2 EXPERIMENTAL PROCEDURES FOR HSI

8.2.1 Sample Collection and Storage

Short-Term Analysis

The red tubers (cv unknown) used in this experiment were sourced from a supermarket in July 2015. These tubers were stored at room temperature for a week to promote sprouting. Split into two groups, these tubers were either left on a windowsill or in a cupboard; the two locations are referred to as light and dark storage respectively.

Long-Term Analysis (Harvest 2015)

Samples of cvs Cultra and Rooster tubers were collected from Country Crest farm on a weekly basis (at the same time as those collected for the tubers used for the Vis/NIR analysis described in CHAPTER 5). Both cultivars were stored in commercial storage units, with conditions of 5 °C and ~90 % RH. The samples were collected from the same wooden crates each week. Ten tubers of each cultivar were used for the analysis every week. Each tuber was cleaned, using a dry brush, on the day of removal from commercial stores. The tubers were placed into a 4 °C fridge ready for analysis on the subsequent day. The tubers were transported to the University of Dublin in a polystyrene box, containing an ice block.

8.2.2 Sample Preparation

Before analysis, the apical end of a fresh tuber was cut off with a depth of 2 cm. The tubers were cut so the surface area undergoing inquisition would sit as parallel to the cylinder light as possible. This was not always simple considering the different tuber shapes. The research in hyperspectral imaging surrounding the issue of quality assessment highlights the idea of non-invasive analysis. However, the shape and size of potato tubers along with the dimensions of hyperspectral system available for this project meant that the tubers needed to be cut before measurements could be made.

8.2.3 Image Acquisition

Hyperspectral images were collected using a Visible (Vis) Desktop Spectral Scanner (DV Optics, Italy). The system consisted of a CCD camera (BASLER vision technologies, Germany), a spectrograph (Specim V10E, Finland) attached to the camera, and a cylinder light diffuser transmitting through fibre optics. The spectral range for this system was 400 – 1000 nm, with 5 nm intervals. The supplied DV optics software (SScanner, Italy) was used for instrument control, data acquisition and file saving (ENVI format). Reflectance calibrations, black and white, was carried out to minimise the difference in relative reflectance between measurements. For sample scans the table speed was set at

20 mm/s and spectra were recorded from the average of 50 scan lines. Each image contained 140*580 pixels.

8.2.4 Data Analysis

Data were pre-treated with a Savitzky-Golay smoothing function and Standard Normal Variate (SNV) normalisation. Wavelengths 460, 530 and 650 nm were used for displaying the hyperspectral data as RGB images. Chl Band Areas were calculated with the same principle as described in CHAPTER 3: after normalisation, all spectra contained within a single image were referenced to a selected Background location; the Chl Band was then extracted and used to calculate the Chl Band Area of each spectrum, giving a value for each pixel across the tuber.

8.3   RESULTS AND DISCUSSION

8.3.1 Short Term Experiment

FIGURE 8:1 displays the eight tubers as RGB images and FIGURE 8:2 displays the tubers coloured according to their Chl Band Areas. The two columns in each figure separate the locations in which the tubers were kept, and the titles state the sprout lengths at the time of analysis. The RGB images for the light-stored tubers show a clear increase in surface greening, by the skin colouring changing from red to dark, from the top to bottom image. Also, the sprouts present have turned black in colour. For the dark stored tubers, no clear surface greening can be observed as the skin remains bright red, and the sprouts have remained yellow in colour. FIGURE 8:2 showed the Chl Areas were unable to easily differentiate between the Eyes and the Background in the tubers kept in light, since Chl was produced all over the surface skin. However, areas of the images are more intense in the places where the sprouts are known to be present, when referring to FIGURE 8:1. In comparison, the tubers kept in dark storage show a clear difference in the intensity of the Chl Band Areas for the Eye than the Background, that appears to become even greater with increased sprout length. An important point is that the sprouts can be seen at the smallest length of 2 mm. As these tubers were shop bought, these tubers would have already been exposed to light. This explains the presence of some Chl in the 'dark storage' tubers.
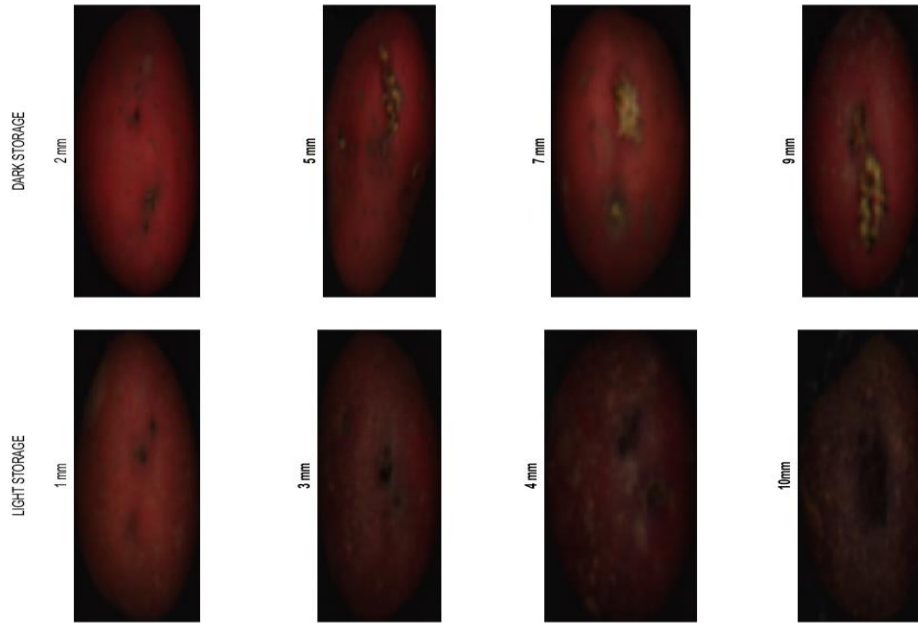
Figure 8:1 RGB images of the eight quick-sprouted tubers analysed by HSI. The columns separate the conditions in which the tubers were kept, and the titles indicate the maximum sprout length present at time of analysis.
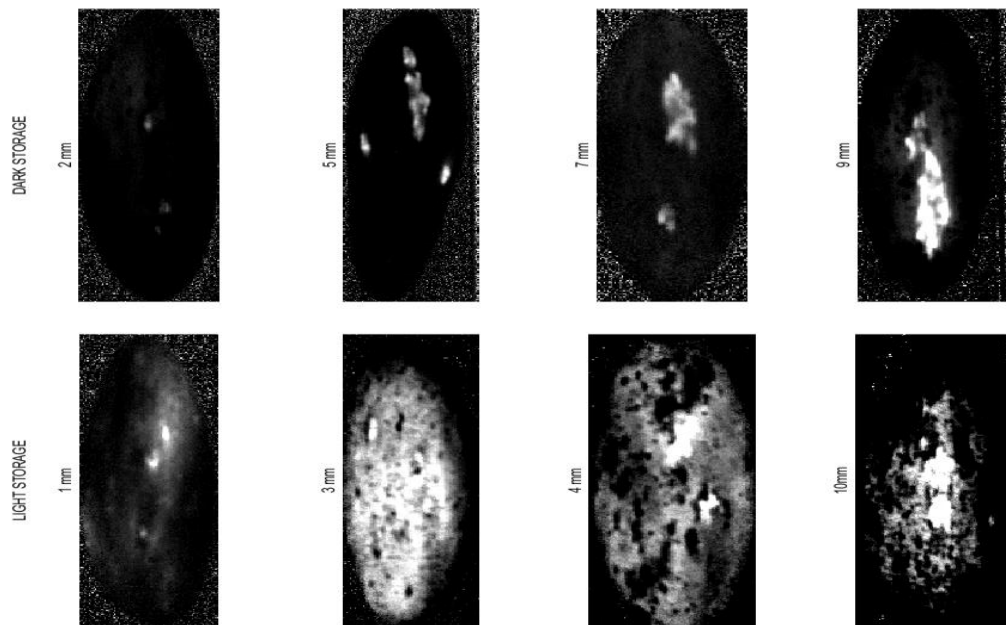
Figure 8:2 Images created using the Chl Band Areas of the eight tubers, analysed by HSI. The columns separate the conditions in which the tubers were kept, and the titles indicate the maximum sprout length present at time of analysis.

FIGURE 8:3 is a representation of the data as a "line measurement" taken over an Eye, analogous to the short-term experiments for the Visible/Near-Infrared analysis (CHAPTER 3). The RGB Image is the same as the image in the bottom rightmost image of FIGURE 8:1; the numbers one to three identify the point measurements that are plotted in the graphs below it. Points one and three are 'Background' areas either side of the Eye, whilst point 2 is the location of the Eye/sprout. The results are consistent with those seen in CHAPTER 3; HSI can also pick up the spectral difference in measurements taken across an Eye.
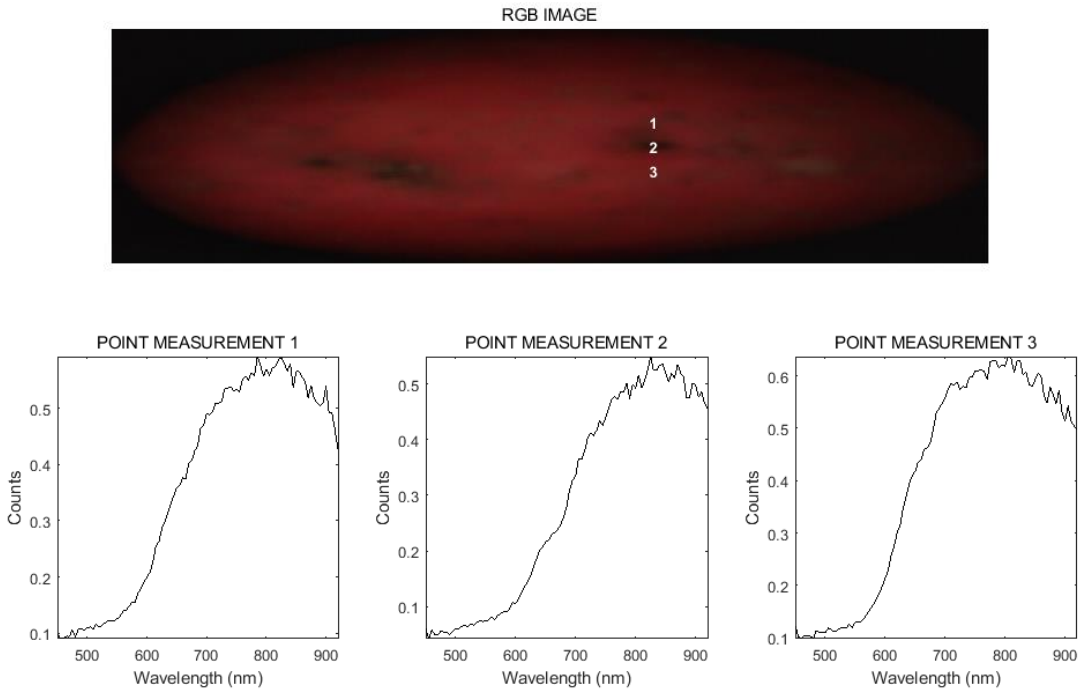
Figure 8:3 Extraction of point measurements from a hyperspectral image, across an Eye. This image is the same as that titled "2 mm" is the previous two Figures. Points 1 and 3 are Background areas, whilst point 2 is of an Eye. The latter shows a greater Chl a absorption centred at ~675 nm.

8.3.2 Long Term Experiment

It is known that Chl was not produced during long term cold storage under the surface skin of the tubers analysed for Harvest 2015 (as discussed in CHAPTER 5). This is confirmed in FIGURE 8:4 and FIGURE 8:5; these figures display the cvs Cultra and Rooster tubers analysed by HSI during the final week of Harvest 2015. As in FIGURE 8:2, these images show the intensity of the Chl Band Area, of each point measurement, captured with the Vis-HSI. It should be noted that by this time all tubers had begun to sprout;
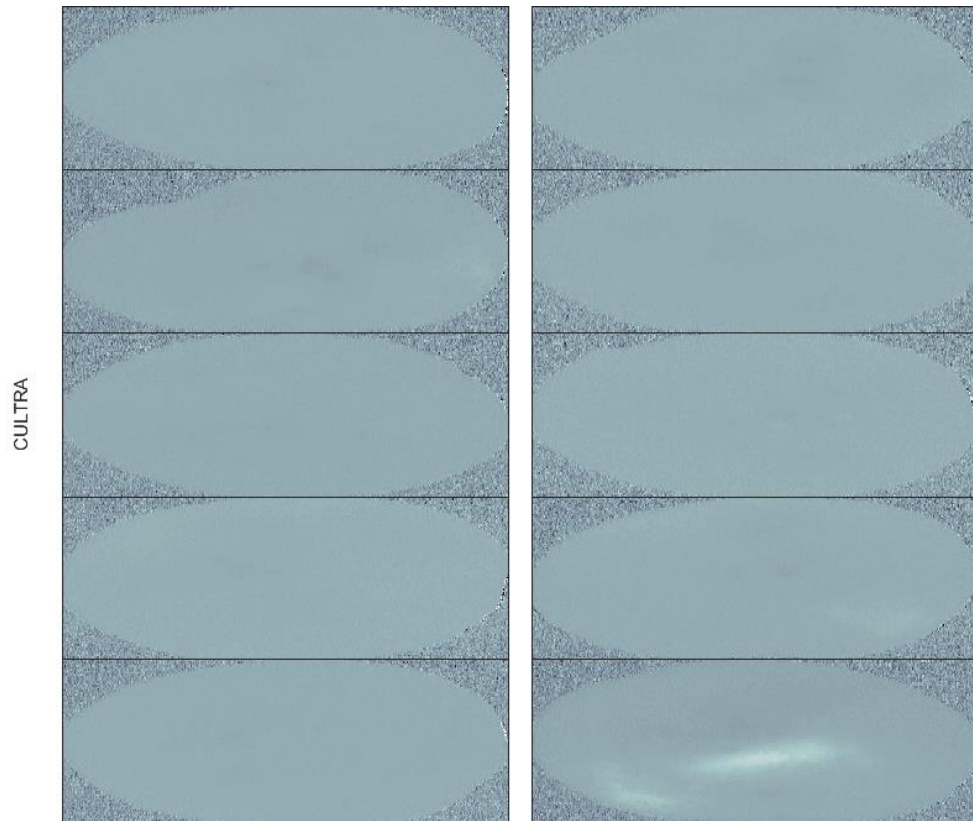
Figure 8:4 Chl Band Areas of the Visible HSI taken of the cv Cultra tubers during the final week of Harvest 2015.
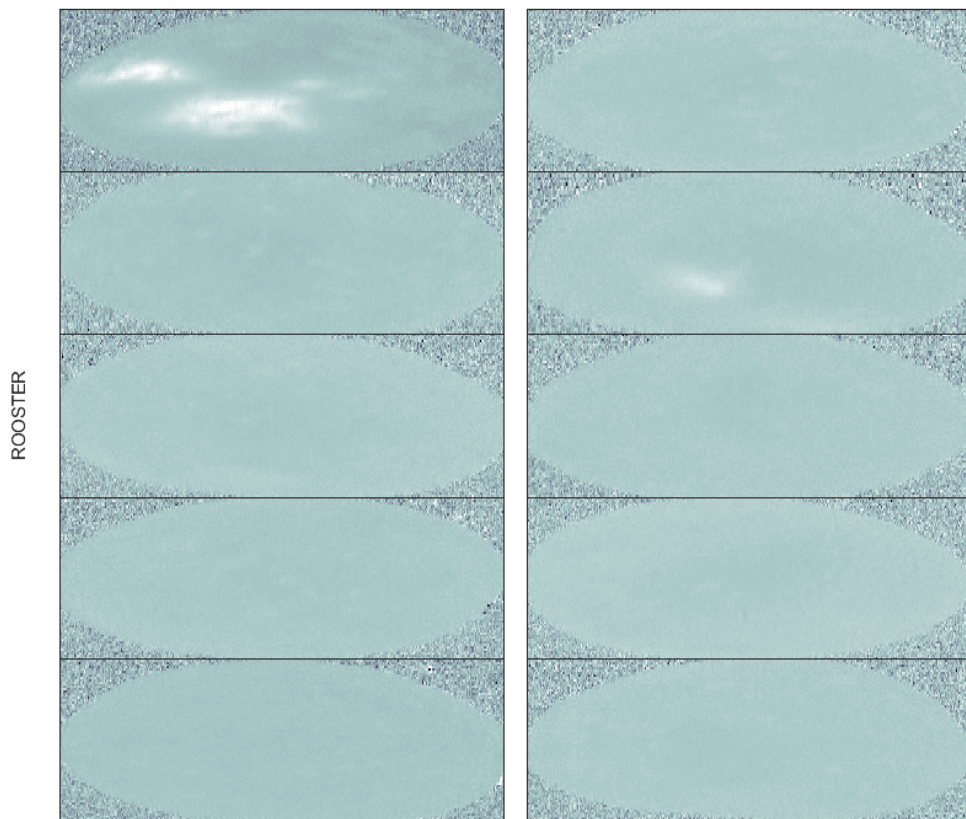
Figure 8:5 Chl Band Areas of the Visible HSI taken of the cv Rooster tubers during the final week of Harvest 2015.
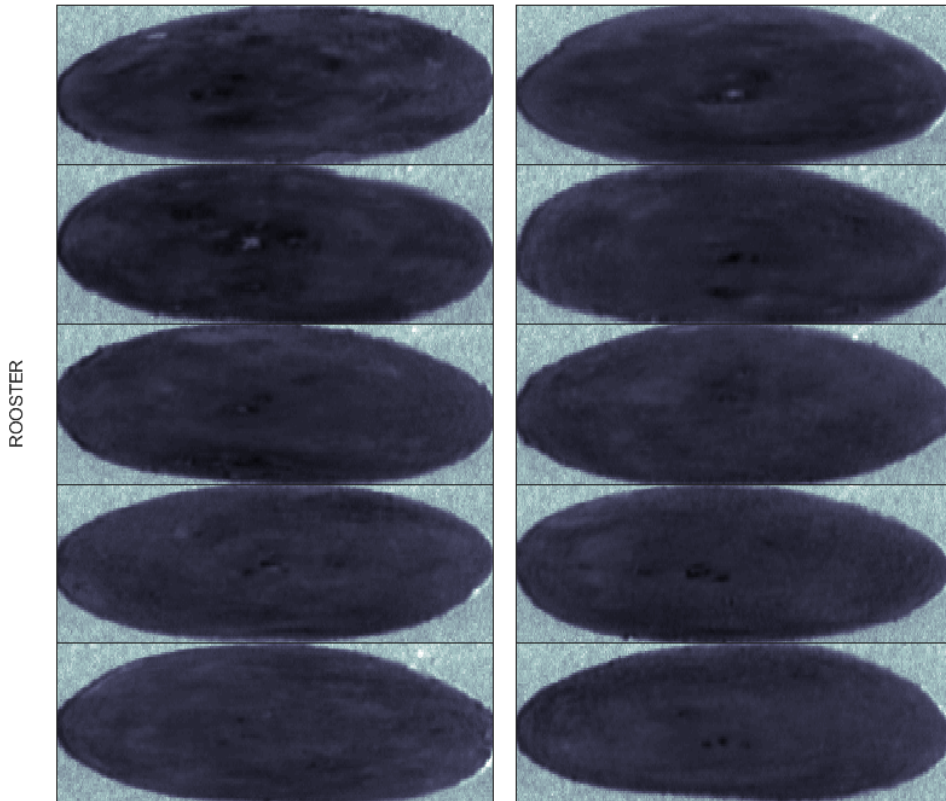
Figure 8:6 Spectral Intensity Ratio (480/800 nm) of the Visible HSI taken of the cv Cultra tubers during the final week of Harvest 2015.
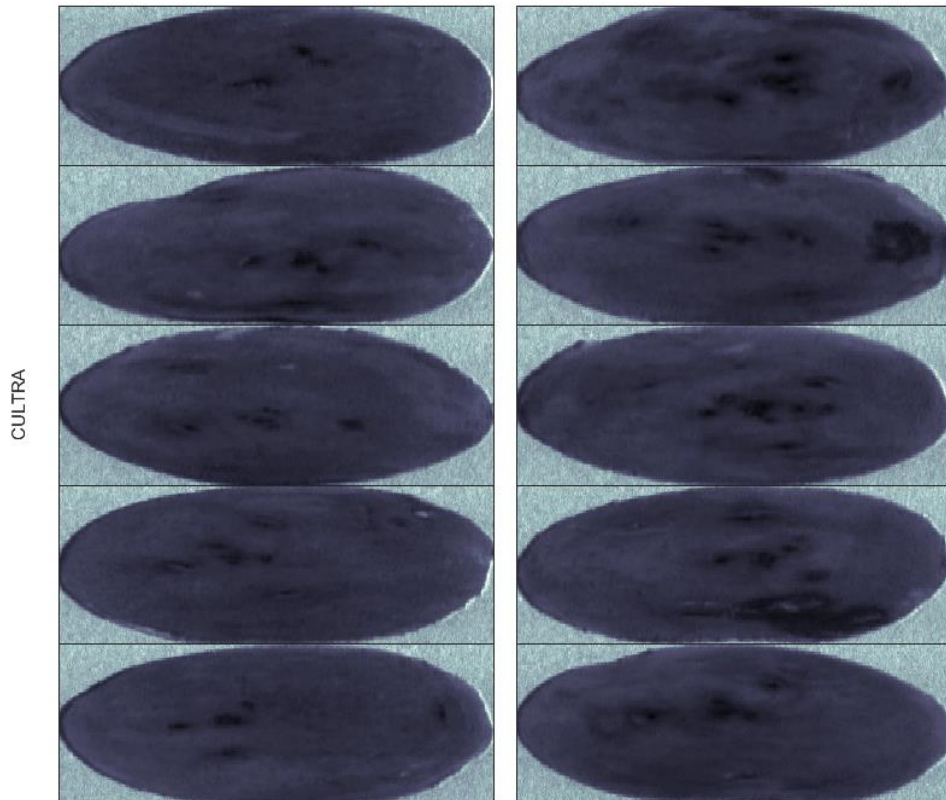
Figure 8:7 Spectral Intensity Ratio (480/800 nm) of the Visible HSI taken of the cv Cultra tubers during the final week of Harvest 2015.

however, it is once again clear that Chl was not produced in dark storage. In both figures, the outline of the tuber can be observed but most of the images are solid in colour, showing that the presence (if any) of Chl is the same across the entire surface of this sample section. Just one tuber from each cv show some differentiated areas (the bottom rightmost for the cv Cultra and top leftmost for cv Rooster). These diffuse spots of greening may be due to partial exposure to light during growth, i.e. the tuber was not fully concealed underground. Notwithstanding the occasional outlier tuber, the results seen in these figures held true for each analysis week; there was no consistent evidence of Chl production under the eyes taking place during dark storage.

Further data analysis was conducted to determine whether the Eyes could be identified and separated from the Background Locations. FIGURE 8:7 and FIGURE 8:6 show the same ten tubers as those in FIGURE 8:4 and FIGURE 8:5. These images are produced by the spectral intensity ratio between 480 (green) and 800 (near-infrared) nm. Each point measurement was normalised by using the maximum spectral value at ~ 800 nm. It was observed that the intensity of the green band was reduced in the spectra taken at the Eye locations in comparison to the Background. The results seen from the cv Cultra, FIGURE 8:7, show this method can be used to establish locations within the image that may be identified as eyes. However, this method also highlights other areas due to defects on the skin, see for example the rightmost tuber on the second row of FIGURE 8:7. This dark spot on the right-hand side of the image is due to a surface defect. Furthermore, this method was not as effective on the cv Rooster tubers, seen by FIGURE 8:6, likely due to its red colouring. Gao et al. (2018) were able to differentiate between non-sprouting and sprouting eye using HSI and specifically the wavelengths 636, 650, 660 and 672 nm. However, the tubers used in their study were shop bought and thus had been exposed to light (in an uncontrolled manner); this meant that the use of the Chl band was possible as Chl a would certainly have been present. However, for tubers kept in dark storage this would not be the case.

8.4 CONCLUSION

Vis-HSI proved sensitive enough to show changes in the presence of Chl under the surface skin of a potato tuber. Analysis of the Chl Bands was also able to identify Eyes from the Background once Chl was present. Agreeing with the results seen by the Vis/NIR data discussed in Chapter 5, the tubers analysed did not show any significant Chl production during storage, nor any differential in Chl production between the Eyes

and Background of a tuber. However, the design of the Harvest 2015 study meant that tubers did not generate Chl during dark storage, and thus it was not possible to conclude whether using HSI as a point measurement of Chl has potential as a means of predicting sprouting. If this equipment had been available in subsequent years, the method of kinetic series analysis would have been investigated. The idea would be to identify potential eye locations and then track the Chl Rate of these points over a period of regular illuminations. In principle, this is likely to yield equivalent results to the fibre-optic spectroscopy approach, and HSI may prove to be a method useful for industry; however, the cost of the technology is currently prohibitive for the sector, especially at the level of small-scale producers.

SUMMARY

This project evolved from the idea of developing a technique and methodology that could supply an indication of potato tuber batch dormancy status. There is currently no crop management tool on the market that is available for this. During potato crop storage, the application of sprouting inhibitors is conducted using only the empirical knowledge of behaviour in dormancy break of past harvest crops. However, it is known that several environmental factors can affect a cultivar's behaviour from season to season (Burton, 1966). This can lead to excess application as the uncertainty can sometime lead to "panic spraying". Due to the concerns on health and safety, there is a growing pressure to reduce the quantity of suppressants used. A crop management tool able to provide a batch dormancy status would provide an indication on when the crop needed to be sprayed. This would not only help with health and safety concerns but also reduce crop losses due to unwanted premature sprouting as well as the cost of the inhibitors themselves. Before this project, the idea of monitoring potato tuber dormancy using Visible/Near-Infrared (Vis/NIR) had not been published.

At the beginning of the project, it was hypothesised that Vis/NIR reflectance measurements, using a fibre-optic probe, made on the buds (Eyes) of potato tubers may be able to detect early-stage tissue changes, before any sprouts emerge. To investigate this, tubers were simply left in warm conditions to drive a non-sprouted Eye to sprout. During this time, Vis/NIR reflectance measurements were recorded at equally spaced time intervals using a fibre-optic probe, aligned directly over an Eye. Known as Static Series measurements, these experiments soon highlighted a change in spectral intensity at 675 nm. This absorbance is known to be due to chlorophyll (Chl) (Friedman and McDonald, 1997, Petermann and Morris, 1985). The first finding was therefore that **Vis/NIR spectroscopy equipped with a fibre-optic probe can track stimulated Chl in potato tubers** at low levels that produce no visible greening. Further analysis showed this is also true for the surface areas without Eyes (referred to as the Background). The degree of Chl production however was found to be significantly less for the Background than an Eye of the same tuber. Another finding therefore was that **the eyes of a tuber have a greater capacity to produce Chl**, compared to the remaining surface skin areas.

The Vis/NIR technique involves illumination of the sample with a suitable light source. Thus, the measurement process inherently acts to stimulate the Chl production in potato tubers, along with any other (e.g. ambient) light sources that are present. Potatoes stored in the dark do not have the systems present to produced chlorophyll, however light

exposure causes amyloplasts to slowly turn into chloroplasts, which leads to the production of Chl (Anstis and Northcot, 1973). This explains the lag phase seen in the Static Series measurements when a tuber had been sourced directly from cold storage. Once a tuber starts to produce Chl, its production is cumulative but requires continuous exposure to light; it ceases if the tuber is returned to the dark. However, once the chloroplasts have been primed, several hours of darkness do not cause any further lag phase once the tuber is returned to the light. **It was found that the spectrometer light source itself was strong enough to drive the Chl production in a tubers surface skin.**

Although the use of fibre-optics allowed for the flexibility of analysis positioning, it introduced problems of sensitivity, specificity and reproducibility. These were heavily investigated throughout the project. The uncertainty (noise) arising directly from the Vis/NIR measurements were found to be low. The problem arose however in the positioning of the probe. Firstly, the Eye "area" was found to be highly localised: alignment of the probe immediately adjacent to the Eye saw a result more characteristic of the Background. The Eye "area" was found to be approximately the width of probe or smaller. Secondly, the non-uniform surface shape of a tuber proved to cause a large variation in spectra collected from the same nominal location when repeated measurements were taken (realignment of the probe). Not only did the depth of the Eye increase the amount of variance seen in the repeated measurements, but also the amount of Chl present under the Eye. These sources of variance were therefore thoroughly investigated, and protocols were established to reduce the impact of measurement error.

Following Static Series experiments, long-term experiments were conducted on four harvest seasons and nine different cvs. The behaviour of Chl production was seen, firstly during Harvest 2014, to have a sigmoidal growth pattern as a function of time. As well as in the Static Series experiments, this pattern was seen again in the Harvest 2017 study. Harvest 2014 showed that;

1 - Chl can still be produced when tubers are kept in storage for several months, (intermittent periods of light were sufficient to stimulate analogous results to those seen previously in Static Series experiments).

2 - The repositioning error seen by individual tubers could be overcome by taking the average values of multiple tubers.

3 - The position of the growth asymptotic phase may have the potential for predicting the dormancy state of a potato crop.

4 - Other wavelength bands, in the Vis/NIR and the Short-Wave NIR, could not be correlated to sprouting.

The experimental design for Harvest 2014 saws the same tubers analysed each week; arguably these tubers would not have been a true representation of the remaining crop left in storage. Following this experiment, the protocol of "analyse and discard" was used to ultimately develop a more acceptable analysis that may be applied in industry.

Harvest 2015 was run as a control: single measurement of cold, dark stored tubers showed that point measurement in storage could not be used as a calibration tool to predict a batch dormancy state. The Vis/NIR data and Hyperspectral Images showed no change in Chl with age or sprouting, proving that the two biological pathways (Chl production and dormancy break) can proceed independently.

However, by using the cumulative Chl Rates of the tuber analysed during Harvest 2017, the results were able to replicate the behaviours seen by Harvest 2014. The time point of dormancy break, respective to the growth phase of the sigmoidal curve, was seen to be highly similar for all three cultivars analysed during this Harvest. A predictive link, therefore, has been seen to be present for multiple cultivars and harvest years. Although cvs had different parameters in their sigmoidal curves, for example cv King Edward tubers having an increased growth rate early on in storage, compared to the others, the five different cvs analysed during Harvests 2014 and 2017 have all shown a link between the activity change of Chl production depending on a tubers state of dormancy.

The challenges that remain concern cultivar-to-cultivar and potentially also harvest-to-harvest variation, but predominantly tuber-tuber variation. The concept of predicting a "batch sprouting date" is not straightforward. Tubers from the same crop can sprout weeks apart. Albeit only a small percentage, some individual tubers can break dormancy months before the batch average. These highly variable behaviours inherently limit the precision of any predictive method used. When the rate of Chl production was analysed according to analysis week for Harvest 2017, no strong link to dormancy break could be found. However, once the quantitative measure of a tuber's individual dormancy state ('Sprouting Age') was incorporated, a much clearer predictive link was seen.

Harvest 2016 highlighted several points that must be considered before this work could be applied into industry. The design of such equipment would need to be carefully planned. The Hamamatsu spectrometer used in SPUD showed great stability and ability to differentiate the Chl band. In addition to its low retail cost, it would be a suitable choice

for this application. However, the unit design of SPUD itself was highly flawed for the placement in industry. The open detector was not suitable for the messy nature of the potato crop. The fixed positioning of this detector also meant that the set up for analysis may be difficult due to the shape of a tuber eye. However, this fixed position also offered support in keeping the tuber in the same position. Tubers were seen to move, particularly in the Vis/NIR protocol, when analysed for an extended period due to water loss. In addition to the design requirements discussed in advance of building the SPUD prototype, the most important requirements for any future development of this crop management tool would include:

1 - Several tubers to be analysed at once, to mitigate tuber-tuber variation.

2 - Fixed analysis environment that could not be changed or interrupted by users (contained box).

3 - Fixed analysis method, so the measurement would not be void due to changes in the experimental set up.

4 - Can be easily cleaned and loose dirt cannot interfere with or block the reflectance measurements.

5 - Pre-illumination of the tubers to remove lag phase variance.

In industry today, in-line HSI systems are used to assess the quality of food. This could be an option for measurement methods for analysis the potato tubers samples. A HSI system, setup for a Kinetic Series analysis, could analyse several tubers for several hours. Line measurement would run over all tubers at equally timed intervals. The data would then be analysed by identifying the sprouts by certain wavelengths, as done in CHAPTER 8. The Chl Rates of these "spots" (identified as Eyes) could then be calculated. This proposed method would be beneficial, in comparison to the Hamamatsu spectrometer, as multiple tubers can be measured at once. However, a clear disadvantage, one of high importance in the commercial market, is the high cost of HSI systems in comparison.

The years of this project have shown that under certain conditions and a precise protocol, the Chl band in Visible spectroscopy can be used to follow the capacity of Chl production in potato tubers, during cold storage. Evidence of a predictive link of this property to the onset of dormancy breaking in the tuber has been established. The research that can be conducted in a laboratory has come to an end; the next step is to translate this research into industry application.

TERM REFERENCE GUIDE

ABBREVIATIONS

Chl   Chlorophyll

CIPC   Chlorpropham

Cv   Cultivar

GA   Gibberellins

HSI   Hyperspectral Imaging

IR   Infrared

NIR   Near-Infrared

RH   Relative Humidity

SNV   Standard Normal Variate

SWIR   Short-Wave Infrared

UV   Ultraviolet

Vis   Visible

DEFINITIONS

Static Series — During 'Static Series' experiments, the probe and tuber were clamped in place throughout the measurement period, fixed on the same position. This was done to remove repositioning error.

Kinetics Spectra — A series of single beam spectra taken from a given position on a tuber surface, divided by the first spectrum in the series (T_i/T_0). The reflectance spectra are then converted to absorbance spectra by taking the $-\log_{10}$. This series may either be taken at the Eye; referred to as *Kinetic Eye spectra*, or Background; as *Kinetic Background Spectra*, of a single tuber.

Absorbance Spectra	The result of a single beam Eye spectrum being referenced to the single beam Background Spectra taken for the same measurement on the same tuber, at the same time point. This reflectance spectrum is then converted into an absorbance spectrum by taking the natural log.
Chl Bands and Chl Areas	A *Chl Band* refers to the extracted region of a spectrum between 620 and 720 nm. The *Chl Area* is the summed area of the Chl Band. Any baseline offset is first removed by using anchor points either side of the Chl Band and subtracting any area under the spectra. For an example and further explanation refer to FIGURE 2. Kinetic, Difference and Kinetic Difference spectra are also analysed by calculating their Chl Bands and Chl Areas. As an example; Kinetic Eye/Background Chl Bands refers to the extraction of the Chl bands in a series of Kinetic spectra; similarly, Difference Chl Bands can be used to refer to the extraction of the Chl band from Difference spectra. The same format of naming has been used for Chl Areas and Chl Rate throughout this Thesis.
Chl Rate	The *Chl Rate* defines the line of best fit gradient calculated from a series of *Kinetic Chl Area* values, excluding any outliers.
Chl Difference Rate	The Difference between the Chl Rates of the Eye and Background kinetic measurements, taken on the same tuber at the same time point.
Sprouting Age	Defined as the day on which a tuber first shows visible signs of dormancy break, i.e. sprouting, as zero. Analysis days before that would therefore have a minus age, and after a positive age. See FIGURE 4:1 as a visual aid.

REFERENCES

Allen, E. J. & Scott, R. K. 1980. An Analysis Of Growth Of The Potato Crop. *The Journal of Agricultural Science,* 94**,** 583-606.

Alpert, N. L., Keiser, W. E. & Szymanski, H. A. 2012. *IR: Theory And Practice Of Infrared Spectroscopy*, Springer Science & Business Media.

Amrein, T. M., Bachmann, S., Noti, A., Biedermann, M., Barbosa, M. F., Biedermann-Brem, S., Grob, K., Keiser, A., Realini, P. & Escher, F. 2003. Potential Of Acrylamide Formation, Sugars, And Free Asparagine In Potatoes: A Comparison Of Cultivars And Farming Systems. *Journal of Agricultural and Food Chemistry,* 51**,** 5556-5560.

Anstis, P. J. P. & Northcot, D. H. 1973. Development of Chloroplasts from Amyloplasts in Potato Tuber Discs. *New Phytologist,* 72**,** 449-464.

Appeldoorn, N. J. G., Sergeeva, L., Vreugdenhil, D., Van Der Plas, L. H. W. & Visser, R. G. F. 2002. In Situ Analysis Of Enzymes Involved In Sucrose To Hexose-Phosphate Conversion During Stolon-To-Tuber Transition Of Potato. *Physiologia plantarum,* 115**,** 303-310.

Appleman, C. 1916. Relation of Oxidases and Catalase to Respiration in Plants. *American Journal of Botany,* 3**,** 223-233.

Appleman, C. O. & Miller, E. 1926a. A chemical and physiological study of maturity in potatoes. *Journal of Agricultural Research,* 33.

Appleman, C. O. & Miller, E. V. 1926b. A Chemical And Physiological Study Of Maturity In Potatoes. *Journal of Agricultural Research,* 33.

Ariana, D., Guyer, D. E. & Shrestha, B. 2006a. Integrating Multispectral Reflectance and Fluorescence Imaging for Defect Detection on Apples. *Computers and Electronics in Agriculture,* 50**,** 148-161.

Ariana, D. P., Lu, R. F. & Guyer, D. E. 2006b. Near-infrared Hyperspectral. Reflectance Imaging for Detection of Bruises on Pickling Cucumbers. *Computers and Electronics in Agriculture,* 53**,** 60-70.

Arnold, M. A. 1992. Fiber-Optic Chemical Sensors. *Analytical chemistry,* 64**,** 1015A-1025A.

Bailey, K. M., Phillips, I. D. J. & Pitt, D. 1978. Role of Buds and Gibberellin in Dormancy and Mobilization of Reserve Materials in Potato-Tubers. *Annals of Botany,* 42**,** 649-657.

Barker, J. 1932. Temperature and Metabolic Balance in the Potato. *Report of Food Investment, London,* 1931**,** 86-90.

Barker, J. 1933. Analytic Studies In Plant Respiration. Iv.—The Relation Of The Respiration Of Potatoes To The Concentration Of Sugars And To The Accumulation Of A Depressant At Low Temperatures. Part I.—The Effect Of Temperature-History On The Respiration/Sugar Relation. *Proceedings of the Royal Society of London,* 112**,** 316-335.

Barnes, M., Duckett, T., Cielniak, G., Stroud, G. & Harper, G. 2010. Visual Detection Of Blemishes In Potatoes Using Minimalist Boosted Classifiers. *Journal of Food Engineering,* 98**,** 339-346.

Barnes, R. J., Dhanoa, M. S. & Lister, S. J. 1989. Standard Normal Variate Transformation and De-trending of Near-Infrared Diffuse Reflectance Spectra. *Applied Spectroscopy,* 43**,** 772-777.

Bauman, R. P. 1962. Absorption Spectroscopy.

Beer, A. 1852. Determination Of The Absorption Of Red Light In Colored Liquids. *Annual Review of Physical Chemistry,* 86**,** 78-88.

Belay, A., Ture, K., Redi, M. & Asfaw, A. 2008. Measurement Of Caffeine In Coffee Beans With Uv/Vis Spectrometer. *Food Chemistry,* 108**,** 310-315.

Bellon-Maurel, V. & McBratney, A. 2011. Near-infrared (NIR) and Mid-infrared (MIR) Spectroscopic Techniques for Assessing the Amount of Carbon Stock in Soils - Critical Review and Research Perspectives. *Soil Biology & Biochemistry,* 43**,** 1398-1410.

Bianchi, G., Lo Scalzo, R., Testoni, A. & Maestrelli, A. 2014. Nondestructive Analysis to Monitor Potato Quality during Cold Storage. *Journal of Food Quality,* 37**,** 9-17.

Birch, C. P. 1999. A New Generalized Logistic Sigmoid Growth Equation Compared With The Richards Growth Equation. *Annals of Botany,* 83**,** 713-723.

Böddi, B., Láng, F. & Soós, J. 1979. A Study of 650 nm Protochlorophyll Form in Pumpkin Seed Coat. *Plant Science Letters,* 16**,** 75-79.

Boyd, W. D. & Duncan, H. J. 1986. Studies On Potato Sprout Suppressants. 7. Headspace And Residue Analysis Of Chlorpropham In A Commercial Box Potato Store. *Potato Research,* 29**,** 217-223.

Bradshaw, J. E. & Ramsay, G. 2009. Potato Origin And Production. *Advances in potato chemistry and technology.* Elsevier.

Brosnan, T. & Sun, D. W. 2002. Inspection and grading of agricultural and food products by computer vision systems - a review. *Computers and Electronics in Agriculture,* 36**,** 193-213.

Brush, S. B., Carney, H. J. & Humán, Z. 1981. Dynamics Of Andean Potato Agriculture. *Economic Botany,* 35**,** 70-88.

Büning-Pfaue, H. 2003. Analysis Of Water In Food By Near Infrared Spectroscopy. *Food Chemistry,* 82**,** 107-115.

Burstall, L., Thomas, M. N. & Allen, E. J. 1987. The Relationship Between Total Yield, Number of Tubers and Yield of Large Tubers in Potato Crops. *The Journal of Agricultural Science,* 108**,** 403-406.

Burton, W. G. 1966. *The Potato,* Wageningen, Holland, Longman Group Limited.

Caldiz, D. O., Fernandez, L. V. & Struik, P. C. 2001. Physiological Age Index: a New, Simple and Reliable Index to Assess the Physiological Age of Seed Potato Tubers Based on Haulm Killing Date and Length of the Incubation Period. *Field Crops Research,* 69**,** 69-79.

Clark, C. J., McGlone, V. A. & Jordan, R. B. 2003. Detection of Brownheart in 'Braeburn' Apple by Transmission NIR Spectroscopy. *Postharvest Biology and Technology,* 28**,** 87-96.

Cline, M. G. 1996. Exogenous Auxin Effects On Lateral Bud Outgrowth In Decapitated Shoots. *Annals of Botany,* 78**,** 255-266.

Coleman, W. K. 1987. Dormancy Release in Potato-Tubers - a Review. *American Potato Journal,* 64**,** 57-68.

Coleman, W. K. 2000. Physiological Ageing of Potato Tubers: A Review. *Annals of Applied Biology,* 137**,** 189-199.

Cottrell, J. E., Duffus, C. M., Paterson, L. & Mackay, G. R. 1995. Properties of Potato Starch - Effects of Genotype and Growing Conditions. *Phytochemistry,* 40**,** 1057-1064.

Cozzolino, D., Esler, M. B., Dambergs, R. G., Cynkar, W. U., Boehm, D. R., Francis, I. L. & Gishen, M. 2004. Prediction of Colour and pH in Grapes using a Diode Array Spectrophotometer (400-1100 nm). *Journal of Near Infrared Spectroscopy,* 12**,** 105-111.

Cunnington, A. & Pringle, R. 2008. Store Manager Guide. Potato Council, Lincolnshire: Agriculture & Horticulture Development Board (AHDB).

Dacal-Nieto, A., Formella, A., Carrión, P., Vazquez-Fernandez, E. & Fernández-Delgado, M. Non–Destructive Detection Of Hollow Heart In Potatoes Using Hyperspectral Imaging. International Conference on Computer Analysis of Images and Patterns, 2011. Springer, 180-187.

Dalla Costa, L., Delle Vedove, G., Gianquinto, G., Giovanardi, R. & Peressotti, A. 1997. Yield, Water Use Efficiency And Nitrogen Uptake In Potato: Influence Of Drought Stress. *Potato Research,* 40**,** 19-34.

Dao, L. & Friedman, M. 1994. Chlorophyll, Chlorogenic Acid, Glycoalkaloid, and Protease Inhibitor Content of Fresh and Green Potatoes. *Journal of Agricultural and Food Chemistry,* 42**,** 633-639.

Datt, B. 1998. Remote Sensing of Chlorophyll a, Chlorophyll b, Chlorophyll a+b, and Total Carotenoid Content in Eucalyptus Leaves. *Remote Sensing of Environment,* 66**,** 111-121.

Davidson, T. 1958. Dormancy in the Potato Tuber and the Effects of Storage Conditions on Initial Sprouting and on Subsequent Sprout Growth. *American Potato Journal,* 35**,** 451-465.

De Weerd, J. W., Hiller, L. K. & Thornton, R. E. 1995. Electrolyte Leakage of Aging Potato Tubers and its Relationship with Sprouting Capacity. *Potato Research,* 38**,** 257-270.

Debon, S. J. J., Tester, R. F., Millam, S. & Davies, H. V. 1998. Effect of Temperature on the Synthesis, Composition and Physical Properties of Potato Microtuber Starch. *Journal of the Science of Food and Agriculture,* 76**,** 599-607.

Donnelly, J. 2002. *Great Irish Potato Famine*, The History Press.

Douglas, L., MacKinnon, G., Cook, G., Duncan, H. J., Briddon, A. & Seamark, S. 2018. Determination Of Chlorpropham (Cipc) Residues, In The Concrete Flooring Of

Potato Stores, Using Quantitative (Hplc Uv/Vis) And Qualitative (Gcms) Methods. *Chemosphere,* 195**,** 119-124.

Edwards, E. J. & Cobb, A. H. 1997. Effect of Temperature on Glycoalkaloid and Chlorophyll Accumulation in Potatoes (Solanum tuberosum L cv King Edward) Stored at Low Photon Flux Density, including Preliminary Modeling using an Artificial Neural Network. *Journal of Agricultural and Food Chemistry,* 45**,** 1032-1038.

Edwards, E. J. & Cobb, A. H. 1999. The Effect of Prior Storage on the Potential of Potato Tubers (Solanum tuberosum L) to accumulate Glycoalkaloids and Chlorophylls during Light Exposure, including Artificial Neural Network Modelling. *Journal of the Science of Food and Agriculture,* 79**,** 1289-1297.

Elbatawi, I. E., Ebaid, M. T. & Hemeda, B. E. 2008. Determination Of Potato Water Content Using Nir Diffuse Reflection Method. *Misr J. Ag. Eng,* 25**,** 1279-1292.

Evans, L. T. 1996. *Crop Evolution, Adaptation and Yield*, Cambridge University Press.

Fifield, F. W. & Kealey, D. 1995. *Principles And Practice Of Analytical Chemistry*, Blackie academic & professional.

Friedman, M. & McDonald, G. M. 1997. Potato Glycoalkaloids: Chemistry, Analysis, Safety, and Plant Physiology. *Critical Reviews in Plant Sciences,* 16**,** 55-132.

Friedman, M., McDonald, G. M. & Filadelfi-Keszi, M. A. 1997. Potato Glycoalkaloids: Chemistry, Analysis, Safety, And Plant Physiology. *Critical Reviews in Plant Sciences,* 16**,** 55-132.

Gao, Y., Li, Q., Rao, X. & Ying, Y. 2018. Precautionary Analysis Of Sprouting Potato Eyes Using Hyperspectral Imaging Technology. *International Journal of Agricultural and Biological Engineering,* 11**,** 153-157.

Garnett, J. M. R., Wellner, N., Mayes, A. G., Downey, G. & Kemsley, E. K. 2018. Using Induced Chlorophyll Production To Monitor The Physiological State Of Stored Potatoes (Solanum Tuberosum L.). *Postharvest Biology and Technology,* 145**,** 222-229.

Gillison, T. C., Jenkins, P. D. & Hayes, J. D. 1987. Some Factors Affecting the Expression of the Physiological Age of Potato Seed Tubers. *Journal of Agricultural Science,* 108**,** 437-451.

Gitelson, A. A. & Merzlyak, M. N. 1996. Signature Analysis of Leaf Reflectance Spectra: Algorithm Development for Remote Sensing of Chlorophyll. *Journal of Plant Physiology,* 148**,** 494-500.

Gitelson, A. A. & Merzlyak, M. N. 1998. Remote Sensing of Chlorophyll Concentration in Higher Plant Leaves. *Synergistic Use of Multisensor Data for Land Processes,* 22**,** 689-692.

Glendinning, D. R. 1983. Potato Introductions And Breeding Up To The Early 20th Century. *New Phytologist,* 94**,** 479-505.

Goetz, A. F. H., Vane, G., Solomon, J. E. & Rock, B. N. 1985. Imaging Spectrometry for Earth Remote-Sensing. *Science,* 228**,** 1147-1153.

Gomez-Castillo, D., Cruz, E., Iguaz, A., Arroqui, C. & Virseda, P. 2013. Effects of Essential Oils on Sprout Suppression and Quality of Potato Cultivars. *Postharvest Biology and Technology,* 82**,** 15-21.

Gowen, A. A., O'Donnell, C. P., Cullen, P. J., Downey, G. & Frias, J. M. 2007. Hyperspectral Imaging - an Emerging process Analytical Tool for Food Quality and Safety Control. *Trends in Food Science & Technology,* 18**,** 590-598.

Graves, C. & Cabieses, F. 2001. *The Potato Treasure of the Andes: From Agriculture to Culture*, International Potato Center.

Gray, D. & Holmes, J. C. 1970. The Effect Of Short Periods Of Shading At Different Stages Of Growth On The Development Of Tuber Number And Yield. *Potato Research,* 13**,** 215-219.

Griffiths, D. W., Bain, H. & Dale, M. F. B. 1998. Effect Of Storage Temperature On Potato (Solanum Tuberosum L.) Tuber Glycoalkaloid Content And The Subsequent Accumulation Of Glycoalkaloids And Chlorophyll In Response To Light Exposure. *Journal Of Agricultural And Food Chemistry,* 46**,** 5262-5268.

Grunenfelder, L. 2005. Physiological Studies Of Light-Induced Greening In Fresh Market Potatoes.

Grunenfelder, L., Hiller, L. K. & Knowles, N. R. 2006a. Color Indices for the Assessment of Chlorophyll Development and Greening of Fresh Market Potatoes. *Postharvest Biology and Technology,* 40**,** 73-81.

Grunenfelder, L. A., Knowles, L. O., Hiller, L. K. & Knowles, N. R. 2006b. Glycoalkaloid Development During Greening of Fresh Market Potatoes (Solanum tuberosum L.). *Journal of Agricultural and Food Chemistry,* 54**,** 5847-5854.

Guimet, F., Ferré, J., Boqué, R. & Rius, F. X. 2004. Application Of Unfold Principal Component Analysis And Parallel Factor Analysis To The Exploratory Analysis Of Olive Oils By Means Of Excitation–Emission Matrix Fluorescence Spectroscopy. *Analytica Chimica Acta,* 515**,** 75-85.

Gull, D. D. & Isenberg, F. M. Lightburn and Off-flavor Development in Potato Tubers Exposed to Fluorescent Lights. Proceedings of the American Society for Horticultural Science, 1958. 446-454.

Gull, D. D. & Isenberg, F. M. Chlorophyll and Solanine Content and Distribution in Four Varieties of Potato Tubers. Proceedings of the American Society for Horticultural Science, 1960. 545-56.

Guo, Q., Wu, W. & Massart, D. L. 1999. The Robust Normal Variate Transform For Pattern Recognition With Near-Infrared Data. *Analytica Chimica Acta,* 382**,** 87-103.

Haase, N. U. & Plate, J. 1996. Properties of Potato Starch in Relation to Varieties and Environmental Factors. *Starch-Starke,* 48**,** 167-171.

Hakim, A., Purvis, A. C., Voipio, I., Pehu, E. & Khatoon, M. Use of Different Nondestructive Techniques to Evaluate Vegetable Quality. International Symposium on Vegetable Quality of Fresh and Fermented Vegetables 483, 1997. 235-244.

Harris, P. M. 1992. *The Potato Crop: The Scientific Basis for Improvement,* London, Chapman and Hall.

Hartmann, A., Senning, M., Hedden, P., Sonnewald, U. & Sonnewald, S. 2011. Reactivation of Meristem Activity and Sprout Growth in Potato Tubers Require Both Cytokinin and Gibberellin. *Plant Physiology,* 155**,** 776-796.

Hawkes, J. G. & Francisco-Ortega, J. 1993. The Early History Of The Potato In Europe. *Euphytica,* 70**,** 1-7.

Hide, G. A. & Boorer, K. J. 1991. Effects Of Drying Potatoes (Solanum Tuberosum L.) After Harvest On The Incidence Of Disease After Storage. *Potato Research,* 34**,** 133-137.

Hide, G. A. & Cayley, G. R. 1987. Effects Of Delaying Fungicide Treatment And Of Curing And Chlorpropham On The Incidence Of Skin Spot On Stored Potato Tubers. *Annals Of Applied Biology,* 110**,** 617-627.

Hill, L. M., Reimholz, R., Schröder, R., Nielsen, T. H. & Stitt, M. 1996. The Onset Of Sucrose Accumulation In Cold-Stored Potato Tubers Is Caused By An Increased Rate Of Sucrose Synthesis And Coincides With Low Levels Of Hexose-Phosphates, An Activation Of Sucrose Phosphate Synthase And The Appearance Of A New Form Of Amylase. *Plant, Cell & Environment,* 19**,** 1223-1237.

Holliday, R., Ivins, J. D. & Milthorpe, F. L. 1963. Effects of Fertilizers Upon Potato Yields and Quality. *The Growth of the Potato, Butterworths, London***,** 248-264.

Hoover, R. 2001. Composition, Molecular Structure, and Physicochemical Properties of Tuber and Root Starches: A Review. *Carbohydrate Polymers,* 45**,** 253-267.

Howard, H. M. 1970. *Genetics Of The Potato Solanum Tuberosum,* London, Logos Press Limited.

Huang, H., Liu, L. & Ngadi, M. O. 2014. Recent Developments in Hyperspectral Imaging for Assessment of Food Quality and Safety. *Sensors,* 14**,** 7248-7276.

Idelberger, C., Sticksel, E. & Mulla, D. J. Spectral Measurements of Sunlight-induced Chlorophyll-fluorescence with Potatoes regarding N-fertilization. Proceedings of the 7th International Conference on Precision Agriculture and Other Precision Resources Management, Hyatt Regency, Minneapolis, MN, USA, 25-28 July, 2004., 2004. Precision Agriculture Center, University of Minnesota, Department of Soil, Water and Climate, 1419-1428.

Iritani, W. M., Thornton, R., Weller, L. & O'leary, G. 1972. Relationships Of Seed Size, Spacing, Stem Numbers To Yield Of Russet Burbank Potatoes. *American Potato Journal,* 49**,** 463-469.

Jenkins, P. D., Gillison, T. C. & Alsaidi, A. S. 1993. Temperature Accumulation and Physiological Aging of Seed Potato-Tubers. *Annals of Applied Biology,* 122**,** 345-356.

Jeong, J. C., Ok, H. C., Hur, O. S. & Kim, C. G. 2008. Prediction of Sprouting Capacity using Near-Infrared Spectroscopy in Potato Tubers. *American Journal of Potato Research,* 85**,** 309-314.

Kaiserli, E. & Chory, J. 2015. The Role of Phytochromes in Triggering Plant Developmental Transitions. *eLS*.

Karafyllidis, D. I., Stavropoulos, N. & Georgakis, D. 1996. The Effect Of Water Stress On The Yielding Capacity Of Potato Crops And Subsequent Performance Of Seed Tubers. *Potato Research,* 39**,** 153-163.

Kidder, A. 1967. A Mochica Potato Bird. *Expedition.* The Penn Museum.

Kim, H. & Lee, S. 1992. Effects of curing and storage conditions on processing quality in potatoes. *Physiological Basis of Postharvest Technologies 343*, 73-76.

Kizil, R., Irudayaraj, J. & Seetharaman, K. 2002. Characterization of Irradiated Starches by Using FT-Raman and FTIR Spectroscopy. *Journal Of Agricultural And Food Chemistry,* 50, 3912-3918.

Kleinkopf, G. E., Oberg, N. A. & Olsen, N. L. 2003. Sprout Inhibition in Storage: Current status, new Chemistries and Natural Compounds. *American Journal of Potato Research,* 80, 317-327.

Kloosterman, B., Navarro, C., Bijsterbosch, G., Lange, T., Prat, S., Visser, R. G. F. & Bachem, C. W. B. 2007. Stga2ox1 Is Induced Prior To Stolon Swelling And Controls Ga Levels During Potato Tuber Development. *The Plant Journal,* 52, 362-373.

Knowles, L. O. & Knowles, N. R. 1990. Changes in Fatty-Acid Composition of Phospholipids from Different Ages of Potato Seed-Tubers during Sprouting. *Annals of Botany,* 65, 217-223.

Knowles, N. R. & Knowles, L. O. 1989. Correlations between Electrolyte Leakage and Degree of Saturation of Polar Lipids from Aged Potato (Solanum-Tuberosum-L) Tuber Tissue. *Annals of Botany,* 63, 331-338.

Kozukue, N., Tsuchida, H. & Freidman, M. 2001. Tracer Studies on the Incorporation of [2-C-14]-DL-Mevalonate into Chlorophylls a and b, alpha-Chaconine, and alpha-Solanine of Potato Sprouts. *Journal of Agricultural and Food Chemistry,* 49, 92-97.

Leemans, V. & Destain, M. F. 2004. A Real-Time Grading Method Of Apples Based On Features Extracted From Defects. *Journal of Food Engineering,* 61, 83-89.

Lehesranta, S. J., Davies, H. V., Shepherd, L. V. T., Nunan, N., McNicol, J. W., Auriola, S., Koistinen, K. M., Suomalainen, S., Kokko, H. I. & Kärenlampi, S. O. 2005. Comparison Of Tuber Proteomes Of Potato Varieties, Landraces, And Genetically Modified Lines. *Plant Physiology,* 138, 1690-1699.

Liu, B., Zhang, N., Wen, Y., Jin, X., Yang, J., Si, H. & Wang, D. 2015. Transcriptomic Changes During Tuber Dormancy Release Process Revealed By Rna Sequencing In Potato. *Journal of biotechnology,* 198, 17-30.

Lu, Z. H., Donner, E., Yada, R. Y. & Liu, Q. 2012. Rheological and Structural Properties of Starches from Gamma-Irradiated and Stored Potatoes. *Carbohydrate Polymers,* 87, 69-75.

Mackinney, G. 1941. Absorption of Light by Chlorophyll Solutions. *Journal of Biological Chemistry,* 140, 315-322.

Ming, W., Du, J., Shen, D., Zhang, Z., Li, X., Ma, J. R., Wang, F. & Ma, J. 2018. Visual Detection Of Sprouting In Potatoes Using Ensemble-Based Classifier. *Journal of Food Process Engineering,* 41, e12667.

Moran, R. 1982. Formulae for Determination of Chlorophyllous Pigments Extracted with N, N-dimethylformamide. *Plant physiology,* 69, 1376-1381.

Moran, R. & Porath, D. 1980. Chlorophyll Determination in Intact Tissues using N, N-dimethylformamide. *Plant Physiology,* 65, 478-479.

Morris, S. C., Graham, D. & Lee, T. H. 1979. Phytochrome Control of Chlorophyll Synthesis in Potato Tubers. *Plant Science Letters,* 17**,** 13-19.

Museum, P. 1939. The Potato-Mother. Expedition Magazine: Kidder, II, .Alfred.

Næs, T., Isaksson, T., Fearn, T. & Davies, T. 2002. *A User Friendly Guide To Multivariate Calibration And Classification*, NIR publications.

Nations, F. a. A. O. o. t. U. 2014. FAOSTAT. Rome, Italy: FAO.

Nicolai, B. M., Beullens, K., Bobelyn, E., Peirs, A., Saeys, W., Theron, K. I. & Lammertyn, J. 2007. Nondestructive Measurement of Fruit and Vegetable Quality by means of NIR Spectroscopy: A Review. *Postharvest Biology and Technology,* 46**,** 99-118.

Norris, K. H. 1964. Design and Development of a New Moisture Meter. *Agriculture Engineering,* 45**,** 370.

O'Neill, J. R. 2009. *Irish Potato Famine*, ABDO.

Olsen, N., Miller, J. & Nolte, P. 2006. *Diagnosis & Management of Potato Storage Diseases*, Idaho Agricultural Experiment Station.

Omayio, D. G., Abong, G. O. & Okoth, M. W. 2016. A Review Of Occurrence Of Glycoalkaloids In Potato And Potato Products. *Current Research in Nutrition and Food Science Journal,* 4**,** 195-202.

Onder, S., Caliskan, M. E., Onder, D. & Caliskan, S. 2005. Different Irrigation Methods And Water Stress Effects On Potato Yield And Yield Components. *Agricultural Water Management,* 73**,** 73-86.

Osborne, B. G. & Fearn, T. 1986. *Near Infrared Spectroscopy In Food Analysis*, Longman Scientific & Technical.

Peirs, A., Lammertyn, J., Ooms, K. & Nicolai, B. M. 2001. Prediction of the Optimal Picking Date of different Apple Cultivars by means of VIS/NIR-spectroscopy. *Postharvest Biology and Technology,* 21**,** 189-199.

Percival, G. C. 1999. The Influence Of Light Upon Glycoalkaloid And Chlorophyll Accumulation In Potato Tubers (Solanum Tuberosum L.). *Plant Science,* 145**,** 99-107.

Petermann, J. B. & Morris, S. C. 1985. The Spectral Responses of Chlorophyll and Glycoalkaloid Synthesis in Potato-Tubers (Solanum-Tuberosum). *Plant Science,* 39**,** 105-110.

Pieterse, L. 2012. *New Tools For Bruise Free Storage* [Online]. SpudSmart.com. Available: http://spudsmart.com/new-tools-for-bruise-free-storage-spud-smart-fall-2012/ [Accessed June 19th 2018].

Qiao, J., Wang, N., Ngadi, M. O. & Baljinder, S. 2005a. Water Content and Weight Estimation for Potatoes Using Hyperspectral Imaging. *American Society of Agricultural Engineers Annual Meeting. Tampa Convention Center. Tampa, Florida.,* 53126.

Qiao, J., Wang, N., Ngadi, M. O. & Baljinder, S. 2005b. Water Content and Weight Estimation for Potatoes using Hyperspectral Imaging. *Published by the American*

Society of Agricultural and Biological Engineers, St. Joseph, Michigan www. asabe. org. Paper.

Rady, A. M. & Guyer, D. E. 2015. Rapid and/or nondestructive quality evaluation methods for potatoes: A review. *Computers and Electronics in Agriculture,* 117**,** 31-48.

Richards, F. J. 1959. A Flexible Growth Function For Empirical Use. *Journal of experimental Botany,* 10**,** 290-301.

Ríos, D., Ghislain, M., Rodríguez, F. & Spooner, D. M. 2007. What Is The Origin Of The European Potato? Evidence From Canary Island Landraces. *Crop Science,* 47**,** 1271-1280.

Roumeliotis, E., Kloosterman, B., Oortwijn, M., Kohlen, W., Bouwmeester, H. J., Visser, R. G. F. & Bachem, C. W. B. 2012. The Effects Of Auxin And Strigolactones On Tuber Initiation And Stolon Architecture In Potato. *Journal of experimental botany,* 63**,** 4539-4547.

Sarkar, N. & Wolfe, R. R. 1985. Feature Extraction Techniques For Sorting Tomatoes By Computer Vision. *Transactions of the ASAE,* 28**,** 970-0974.

Savitzky, A. & Golay, M. J. E. 1964. Smoothing And Differentiation Of Data By Simplified Least Squares Procedures. *Analytical chemistry,* 36**,** 1627-1639.

Schippers, P. A. 1977. Rate of Respiration of Potato Tubers during Storage .1. Review of Literature. *Potato Research,* 20**,** 173-188.

Schmilovitch, Z., Mizrach, A., Hoffman, A., Egozi, H. & Fuchs, Y. 2000. Determination of Mango Physiological Indices by Near-infrared Spectrometry. *Postharvest Biology and Technology,* 19**,** 245-252.

Scotter, C. 1990. Use of Near Infrared Spectroscopy in the Food Industry with Particular Reference to its Applications to on/in-line Food Processes. *Food Control,* 1**,** 142-149.

Sergeeva, L. I., Claassens, M. M. J., Jamar, D. C. L., van der Plas, L. H. W. & Vreugdenhil, D. 2012. Starch-related Enzymes during Potato Tuber Dormancy and Sprouting. *Russian Journal of Plant Physiology,* 59**,** 556-564.

Shin, K. S., Chakrabarty, D. & Paek, K. Y. 2002. Sprouting Rate, Change Of Carbohydrate Contents And Related Enzymes During Cold Treatment Of Lily Bulblets Regenerated In Vitro. *Scientia Horticulturae,* 96**,** 195-204.

Sibma, L. 1970. Relation Between Total Radiation And Yield Of Some Field Crops In The Netherlands. *Netherlands Journal of Agricultural Science,* 18**,** 125-31.

Skoog, D. A., West, D. M., Holler, F. J. & Crouch, S. 2013. *Fundamentals Of Analytical Chemistry*, Nelson Education.

Smith, D. B., Roddick, J. G. & Jones, J. L. 1996. Potato Glycoalkaloids: Some Unanswered Questions. *Trends in Food Science & Technology,* 7**,** 126-131.

Solé, J., Bausa, L. & Jaque, D. 2005. *An Introduction to the Optical Spectroscopy of Inorganic Solids*, Wiley.

Sonnewald, U. 2001. Control Of Potato Tuber Sprouting. *Trends In Plant Science,* 6**,** 333-335.

Sorce, C., Lorenzi, R., Ceccarelli, N. & Ranalli, P. 2000. Changes in Free and Conjugated IAA during Dormancy and Sprouting of Potato Tubers. *Australian Journal of Plant Physiology,* 27**,** 371-377.

Sorce, C., Piaggesi, A., Ceccarelli, N. & Lorenzi, R. 1996. Role and Metabolism of Abscisic acid in Potato Tuber Dormancy and Sprouting. *Journal of Plant Physiology,* 149**,** 548-552.

Sowokinos, J. R., Hayes, R. J. & Thill, C. A. 2018. Coordinated Regulation of Cold Induced Sweetening in Tetraploid Potato Families by Isozymes of UDP-Glucose Pyrophosphorylase and Vacuolar Acid Invertase. *American Journal of Potato Research,* 95**,** 487-494.

Spychalla, J. P. & Desborough, S. L. 1990. Fatty-Acids, Membrane-Permeability, and Sugars of Stored Potato-Tubers. *Plant Physiology,* 94**,** 1207-1213.

Storey, M. & Briddon, A. 2018. *Be CIPC Compliant* [Online]. Sutton Bridge Crop Storage Research: Potato Industry CIPC Stewardship Group. Available: http://www.cipccompliant.co.uk [Accessed 14th August 2018].

Su, W. H., Liu, G. S., He, J. G., Wang, S. L., He, X. G., Wang, W. & Wu, L. G. 2014. Detection of External Defects on Potatoes by Hyperspectral Imaging Technology and Image Processing Method. *Journal of Zhejiang University (Agriculture and Life Sciences),* 40.

Sundbom, E., Strand, M. & Hällgren, J. 1982. Temperature-Induced Fluorescence Changes A Screening Method for Frost Tolerance of Potato (Solanum Sp.). *Plant physiology,* 70**,** 1299-1302.

Suttle, J. C. 2004. Physiological Regulation of Potato Tuber Dormancy. *American Journal of Potato Research,* 81**,** 253-262.

Svanberg, S. 2012. *Atomic and Molecular Spectroscopy: Basic Aspects and Practical Applications*, Springer Berlin Heidelberg.

Tester, R. F. & Karkalas, J. 2001. The Effects of Environmental Conditions on the Structural Features and Physico-Chemical Properties of Starches. *Starch-Starke,* 53**,** 513-519.

Tester, R. F., Karkalas, J. & Qi, X. 2004. Starch - Composition, fine Structure and Architecture. *Journal of Cereal Science,* 39**,** 151-165.

Vanderzaag, D. E. & Vanloon, C. D. 1987. Effect of Physiological Age on Growth Vigor of Seed Potatoes of 2 Cultivars .5. Review of Literature and Integration of Some Experimental Results. *Potato Research,* 30**,** 451-472.

Vanittersum, M. K., Aben, F. C. B. & Keijzer, C. J. 1992. Morphological-Changes in Tuber Buds during Dormancy and Initial Sprout Growth of Seed Potatoes. *Potato Research,* 35**,** 249-260.

Vanittersum, M. K. & Scholte, K. 1992. Shortening Dormancy of Seed Potatoes by Storage-Temperature Regimes. *Potato Research,* 35**,** 389-401.

Vansoest, J. J. G., Dewit, D., Tournois, H. & Vliegenthart, J. F. G. 1994. Retrogradation of Potato Starch as Studied by Fourier-Transform Infrared-Spectroscopy. *Starch-Starke,* 46**,** 453-457.

Vijay, P., Ezekiel, R. & Pandey, R. 2018. Use of CIPC as a potato sprout suppressant: health and environmental concerns and future options. *Quality Assurance and Safety of Crops & Foods,* 10**,** 17-24.

Viola, R., Pelloux, J., Van der Ploeg, A., Gillespie, T., Marquis, N., Roberts, A. G. & Hancock, R. D. 2007a. Symplastic Connection is Required for Bud Outgrowth following Dormancy in Potato (Solanum tuberosum L.) Tubers. *Plant Cell and Environment,* 30**,** 973-983.

Viola, R., Pelloux, J., van der Ploeg, A., Gillespie, T., Marquis, N., Roberts, A. G. & Hancock, R. D. 2007b. Symplastic Connection Is Required For Bud Outgrowth Following Dormancy In Potato (Solanum Tuberosum L.) Tubers. *Plant, Cell & Environment,* 30**,** 973-983.

Virgin, H. I. & Sundqvist, C. 1992. Pigment Formation in Potato-Tubers (Solanum-Tuberosum) Exposed to Light Followed by Darkness. *Physiologia Plantarum,* 86**,** 587-592.

Visser, R. G. F., Vreugdenhil, D., Hendriks, T. & Jacobsen 1994. Gene Expression And Carbohydrate Content During Stolon To Tuber Transition In Potatoes (Solanum Tuberosum). *Physiologia Plantarum,* 90**,** 285-292.

Wang, L. & Zhao, C. 2016. *Hyperspectral Image Processing*, Springer.

Wang, Q., Cao, Y., Zhou, L., Jiang, C., Feng, Y. & Wei, S. 2015. Effects Of Postharvest Curing Treatment On Flesh Colour And Phenolic Metabolism In Fresh-Cut Potato Products. *Food Chemistry,* 169**,** 246-254.

Watson, D. J. 1963. Some Features Of Crop Nutrition. *The Growth Of The Potato. London: Butterworth***,** 233-237.

Wellner, N. & Kemsley, K. 2017. *Spectroscopy Method and System*. UK patent application 15/270,643

Williams, C. 14th September 2017. *RE: Meeting at Produce World.* Type to GARNETT, J. M. R.

Williams, P. & Norris, K. 1987. *Near-Infrared Technology in the Agricultural and Food Industries (NIR-Technologie in der Landwirtschaft und Lebensmittelindustrie)*.

Wiltshire, J. J. J. & Cobb, A. H. 1996. A Review of the Physiology of Potato Tuber Dormancy. *Annals of Applied Biology,* 129**,** 553-569.

Wise, R. R. 2006. The Diversity of Plastid Form and Function. *In:* WISE, R. T. R. & HOOBER, J. K. (eds.) *The Structure and Function of Plastids.* Dordrecht: Springer Netherlands.

Wolfbeis, O. S. 2008. Fiber-Optic Chemical Sensors And Biosensors. *Analytical chemistry,* 80**,** 4269-4283.

Yao, H. B., Hruska, Z., Kincaid, R., Brown, R. L., Bhatnagar, D. & Cleveland, T. E. 2013. Detecting Maize Inoculated with Toxigenic and Atoxigenic Fungal Strains with Fluorescence Hyperspectral Imagery. *Biosystems Engineering,* 115**,** 125-135.

Young, M. A., Stuart, D. A., Lyandres, O., Glucksberg, M. R. & Van Duyne, R. P. 2004. Surface-Enhanced Raman Spectroscopy With A Laser Pointer Light Source And Miniature Spectrometer. *Canadian Journal Of Chemistry,* 82**,** 1435-1441.

Yuan, B., Nishiyama, S. & Kang, Y. 2003. Effects Of Different Irrigation Regimes On The Growth And Yield Of Drip-Irrigated Potato. *Agricultural Water Management,* 63**,** 153-167.

Yusuph, M., Tester, R. F., Ansell, R. & Snape, C. E. 2003. Composition and Properties of Starches Extracted from Tubers of Different Potato Varieties Grown under the same Environmental Conditions. *Food Chemistry,* 82**,** 283-289.

Zalacain, A., Ordoudi, S. A., Blázquez, I., Díaz-Plaza, E. M., Carmona, M., Tsimidou, M. Z. & Alonso, G. L. 2005. Screening Method For The Detection Of Artificial Colours In Saffron Using Derivative Uv-Vis Spectrometry After Precipitation Of Crocetin. *Food Additives & Contaminants,* 22**,** 607-615.

Zhou, L., Chalana, V. & Kim, Y. 1998. Pc-Based Machine Vision System For Real-Time Computer-Aided Potato Inspection. *International Journal of Imaging Systems and Technology,* 9**,** 423-433.

APPENDIX 1

```matlab
%% CHAPTER THREE
%
% Script used to create the figures contain in chapter three. The
% following read analysis and displays the short-term experiments
% explained in my thesis. Within are three self-written functions:
% CorrectVis, ConvertVis and ColorPlots.
%
% J. Garnett, July 2018



%% FIGURES 3 - 7

% % Create Idx of Static Series Experiments:
Exp(1,:) = {2014 'MARIS PIPER HAREVST 2014'
'U:\2014HarvestData\EpisodicData\GsMarisPiper\2014_11_13\Vis'};
Exp(2,:) = {2014 'HERMES HARVEST 2014'
'U:\2014HarvestData\EpisodicData\Hermes\2015_02_27\Eye'};
Exp(3,:) = {2015 'CULTRA HARVEST 2015' 'U:\2015HarvestData\Visible-
Infrared\WeekendExperiments'};
Exp(4,:) = {2016 'ROYAL HARVEST 2016'
'U:\2017SummerTests\20170727\Side'};
Exp(5,:) = {2018 'WHITE HARVEST 2017' 'U:\2018Tests\LONGStatic'};


% % Select Experiment to Look At:
exp = 1; % Run through 1 - 5 to get the five figures


% % Load Spectra and Input into a Spectra Variable:
cd(Exp{exp,3});
D = dir('*.EP*'); FileiD = cellstr(char(D.name));
% Read data..
file = fopen(FileiD{1,1});
data = fread(file,'single');
fclose(file);
% Reshape data into a suitable matrix..
Spectra = reshape(data,2051,length(data)/2051); Spectra =
Spectra(11:end, :);
Wavelength = linspace(data(9,1), data(9,1) + (data(7,1))*2051,
2051); Wavelength = Wavelength(11:end)';


% % Alterations for Specific Files:
if exp == 1
    Spectra = Spectra(1:sum(Spectra(:, end) ~= 0), :); % cut off
extra "zeros" at the end of the matrix
    [w,s] = size(Spectra);
    Wavelength = linspace(data(9,1), 1100, w); % create new size
wavelength range
elseif exp == 2
    Spectra = Spectra(:, (1:2:57)); % Has a repeating spectra
    [w,s] = size(Spectra);
    Wavelength = linspace(data(9,1), data(9,1) + (data(7,1)-
0.06)*2051, w);
elseif exp == 4
    Spectra = Spectra(sum(Spectra(:, 1) == 0):end-1, 1:5:end); % cut
off extra "zeros" at beginning and take every 5 spectra
    [w,s] = size(Spectra);
    Wavelength = linspace(Wavelength(1), Wavelength(end), w); %
```

```matlab
elseif exp == 5
    Spectra = Spectra(:, 1:100); % Cut data short as tuber moved
    [w,s] = size(Spectra);
else
    [w,s] = size(Spectra);
end


% % Spectra Corrections/Kinetic Conversions:
[Spectra] = CorrectVis(Spectra, 0, 0); % self written function
"CorrectVis"
[Absorb, NW, Area] = ConvertVis(Spectra, Wavelength); % self written
function "ConvertVis"


% % Create Figure:
Color = ColorPlots(3, s); % Colour scheme, self written function
"ColorPlots"
[S] = SubplotPositions(1, 3, 0.1, 0.07, 0.05, 0); % Subplot
positioning
% Plot one - single beam spectra..
close all; figure('Position', [10 50 950 950])
subplot('Position', S(1,:))
p = plot(Wavelength,Spectra);
title('SINGLE BEAM SPECTRA', 'fontweight', 'normal')
xlabel('Wavelength (nm)'); ylabel({Exp{exp,2}; ''; 'Signal
(counts)'})
axis square tight;
if Wavelength(1)>400 % Different axis for the two spectrometers used
    xlim([500,1100]);
else
    xlim([400,1100]);
end
for c = 1:s % Set graduated color for time order
    set(p(c),'Color',Color(c,:))
end
% Plot two - kinetic chl bands..
subplot('Position', S(2,:))
p = plot(NW, Absorb);
title('KINETIC CHL BANDS', 'fontweight', 'normal')
xlabel('Wavelength (nm)'); ylabel('Differential Absorbance')
axis square tight; xlim([620,720]);
for c = 1:s
    set(p(c),'Color',Color(c,:))
end
% Create variable of experiment duration..
if exp == 2
    Time = linspace(0, (data(5)+120000)/3600000 * ((s*2)-1), s);
elseif exp == 4
    Time = linspace(0, (data(5)+120000)/3600000 * ((s*5)-1), s);
else
Time = linspace(0, (data(5)+120000)/3600000 * (s-1), s);
end
% Plot three - kinetic chl areas..
subplot('Position', S(3,:))
for c = 1:s
    plot(Time(c), Area(1,c), '.', 'Color', Color(c,:),
'markersize',10);
    hold on
end
title('KINETIC CHL AREAS', 'fontweight', 'normal')
axis square tight
xlabel('Time (hours)'); ylabel('Chl Band Areas')
```

```matlab
%% FIGURE 8

% % Load Spectra and Create (Wav/Spectra) Variables:
cd('U:\2017SummerTests\IntermittentLight');
D = dir('*.ssm'); FileiD = cellstr(char(D.name));
% Read into spectra matrix..
for x = 1:length(FileiD)
        data = dlmread(char(FileiD(x)),' ',2,0);
        Spectra(:,x) = [data(1:1018,4);data(1019:end,3)];
end
Wavelength = [data(1:1018,2);data(1019:end,1)];

% % Spectra Corrections/Kinetic Conversions:
[Spectra] = CorrectVis(Spectra, 0, 0);
[Absorb, NW, Area] = ConvertVis(Spectra, Wavelength);

% % Create Figure:
Color = [ColorPlots(2,12); ColorPlots(3,13); ColorPlots(4,11)]; %
Colour scheme
[S] = SubplotPositions(1, 2, 0.08, 0.08, 0.05, 0); % Subplot
positioning
% Plot one - kinetic chl bands..
close all; figure('Position', [10 50 950 950])
subplot('Position', S(1,:))
p = plot(NW, Absorb);
xlabel('Wavelength (nm)')
ylabel('Differential Absorbance')
title('KINETIC CHL BANDS', 'fontweight', 'normal')
axis tight; xlim([620,720]);
for c = 1:length(p)
    set(p(c),'Color',Color(c,:))
end
% Plot two - kinetic chl areas..
subplot('Position', S(2,:))
T = str2num(FileiD{1,1}(1:2))+ str2num(FileiD{1,1}(3))/6;
for c = 1:size(Spectra,2)
    t = (str2num(FileiD{c,1}(1:2))+ str2num(FileiD{c,1}(3))/6) - T;
    p(c) = plot(t,Area(c),'Color',Color(c,:), 'marker',
'.','markersize',12);
    hold on
end
xlabel('Time (hours)')
ylabel('Chl Band Area')
title('KINETIC CHL AREAS', 'fontweight', 'normal')
axis square tight
l = legend([p(6), p(21), p(31)], 'Day 1', 'Day 2', 'Day 3',
'orientation', 'horizontal');
l.Position = [0.78 0.77 0.14 0.03];


%% FIGURE 9

% % Load Spectra and Create Variables:
cd('U:\2018Tests\19.02.18')
file = fopen('OrSprtd.EP1');
data = fread(file,'single');
fclose(file);
Spectra = reshape(data,2051,length(data)/2051);
Time = linspace(0,54,size(Spectra,2));  % Measurement time
```

```matlab
Spectra = Spectra(11:end, 10:4:end); Time = Time(10:4:end); % Take
every 4 measurements to uncrowd plot
Wavelength = linspace(data(9,1), data(9,1) + (data(7,1))*2051,
2051); Wavelength = Wavelength(11:end)';
% Index for when lights were illuminated..
Lights = [find(Time<6), find(Time>23& Time<30.1), find(Time>48)];


% % Spectra Corrections/Kinetic Conversions:
[Spectra] = CorrectVis(Spectra, 0, 0);
[Absorb, NW, Area] = ConvertVis(Spectra, Wavelength);


% % Create Figure:
ColorB = ColorPlots(3,3); ColorG = ColorPlots(4,3); % Colour scheme
[S] = SubplotPositions(1, 2, 0.08, 0.08, 0.05, 0); % Subplot
positioning
% Plot one - kinetic chl bands..
close all; figure('Position', [10 50 950 950])
subplot('Position', S(1,:))
p = plot(NW, Absorb, 'Color', ColorB(1,:));
xlabel('Wavelength (nm)')
ylabel('Differential Absorbance')
title('KINETIC CHL BANDS', 'fontweight', 'normal')
axis tight; xlim([640,720]);
for c = 1:length(Lights)
    set(p(Lights(c)), 'Color', ColorG(3,:))
end
% Plot two - kinetic chl areas..
subplot('position',S(2,:))
p = plot(Time,Area, '.', 'Color', ColorB(1,:), 'markersize',12);
hold on
for c = 1:length(Lights)
    pp = plot(Time(Lights(c)),Area(Lights(c)), '.', 'Color',
ColorG(3,:), 'markersize',12);
    hold on
end
xlabel('Time (hours)')
ylabel('Chl Band Area')
title('KINETIC CHL AREAS', 'fontweight', 'normal')
axis square tight
l = legend([p(1), pp(1)], 'Lights ON', 'Lights OFF', 'orientation',
'horizontal');
l.Position = [0.79 0.76 0.14 0.03];


%% FIGURE 10

% % Load Spectra and Create (Wav/Spectra) Variables:
cd('U:\2017SummerTests\20170628\1')
D = dir; FileiD = {D(3:end).name};
for x = 1 : length(FileiD)
    data = dlmread(char(FileiD(x)),' ', 2, 0);
    Spectra(:,x) = [data(1:1018,4); data(1019:end,3)];
end
Wavelength = [data(1:1018,2); data(1019:end,1)];

% % Create Figure (Plot One - Raw Spectra):
Color = ColorPlots(3, 3); % Colour scheme
[S] = SubplotPositions(1, 2, 0.08, 0.08, 0.05, 0); % Subplot
positioning
close all; figure('Position', [10 50 950 950])
```

```matlab
subplot('Position', S(1,:))
plot(Wavelength, Spectra(:,1:20), 'color', Color(2,:));
axis tight square
title('RAW SINGLE BEAM SPECTRA', 'fontweight', 'normal');
xlabel('Wavelength (nm)');
ylabel('Signal (counts)')


% % Spectra Corrections:
[Spectra] = CorrectVis(Spectra, 0, 0);

% % Create Figure (Plot One - Normalised Spectra):
subplot('Position', S(2,:))
plot(Wavelength, Spectra, 'color', Color(2,:));
axis tight; axis square
title('NORMALISED SPECTRA', 'fontweight', 'normal');
xlabel('Wavelength (nm)');
ylabel('Signal (counts)')


%% FIGURE 11

% % Load Spectra For Deep Set Eye:
cd('G:\2017SummerTests\20170830\DeepEye');
D = dir; FileiD = {D(3:end).name};
for x = 1:length(FileiD)
    data = dlmread(char(FileiD(x)),' ', 2, 0);
    Spectra(:,x) = [data(1:1018,4); data(1019:end,3)];
end
Wavelength = [data(1:1018,2); data(1019:end,1)];

% % Create Figure (Plot One - Raw Spectra):
Color = ColorPlots(3, 3); % Colour
S = [0.08 0.55 0.17 0.34; 0.29 0.55 0.17 0.34; 0.50 0.55 0.17 0.34;
0.08 0.15 0.17 0.34; 0.29 0.15 0.17 0.34; 0.50 0.15 0.17 0.34; 0.71
0.34 0.17 0.34]; % Subplot positioning
close all; figure('Position', [10 50 1900 950])
subplot('Position', S(1,:))
plot(Wavelength, Spectra(:,1:10), 'Color', Color(2,:))
axis tight; xlim([490 1200])
title({'RAW SINGLE BEAM SPECTRA'; ''}, 'fontweight', 'normal');
xlabel('Wavelength (nm)');
ylabel({'DEEP-SET EYE';'';'Signal (counts)'})

% % Spectra Corrections:
[Spectra] = CorrectVis(Spectra, 0, 0);

% % Plot Two and Three - Normalised Spectra
subplot('Position', S(2,:))
plot(Wavelength, Spectra, 'Color', Color(2,:));
axis tight; xlim([490 1200])
title({'NORMALISED SPECTRA'; ''}, 'fontweight', 'normal');
xlabel('Wavelength (nm)');
ylabel('Signal (counts)')
% Close up..
subplot('Position', S(3,:))
plot(Wavelength, Spectra, 'Color', Color(2,:));
axis tight; xlim([620 720]);
title({'CHL BAND OF SPECTRA'; ''}, 'fontweight', 'normal');
xlabel('Wavelength (nm)');
ylabel('Signal (counts)')
```

```matlab
% % Load Spectra For Shallow Eye:
cd('G:\2017SummerTests\20170830\ShallowEye');
for x = 1:length(FileiD)
    data = dlmread(char(FileiD(x)),' ', 2, 0);
    Spectra2(:,x) = [data(1:1018,4); data(1019:end,3)];
end


% % Plot Four - Raw Spectra:
subplot('Position', S(4,:))
plot(Wavelength, Spectra2(:,1:10), 'Color', Color(2,:))
axis tight; xlim([490 1200])
xlabel('Wavelength (nm)');
ylabel({'SHALLOW-SET EYE';'';'Signal (counts)'})


% % Spectra Corrections:
[Spectra2] = CorrectVis(Spectra2, 0);


% % Plot Five and Six - Normalised Spectra
subplot('Position', S(5,:))
plot(Wavelength, Spectra2, 'Color', Color(2,:));
axis tight; xlim([490 1200])
xlabel('Wavelength (nm)');
ylabel('Signal (counts)')
% Close up..
subplot('Position', S(6,:))
plot(Wavelength, Spectra2, 'Color', Color(2,:));
axis tight; xlim([620 720]);
xlabel('Wavelength (nm)');
ylabel('Signal (counts)')



% % BoxPlot - Variance in Signal at 675 nm
subplot('Position', S(7,:))
boxplot([Spectra(Wavelength == 675, :)', Spectra2(Wavelength == 675, ...
:)'], 'labels', {'DEEP-SET EYE','SHALLOW-SET EYE'}, 'width', 0.8)
b = findobj(gca, 'type', 'line');
set(b(1:2), 'markeredgecolor', Color(1, :))
set(b(3:6), 'color', Color(2, :), 'linewidth', 1.5)
ylabel('Signal (Counts)')
title('SIGNAL AT 675 NM', 'fontweight', 'normal')



%% FIGURE 12

% % Load Spectra and Create (Wav/Spectra) Variables:
cd('U:\2017SummerTests\20170801\Distance\Eye');
D = dir; FileiD = {D(3:end).name};
for x = 1:length(FileiD)
    cd('U:\2017SummerTests\20170801\Distance\Eye');
    data = dlmread(char(FileiD(x)),' ', 2, 0);
    Eye(:,x) = [data(1:1018,4); data(1019:end,3)];
    cd('U:\2017SummerTests\20170801\Distance\Bac');
    data = dlmread(char(FileiD(x)),' ', 2, 0);
    Bac(:,x) = [data(1:1018,4); data(1019:end,3)];
end
Wavelength = [data(1:1018,2); data(1019:end,1)];
```

```matlab
% % Create Figure:
Color = ColorPlots(3, 10); % Colour scheme
[S] = SubplotPositions(2, 3, 0.1, 0.07, 0.05, 0); % Subplot
positioning
% Plot one - raw eye single beam spectra..
close all; figure('Position', [10 50 950 950])
subplot('Position', S(1,:))
p = plot(Wavelength, Eye);
title({'RAW SINGLE BEAM SPECTRA'; ''}, 'fontweight', 'normal');
xlabel('Wavelength (nm)');
ylabel({'EYE DATA';'';'Signal (counts)'})
axis tight; xlim([490 1200])
% Plot four - raw background single beam spectra..
subplot('Position', S(4,:))
i = plot(Wavelength, Bac);
xlabel('Wavelength (nm)');
ylabel({'BACKGROUND DATA';'';'Signal (counts)'})
axis tight; xlim([490 1200])
text(800,Bac(find(Wavelength == 800),10), '\leftarrow Max Distance',
'fontsize', 8);
text(800,Bac(find(Wavelength == 800),1), '\leftarrow Min Distance',
'fontsize', 8);
for x = 1:10
    set(p(x,1),'Color',Color(x,:));
    set(i(x,1),'Color',Color(x,:));
end

% % Spectra Corrections:
[Eye] = CorrectVis(Eye, 0, 0);
[Bac] = CorrectVis(Bac, 0, 0);

% % Plots of Normalised Data:
subplot('Position', S(2,:))
p = plot(Wavelength, Eye);
title({'NORMALISED SPECTRA'; ''}, 'fontweight', 'normal');
xlabel('Wavelength (nm)');
ylabel('Signal (counts)')
axis tight; xlim([490 1200])
subplot('Position', S(5,:))
i = plot(Wavelength, Bac);
xlabel('Wavelength (nm)');
ylabel('Signal (counts)')
axis tight; xlim([490 1200])
% Close-up of eye chl band..
subplot('Position', S(3,:))
j = plot(Wavelength, Eye);
title({'CHL BAND OF SPECTRA'; ''}, 'fontweight', 'normal');
xlabel('Wavelength (nm)');
ylabel('Signal (counts)')
axis tight; xlim([620 720])
% Close-up of background chl band..
subplot('Position', S(6,:))
k = plot(Wavelength, Bac);
xlabel('Wavelength (nm)');
ylabel('Signal (counts)')
axis tight; xlim([620 720])
for x = 1:10
    set(p(x,1),'Color',Color(x,:));
    set(i(x,1),'Color',Color(x,:));
    set(j(x,1),'Color',Color(x,:));
    set(k(x,1),'Color',Color(x,:));
```

```matlab
    end


%% FIGURE 13

% % Load Spectra and Create (Wav/Spectra) Variables:
% Day one..
cd('U:\2017SummerTests\20170731\!!');
% Read eye A and B data..
D = dir('*.ssm'); FileiD1 = {D(3:end).name};
for x = 1:length(FileiD1)
    data = dlmread(char(FileiD1(x)),' ', 2, 0);
    Spectra(:,x) = [data(1:1018,4); data(1019:end,3)];
end
% Read eye C data..
file = fopen('1523C.EP1');
data = fread(file,'single');
fclose(file);
% Reshape data into a suitable matrix..
SpectraC = reshape(data,2051,length(data)/2051); SpectraC =
SpectraC(182:end-200, :);
% Day two..
cd('U:\2017SummerTests\20170801\!!');
% Read eye A and B data..
D = dir('*.ssm'); FileiD2 = {D(3:end).name};
for x = 1:length(FileiD2)
    data = dlmread(char(FileiD2(x)),' ', 2, 0);
    Spectra(:, x+length(FileiD1)) = [data(1:1018,4);
data(1019:end,3)];
end
% Wavelength variable..
Wavelength = [data(1:1018,2); data(1019:end,1)];
% Read eye C data..
file = fopen('1548C.EP1');
data = fread(file,'single');
fclose(file);
% Reshape data into a suitable matrix..
SpectraC2 = reshape(data,2051,length(data)/2051); SpectraC2 =
SpectraC2(182:end-200, :);

% % Spectra Corrections:
[Spectra] = CorrectVis(Spectra, 0, 0);
[SpectraC] = CorrectVis([SpectraC,SpectraC2], 0, 0);

% % Seperate Eye A and Eye B and Calculate Chl Areas:
FileiD = [FileiD1 FileiD2];
A = find(contains(FileiD,'A')); B = find(contains(FileiD,'B'));
SpectraA = Spectra(:, A); SpectraB = Spectra(:, B);

% % Kinetic Calculations:
[~, ~, AreaA] = ConvertVis(SpectraA, Wavelength);
[~, ~, AreaB] = ConvertVis(SpectraB, Wavelength);
[~, ~, AreaC] = ConvertVis(SpectraC, Wavelength);

% % Create a Variable of Analysis Time:
% For eye A and B..
for x = 1:length(A)
    Time(1,x) =
str2num(FileiD{1,A(x)}(1:2))+(str2num(FileiD{1,A(x)}(3:4))/60);
end
```

```matlab
Time(1,58:107) = Time(1,58:107) + 24; Time = Time - Time(1,1);
% For eye C..
TimeC = linspace(Time(57)+0.1, Time(58)-0.1, (size(SpectraC,2)-
size(SpectraC2,2)));
TimeC = [TimeC, repmat(Time(end),1,size(SpectraC2,2)) +
cumsum(repmat(0.09, 1, size(SpectraC2,2)))];


% % Create Figure:
Color = ColorPlots(3, 3); % Colour scheme
close all; figure('Position', [10 50 500 950])
plot(Time, AreaA, '.', 'Color', Color(1,:), 'Markersize', 8)
hold on
plot(Time, AreaB, '.', 'Color', Color(3,:), 'Markersize', 8)
hold on
plot(TimeC, AreaC, '.', 'Color', Color(2,:), 'Markersize', 8)
title('KINETIC CHL AREAS OF 3 EYES FROM A SINGLE TUBER',
'fontweight', 'normal')
xlabel('Time (Hours)'); ylabel('Chl Band Area')
legend('Eye 1 (Apical)', 'Eye 2 (Side)', 'Eye 3', 'location',
'southeast')
axis tight square


%% FIGURE 14

% % Load Spectra and Create Variables:
% Day one..
cd('U:\2017SummerTests\LineMeasurement\1')
D = dir; FileiD = {D(3:end).name};
for y = 1 : length(FileiD)
    data = dlmread(char(FileiD(y)),' ', 2, 0);
    Spectra1(:,y) = [data(1:1018,4); data(1019:end,3)];
end
% Extract time for day one..
iD = char(FileiD); T1 = unique(cellstr(iD(:,1:4)));
% Day two..
cd('U:\2017SummerTests\LineMeasurement\2')
D = dir; FileiD = {D(3:end).name};
for y = 1 : length(FileiD)
    data = dlmread(char(FileiD(y)),' ', 2, 0);
    Spectra2(:,y) = [data(1:1018,4); data(1019:end,3)];
end
% Extract time for day two..
iD = char(FileiD); T2 = unique(cellstr(iD(:,1:4)));
% Day three..
cd('U:\2017SummerTests\LineMeasurement\3')
D = dir; FileiD = {D(3:end).name};
for y = 1 : length(FileiD)
    data = dlmread(char(FileiD(y)),' ', 2, 0);
    Spectra3(:,y) = [data(1:1018,4); data(1019:end,3)];
end
% Extract time for day three..
iD = char(FileiD); T3 = unique(cellstr(iD(:,1:4)));
% Wavelength variable..
Wavelength = [data(1:1018,2); data(1019:end,1)];
% Time variable..
for x = 1:3
    Time(1,x) = str2num(T1{x,1}(1:2))+(str2num(T1{x,1}(3:4))/60)-
9.2;
    Time(1,x+3) =
str2num(T2{x,1}(1:2))+(str2num(T2{x,1}(3:4))/60)+(24-9.2);
```

```matlab
    Time(1,x+6) =
str2num(T3{x,1}(1:2))+(str2num(T3{x,1}(3:4))/60)+(48-9.2);
end

% % Spectra Corrections/Kinetic Conversions:
[Spectra] = CorrectVis([Spectra1, Spectra2, Spectra3], 0, 1);
Idx = repmat(1:5,1,9);
[~, ~, Area1] = ConvertVis(Spectra(:,Idx==1), Wavelength);
[~, ~, Area2] = ConvertVis(Spectra(:,Idx==2), Wavelength);
[~, ~, Area3] = ConvertVis(Spectra(:,Idx==3), Wavelength);
[~, ~, Area4] = ConvertVis(Spectra(:,Idx==4), Wavelength);
[~, ~, Area5] = ConvertVis(Spectra(:,Idx==5), Wavelength);

% % Create Figure:
Color = [ColorPlots(2,3); ColorPlots(3,3); ColorPlots(4,3)]; %
Colour scheme
[S] = SubplotPositions(2, 3, 0.1, 0.07, 0.1, 0); % Subplot
positioning
close all; figure('Position', [10 50 950 950])
% Plot one - position one..
ax(1) = subplot('Position', S(1,:));
h = scatter(Time, Area1, 'fill'); axis tight; ylim([0 6])
% Plot two - position two..
ax(2) = subplot('Position', S(4,:));
i = scatter(Time, Area2, 'fill'); axis tight; ylim([0 6])
% Plot three - position three..
ax(3) = subplot('Position', S(5,:));
j = scatter(Time, Area3, 'fill'); axis tight; ylim([0 6])
% Plot four - position four..
ax(4) = subplot('Position', S(6,:));
k = scatter(Time, Area4, 'fill'); axis tight; ylim([0 6])
% Plot five - position five..
ax(5) = subplot('Position', S(3,:));
l = scatter(Time, Area5, 'fill'); axis tight; ylim([0 6])
% Set colour scheme..
set([h,i,j,k,l], 'CData', Color);
set(ax, 'ylim', [0 10])
for x = 1:length(ax)
    xlabel(ax(x), 'Time (Hours)')
    ylabel(ax(x), 'Chl Band Area');
    title(ax(x), ['POSITION ' num2str(x)], 'fontweight', 'normal')
end
% Input image...
cd('U:\2017SummerTests');
Image = imread('IMG_5191.JPG');
subplot('Position', S(2,:))
image(Image)
axis square off;




function [Spectra] = CorrectVis(Spectra, SmoothData, MeanReplicas)
%%
% CORRECTVIS
% Corrections of smoothing (if needed), SNV normalisation and
% baseline adjustment for the Vis/NIR spectral data.
%
% J.Garnett, July 2018

%%
```

```matlab
% % (If Required) Smooth Spectral Data:
if SmoothData == 1
    Spectra = smoothdata(Spectra, 'sgolay', 21);
else
end

% % SNV Normalisation:
[w,s] = size(Spectra);
for y = 1:s % Run through one spectra at a time
    Spectra(:,y) = (Spectra(:,y)-
mean(Spectra(:,y))*ones(w,1))./(std(Spectra(:,y))*ones(w,1));
end

% % Shift Baseline to Zero:
Spectra = Spectra - repmat(min(Spectra),w,1);

% % (If Required) Average Replicas:
if MeanReplicas == 1
    Idx = 3:3:size(Spectra,2);
    for x = 1:length(Idx)
        S(:,x) = mean(Spectra(:,Idx(x)-2:Idx(x)),2);
    end
    Spectra = S;
else
end




function [AbsorbanceSpec, NewWavelength, ChlArea] =
ConvertVis(Spectra, Wavelength)
%%
% CONVERTVIS
% Convert single beam spectra to kinetic (absorbance) spectra and
% calculate chl areas.
%
% J.Garnett, July 2018

%%
[~,s] = size(Spectra);

% % Find Absorbance Spectra:
W = Wavelength>549 & Wavelength<901; % Find wavelength range where
noise from I/I0 is not created
AbsorbanceSpec = Spectra(W,:)./repmat(Spectra(W,1),1,s);
AbsorbanceSpec(AbsorbanceSpec<0) = 0; % Remove non-intergers
AbsorbanceSpec = log10(AbsorbanceSpec)*(-1);

% % Create New Wavelength Variable
NewWavelength = Wavelength(W);

% % Calculate Chl Ares
W = NewWavelength>640 & NewWavelength<710; % Anchor points used
either side of the Chl band
Offsets = zeros(sum(W),s);
for y = 1:s % Create matrix of lines (one for each spectra) between
the two anchor points
    Offsets(:,y) = linspace(AbsorbanceSpec(find(W==1, 1),y),
AbsorbanceSpec(find(W==1, 1, 'last'),y), sum(W))';
end
```

```matlab
ChlArea = sum(AbsorbanceSpec(W,:))-sum(Offsets); % Find some of peak
minus area underneath




function [color] = ColorPlots(ColorChange, NumberOfPlots)
%%
% COLORPLOTS
% Creates a colour index for a gradual change between two colours,
% input no of colours need in "NumberOfPlots"
% ColorChange; for Red2Cyan use 1
%              for Red2Red use 2
%              for Blue2Blue use 3
%              for Green2Green use 4
%
% J.Garnett, July 2018


%%
% Red2Cyan
if ColorChange == 1
   color = zeros(NumberOfPlots, 3);
   color(:,1) = flipud((0:(NumberOfPlots-1))'/(NumberOfPlots-1));
   color(:,2) = ((0:(NumberOfPlots-1))'/(NumberOfPlots-1));
   color(:,3) = ((0:(NumberOfPlots-1))'/(NumberOfPlots-1));
% Red2Red
elseif ColorChange == 2
       color = zeros(NumberOfPlots, 3);
       color(:,1) = linspace(0.3, 1, NumberOfPlots);
       color(:,3) = flipud(linspace(0, 0.3, NumberOfPlots));

% Blue2Blue
elseif ColorChange == 3
       color = zeros(NumberOfPlots, 3);
       color(:,2) = linspace(0, 1, NumberOfPlots);
       color(:,3) = linspace(0.3, 1, NumberOfPlots);

% Green2Green
elseif ColorChange == 4
       color = zeros(NumberOfPlots, 3);
       color(:,2) = linspace(0.2, 0.8, NumberOfPlots);
end
```
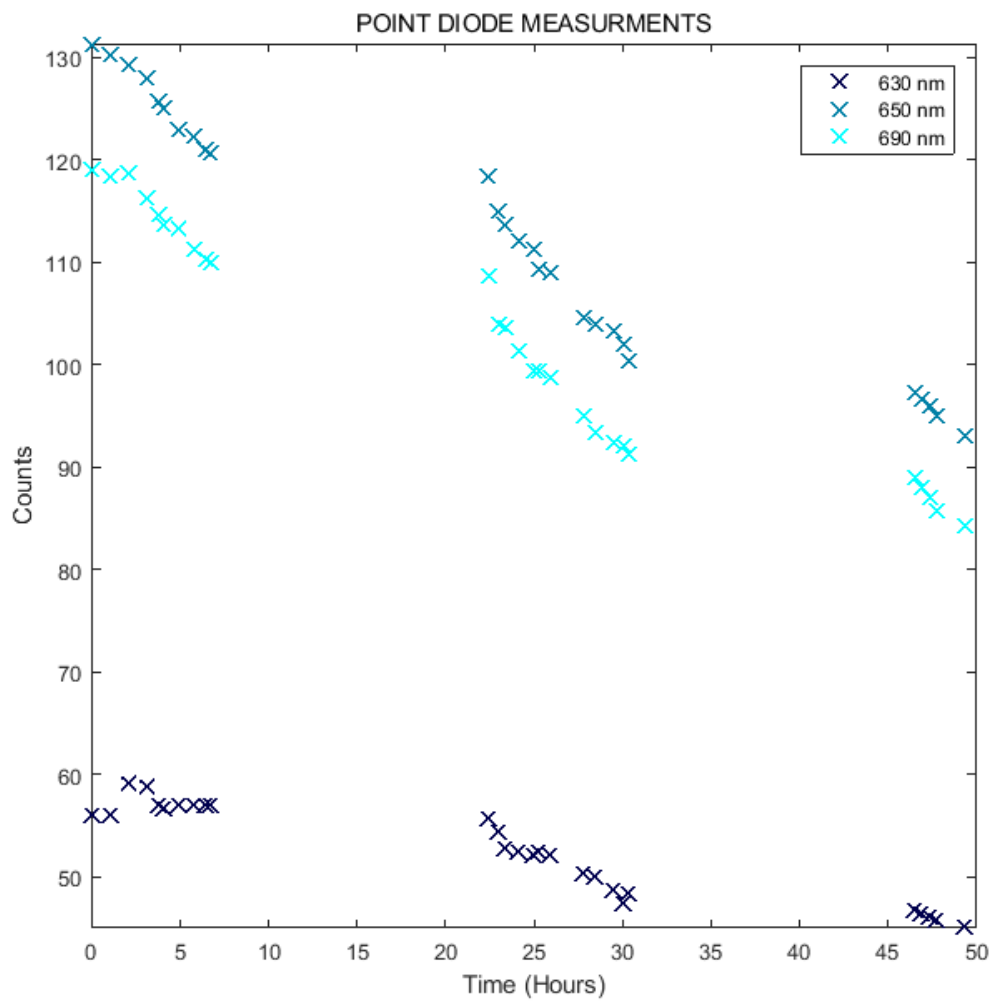
APPENDIX 2

Figure 13:1 Example of measurements recorded using the three-diode component on the SPUD equipment. Shop bought cv King Edward tuber was monitored for 50 hours, January 2016. The tuber was irradiated with laboratory lighting during analysis period and left in darkness for the periods in-between (i.e. ~ 8 – 22 and 31 – 46). The tuber was fixed into position over the diodes using a clamp.